DISSERTATION

PROTEOMIC AND MOLECULAR BIOLOGICAL STUDIES ON COMPONENTS OF THE MIH SIGNALING PATHWAY IN THE CRUSTACEAN MOLTING GLAND FROM LAND CRAB, *GECARCINUS LATERALIS*

Submitted by

SUNG GU LEE

Graduate Degree Program

In Cell and Molecular Biology

In partial fulfillment of the requirements

For the Degree of Doctor of Philosophy

Colorado State University

Fort Collins, Colorado

Summer 2006

COLORADO STATE UNIVERSITY

May 15, 2006

WE HEREBY RECOMMEND THAT THE DISSERTATION PREPARED UNDER OUR SUPERVISION BY SUNG GU LEE ENTITLED PROTEOMIC AND MOLECULAR BIOLOGICAL STUDIES ON COMPONENTS OF THE MIH SIGNALING PATHWAY IN THE CRUSTACEAN MOLTING GLAND FROM LAND CRAB, *GECARCINUS LATERALIS* BE ACCEPTED AS FULFILLING IN PART REQUIREMENTS FOR THE DEGREE OF DOCTOR OF PHILOSOPHY.

Committee on Graduate Work

Deborah Garrity

James R Bamburg

Donald L. Mykles
Advisor

Department Head

ABSTRACT OF DISSERTATION

PROTEOMIC AND MOLECULAR BIOLOGICAL STUDIES ON COMPONENTS OF THE MIH SIGNALING PATHWAY IN THE CRUSTACEAN MOLTING GLAND FROM LAND CRAB, *GECARCINUS LATERALIS*

Regulation of the molting cycle in decapod crustaceans is mainly controlled by the X-organ/sinus gland (XO/SG) complex and the Y-organ (YO). Molt-inhibiting hormone (MIH), is produced in XO/SG complex, and regulates ecdysteroidogenesis in the YO. The goal of this study was to characterize components of the MIH signaling pathway. The eyestalk is the main endocrine system to produce MIH in crustaceans, and eyestalk ablation (ESA) causes significant increases in hemolymph ecdysteroid of land crabs. However, MIH immunoprecipitation of YO extracts showed that the MIH or MIH-like peptide(s) was/were not decreased even after 3 days post ESA. Further analysis of the MIH-immunoprecipitated samples by two-dimensional gel electrophoresis showed the presence of putative MIHBPs (MIH-binding proteins) in the YOs of intact animals. This suggests that MIHBP(s) may facilitate the binding of MIH to receptor, which would result in the suppression of ecdysteroidogenesis. MIHBPs were shown at 35 kDa, pI 7.6 and 32 kDa, pI 8.0. These proteins remain to be identified, but preliminary sequences obtained by tandem mass spectrometry showed they are related. MIH induces at least 60-fold increase in cGMP in the YO. Three guanylyl cyclases (GCs) were cloned from land crabs and each GC expression was investigated after ESA to identify which GC is regulated in the Y-organ. RT-PCR revealed that expression of both NO-sensitive (Gl-GC-Iβ) and NO-insensitive soluble (Gl-GC-III) GCs increased in response to elevated

ecdysteroid induced by ESA. One of the receptor guanylyl cyclase isoforms found in this study, Gl-GC-II(+18), was expressed predominantly in striated muscle. Semi-quantitative PCR and statistical analysis showed that the expressional change of this isoform was significant only in claw muscle in response to elevated ecdysteroid induced by ESA. The response of Gl-GC-II(+18) to elevated ecdysteroid in claw muscle indicates that a specific ligand binds to this receptor and triggers a series of signaling cascades for claw muscle atrophy, eventually inducing molting. Total protein extracts of Y-organs from intact and ES ablated animals were analyzed to discover potential candidates of MIH signaling by two-dimensional gel electrophoresis, image analysis, and proteome clustering. As a result, more than 3-fold increases in 170 proteins and 3-fold decreases in 89 proteins out of total 543 proteins were identified, suggesting that expression proteomics has a powerful potential as a high-throughput target screening system. Phosphoproteins purified from Y-organs were analyzed by two-dimensional gel electrophoresis. ESA caused significant changes in the levels of phosphoproteins. These proteins were selected as putative candidates for molt-regulating factors. One of these phosphoproteins was detected on a Western blot of ESA Y-organ extracts probed with an anti-NOS antibody. Peptide mass fingerprinting analysis confirmed that the protein was land crab NOS. These results indicate that NOS phosphorylation is associated with YO activation in ESA animals. A MIH signaling pathway involving NOS and NO-sensitive GC is proposed.

Sung Gu Lee
Graduate Program in Cell and Molecular Biology
Colorado State University
Fort Collins, CO 80523
Summer 2006

ACKNOWLEDGMENTS

I would like to give my first thanks to God who planned and gave me the opportunity and the strength to accomplish my degree.

I would like to deeply thank Dr. Donald L. Mykles, my advisor for his scientific guidance, support, for understanding of my situation as a foreign student, and for introducing me into the world of crustacean biology. I would also like to thank my committee members Drs. Anireddy S.N. Reddy, Deborah M. Garrity, and James R. Bamburg for their consistent encouragement and guidance. I am very grateful to Dr. Henry Thompson and Dr. Bamburg who willingly let me use their 2-DE facilities. I am also thankful Dr. Watson's lab for providing the MIH antibody. I am indebted so much to Dr. Kara Lee for sharing her knowledge on crustacean biology. I wish to thank Matthew Thompson for his frequent help in/out the lab, and being a wonderful friend, and Dr. Joseph Covi for reviewing and making suggestions in this manuscript, as well as for his good friendship. My thanks also go to the past and present crab lab members, Dr. Scott Medler, Kitty Brown, Luisa Batista, Laura Baker, Rachelle Doran, Travis Lilley, Jo Hoppes, Stephanie Spenny, Lindsey Progen, Erica Chao, Tyler Zarubin, Natalie Wasmundt, Brandon Bader, Lindsey Brier, Danielle Dennis, Keith Dmytrow, April Flack, Andrea Gomez, Lindsay Martin, Stephanie Melzer, Jocelyn Riehl, and Kristin Van Ort.

I would also like to thank many Korean friends in Fort Collins and my two close friends Drs. HakJun Kim in Vanderbilt University and HyunWoo Kim in Pukyung National University.

Finally, I would like to thank my wife JooHyun Hahm, daughter YeJin, and son YeJun for their continuous support and love without which I would not have succeeded. I also thank my parents and parents-in-law for their continuous prayers and personal sacrificing.

TABLE OF CONTENTS

CHAPTER ONE

INTRODUCTION

Overview of the crustacean molting cycle

Crustaceans, like other arthropods, grow by periodic shedding of their old exoskeleton, which is known as molting or ecdysis. Major metabolic events associated specifically with growth are observed before and after ecdysis. 'Molting' concerns all the processes involved in ecdysis including degradation and synthesis of the exoskeleton, formation of gastroliths in some species, atrophy and restoration of somatic muscle in the claws, and regeneration of lost appendages (Skinner, 1985). Drach categorized the molting cycle into five stages (A to E) based on hardness of specific regions of the exoskeleton (Drach, 1939).

As shown in Figure 1-1, by observing sequential alterations in the epidermis of land crabs (*Gecarcinus lateralis*), Skinner explained the molting cycle at the cellular level (Skinner, 1962). Stage A comes immediately after ecdysis (Stage E), and lasts one to two days. In this stage, gastroliths are completely dissolved and epidermal cell size in the integument is decreased. In Stage B, the endocuticle layers of the exoskeleton are formed at about 7 μm a day and muscle in the chela grows. Through stage C, the exoskeleton becomes harder by calcification and thickening of the endocuticle layer. The formation of the membranous layer of the exoskeleton is observed at the end of postmolt

or metecdysis (stages A through C3) (Carlisle and Dohrn, 1953). Stage C4 is the intermolt or anecdysis period, and is the longest period in the molting cycle. It continues for about 10 or 11 months in land crabs. The premolt or proecdysis period usually starts about 2 months before ecdysis and this period can be divided into 5 substages (from D0 to D4) based on structural changes at the cellular level. Premolt is triggered by increasing concentrations of ecdysteroids in the hemolymph. Stage D0 begins gastrolith formation and claw muscle atrophy. The first sign of premolt in integumentary tissues is apolysis, the separation of epidermis from the old exoskeleton in stage D1 (Jenkin and Hinton, 1966). During stage D2, the epidermis secretes a new epicuticle and exocuticle. Hemolymph ecdysteroid concentrations increase through stage D2 and reach a peak in stage D3. In stage D4 the hemolymph turns pink because astaxanthin is resorbed from the old exocuticle. Astaxanthin, a carotenoid pigment that is not synthesized by crustaceans, is a component of the exoskeleton of many crustacean species. Changes in the concentration of astaxanthin in the hemolymph have been used as an index of an animal's progress through premolt (Skinner, 1985). Degradation of the old exoskeleton continues up to ecdysis. Any lost limb regeneration also happens during this stage. Epidermal cell size in the integument begins to decrease just prior to ecdysis, and decreases until it reaches a size comparable to that of intermolt animals. Stage E (ecdysis) begins with opening of the old exoskeleton (the passive phase) and continues until the old exoskeleton is completely removed from the animal (the active phase) (Skinner, 1985). Ecdysis lasts for up to a day.

The length of the molting cycle increases as animals age. Molting cycles in larvae are usually a few days or weeks. The first seven molt cycles of the amphipod

Traskorchestia traskiana are as short as a few days (Soyez and Kleinholz, 1977). Some species enter a terminal intermolt at the puberty molt and no longer molt under unstressed conditions (Skinner, 1985). Molting cycles are affected by environmental conditions. The effect of temperature has been reported for various crustaceans (Chang and Bruce, 1980; Hughes, 1972). In American lobster, *Homarus americanus,* the molting cycle is shortened by increasing the temperature from natural conditions (below 10°C) to higher temperature (22-24°C). Low temperature delays molting in the fiddler crab, *Uca pugnax* (Passano, 1960). The effect of light appears to be variable in different species (Stephens, 1955; Weis, 1976). Although environmental signals may affect the molt cycle, it is likely that internal signals determine an animal's response to external factors (Skinner, 1985).

Hormonal regulation of molting in decapod crustaceans

The internal signal controlling the molting cycle is the steroid hormone 20-hydroxyecdysone (20E) (Hoffmann and Porchet, 1984). Ecdysteroids are polyhydroxylated C-27 steroids derived from cholesterol. Although a variety of ecdysteroids are present, the dominant ecdysteroid in the hemolymph is 20E in most species. Ecdysteroids are synthesized and secreted from the Y-organs (YOs), a pair of epitheliod glands located in the anterior cephalothoraxes (Lachaise et al., 1993). The YOs are small, compact structures, that are no more than a few millimeters in diameter even in large species, such as the crab *Cancer magister* (Hoffman, 1967). YO cells are of a single type and have many mitochondria and smooth endoplasmic reticulum, which are the distinctive characteristics of steroid-secreting cells (Buchholz and Adelung, 1980). Like other arthropods, crustaceans lack squalene synthetase, which is the enzyme that

catalyzes the conversion of farnesyl pyrophosphate to squalene, the precursor of cholesterol. Consequently, they lack the ability to synthesize cholesterol. Instead, crustaceans utilize cholesterol as a precursor for steroid hormone synthesis (Karlson and Hoffmeister, 1963; Spaziani and Kater, 1973; Vensel et al., 1984; Watson and Spaziani, 1985; Willig and Keller, 1976). This cholesterol must be obtained directly from the diet or from converting ingested phytosterols (Grieneisen, 1994). In crustaceans, cholesterol has been shown to be taken up by the high density lipoprotein (HDL)-cholesterol complex which then binds to the HDL receptor on the YO membrane, followed by endocytosis (Kang and Spaziani, 1995a; Kang and Spaziani, 1995b; Kang and Spaziani, 1995c).

Even though it is known that ecdysteroids are derived from dietary cholesterol, the biosynthetic pathway is still unknown except for the first step (conversion of cholesterol to 7-dehydrocholesterol) and last step (hydroxylations at carbons 2, 22, and 25), which yields 5 beta-ketodiol (2, 22, 25 trideoxyecdysone) (Grieneisen, 1994; Lachaise et al., 1986; Rees, 1989). The enzyme necessary for conversion of 20E from ecdysone is ecdysone 20-monooxygenase, and is found in the mitochondrial and/or microsomal fractions of many different species and tissues (Grieneisen, 1992; Rees and Isaac, 1985; Smith, 1985). The rate of ecdysteroid synthesis depends on the availability of dietary cholesterol and its access to enzymes through short-lived carrier proteins, the activity of steroidogenic enzymes, and the availability of enzyme cofactors, mainly NADPH for cytochrome P450 monooxygenases (Baghdassarian et al., 1996).

The general titer of circulating ecdysteroids is low during intermolt in crustaceans. It increases dramatically in premolt, reaches a peak during mid to late premolt, and then

declines to basal levels just before ecdysis, which is kept at low levels during postmolt (Chang, 1989; Steele and Vafapoulou, 1989). However, in some species, such as *Uca*, ecdysteroid concentrations show small transient peaks in intermolt and premolt stages (Hopkins, 1983; Hopkins, 1992). Nonetheless, in most cases, ecdysteroid titer increases in mid to late premolt and decreases dramatically prior to ecdysis.

Roles of molt-inhibiting hormone (MIH) on crustacean molting gland

The YOs are regulated negatively by a neuropeptide, molt-inhibiting hormone (MIH). MIH is produced and released from the X-organ/sinus gland (XO/SG) complex in the eyestalk ganglia and has an inhibitory effect on the Y-organs by suppressing ecdysteroid synthesis. The existence of MIH was suggested by the fact that eyestalk ablation leads to rapid increase in ecdysteroid titer in hemolymph and induces molting (Passano, 1953). Injection of eyestalk extracts into eyestalkless animals at specific stages of the molting cycle lengthens the duration of the cycle (Ranga Rao, 1965; Soyez and Kleinholz, 1977). However, regulation of ecdysteroidogenesis in the Y-organs is more complex. For example, eyestalk ablation does not shorten the molting cycle in females undergoing vitellogenesis (Lachaise et al., 1992), and some species show continuous fluctuation of ecdysteroid titer in the molt cycle without eyestalks (Chang, 1985; Hopkins, 1983). In addition, as crustacean hyperglycemic hormone (CHH), gonad-inhibiting hormone (GIH), and mandibular organ-inhibiting hormone (MOIH) are also expressed in the X-organ, eyestalk ablation may cause imbalances in other physiological processes. Thus, regulation of the molting cycle is not simply a suppression of the Y-organ by MIH.

It involves a complex interaction between reproduction, growth, and environmental factors.

MIH sequences have been characterized in several decapod crustaceans. *In vivo* assays were employed in the isolation of an 8.7 kDa peptide from the sinus glands of *Homarus americanus* (Chang et al., 1987). Once the amino acid sequence of MIH was determined (Chung et al., 1996; Webster, 1991), the complete cDNA sequence was reported (Klein et al., 1993; Lee et al., 1995). Recently, a genomic DNA study of *Cancer parurus* showed that at least two copies of MIH genes exist (Lu et al., 2000). The MIH genes of *Cancer feriatus* and *C. pagurus* consist of three exons and two introns, and span approximately 4.3 kb (Chan et al., 1998; Lu et al., 2000). The 5' flanking regions of MIH genomic DNA contain several potential binding sites for known transcription factors, such as cAMP response element binding protein, putative Cf1/USP, and Broad Complex Z2 (Chan et al., 1998; Lu et al., 2000). The brachyuran MIHs share high sequence similarity. They encode a 113 amino acid prohormone (proMIH) composed of a 35-amino acid residue signal peptide and a 78-amino acid mature peptide (Watson et al., 2001). MIH contains six cysteine residues which are characteristic of the crustacean hyperglycemic hormone (CHH) peptide family (Keller, 1992). A structural study suggests that the first α-helix near the N-terminus and C-terminal region are essential for MIH function (Katayama et al., 2003).

MIH mRNA is detected in eyestalk neural ganglia (Umphrey et al., 1998). It is expressed at lower levels in brain, fertilized eggs, embryos, and larvae (Chan et al., 1998). Recently, MIH polyclonal antibody raised to a unique amino acid sequence of MIH from blue crab (Lee and Watson, 2002) showed strong immunoreactivity in second limb

regenerate but not in primary limb regenerate in land crab (*Gecarcinus lateralis*) (K.J, Lee, personal communication). These findings of nontraditional sites of MIH expression suggest a possible alternate mode of action such as a neuromodulator or neurotransmitter (Watson et al., 2001).

Cyclic nucleotides and protein kinases in the Y-organ

The signal transduction pathway of MIH is poorly understood. cDNA encoding high affinity MIH receptors in the YO membrane have yet to be characterized. Both cAMP and cGMP have been implicated as second messengers, although cGMP appears to be the main messenger regulating YO ecdysteroidogenesis. MIH induces a transient 2-fold increase of cAMP and more than 60-fold increase in cGMP in the Y-organs (Saidi et al., 1994). Activation of adenylate cyclase or inhibitors of phosphodiesterase each mimicked the inhibitory MIH function (Mattson and Spaziani, 1985). cAMP also has been shown to inhibit the receptor-mediated uptake of precursor cholesterol (Kang and Spaziani, 1995c). In previous studies, both cAMP and cGMP were suggested to have roles in mediating MIH action, but the relation of two signaling pathways still remains to be elucidated (Spaziani et al., 1999).

A signaling pathway including cGMP dependent kinase (PKG) is involved in inhibiting the YOs (Baghdassarian et al., 1996). The substrates of either the PKG or PKA are not known. However, in the YOs of the crayfish (*Orconectes limosus*), 95 kDa phosphoprotein increased during premolt and became the dominant phosphoprotein at stage D_1, while 68 kDa (pp68) and 17 kDa phosphoproteins decreased (Böcking and Sedlmeier, 1994). None of these proteins have been identified, but these data strongly

suggest that protein phosphorylation/dephosphorylation is involved in regulation of ecdysteroidogenesis. Tyrosine kinases have also been studied in regulation of ecdysteroid synthesis (Spaziani et al., 1999). Inhibitors of soluble tyrosine kinases inhibited ecdysteroid synthesis, thus tyrosine kinase has been considered to be affected by the MIH signaling pathway.

My graduate work has focused on identifying components of the MIH signaling pathway in the YO from blackback land crab, *Gecarcinus lateralis*. This dissertation is organized into five chapters. Chapter one is an introduction. In chapter two, the isolation of MIHBP(s) is described. Chapter three reports the cloning of three guanylyl cyclases (NO-sensitive soluble GC, receptor membrane GC, and NO-insenstive soluble GC) from land crab and determines effects of elevated ecdysteroid on their expression. Chapter four reports high-throughput expression proteomic approaches for identifying molt-regulating factors in the YO and identifies nitric oxide synthase (NOS) phosphorylation/dephosphorylation in the YO. Chapter five is a summary and outlines future directions of the research. Appendices are included that contain cloning and expression of land crab myostatin (Gl-Mstn); expression of EcR, RXR isoforms, and E75 in land crab tissues; tissue distribution of land crab NOS; two-dimensional electrophoresis analysis of total extracts of limb buds; and Tandem MS/MS analysis of MIHBPs using Agilent Ion-Trap in a nanospray mode.

Fig. 1-1. Crustacean molting cycle.

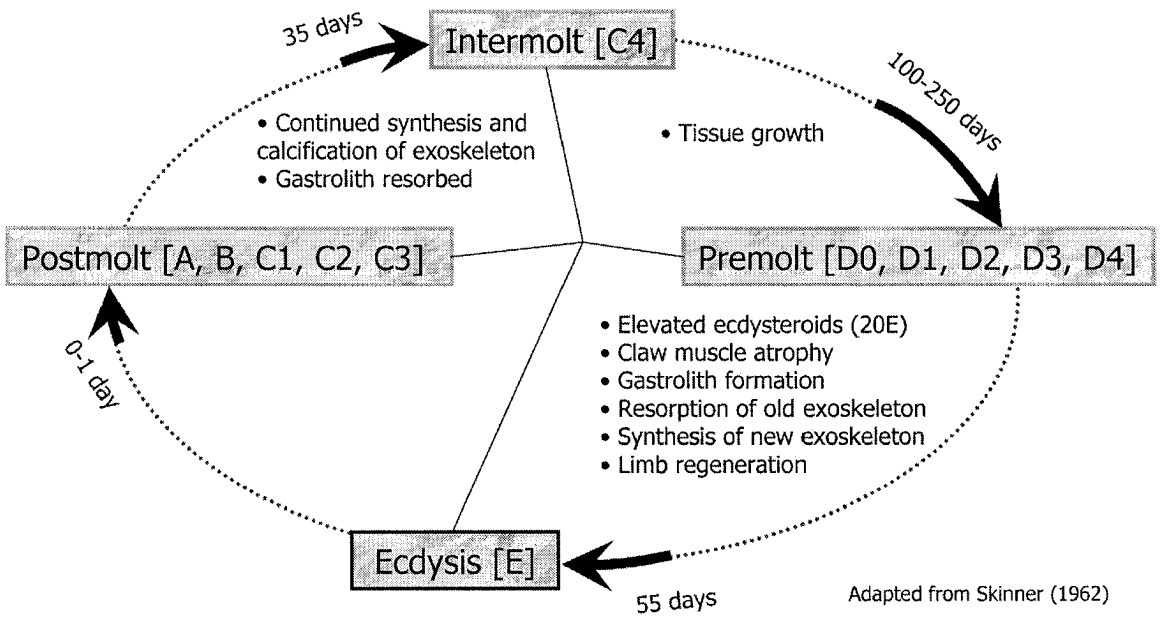

CHAPTER TWO

IDENTIFICATION OF MIH-BINDING PROTEINS (MIHBPS) BY CELL-MAP PROTEOMICS

Abstract

Regulation of the molting cycle in decapod crustaceans is mainly controlled by the X-organ/sinus gland (XO/SG) complex and the Y-organ. Molt-inhibiting hormone (MIH), is produced in XO/SG complex, and regulates ecdysteroidogenesis in the Y-organ. Eyestalk ablation (ESA) causes a rapid increase of ecdysteroid titers and induces molting. However, little information is known about the pathways for inhibition of ecdysteroidogenesis in the Y-organ after MIH triggers the signal cascade from its receptor on the Y-organ membrane. In an effort to determine which proteins are involved in Y-organ ecdysteroidogenesis, cell-map proteomic approaches were used. Eyestalks are the main endocrine system to produce MIH in crustaceans, and eyestalk ablation (ESA) caused significant increases in hemolymph ecdysteroid of land crabs. However, the MIH amount was not decreased in ES-ablated Y-organ extracts. The MIH-immunoprecipitated samples were subjected to two-dimensional gel electrophoresis, and then analyzed by Western blot and silver staining. As a result, putative MIHBPs (MIH-binding proteins) were observed only in Y-organ from intact animals, suggesting that MIHBPs could be critical regulators for ecdysteroidogenesis. The similar binding proteins were observed in

2° limb bud (LB) not in 1° LB, as 2° LB is known to produce MIH-like peptide (LAFpro). Some internal peptide sequences were determined by tandem mass spectrometry, but cloning of the MIHBPs was not successful by using deduced primer sets. These proteins remain to be identified. Our data suggest that the currently accepted molting control model should be reconsidered. The determination of MIHBP sequences would provide insight into crustacean molting regulation mechanisms.

Introduction

Molting, like many other physiological processes, is regulated by a neuropeptide, molt-inhibiting hormone (MIH), which is produced and released from the X-organ/sinus gland (XO/SG) complex in the eyestalk ganglia. The molting gland, the Y-organ, is regulated negatively by MIH, which suppresses Y-organ ecdysteroid synthesis. MIH activates protein kinases in the Y-organs *in vitro* via increases in cAMP and cGMP (Baghdassarian et al., 1996; Böcking and Sedlmeier, 1994; Saidi et al., 1994; Sedlmeier and Fenrich, 1993; Von Gliscynski and Sedlmeier, 1993). Ca^{2+} is regulated at an optimal level for ecdysteroidogenesis since intracellular Ca^{2+} is inhibitory at extreme concentrations (Spaziani et al., 2001). The Y-organ membranes of crab are thought to have different receptors for MIH and crustacean hyperglycemic hormone (CHH) (Webster, 1993) since these two neuropeptides differ in their surface structure (Katayama et al., 2003).

The existence of MIH was first suggested by the fact that eyestalk ablation (ESA) leads to a rapid increase in ecdysteroid titer in the hemolymph and induces molting (Passano, 1953). Injection of eyestalk extracts into eyestalkless animals at specific stages of the molting cycle lengthens the duration of the cycle (Ranga Rao, 1965; Soyez and Kleinholz, 1977). However, regulation of ecdysteroidogenesis in the Y-organs is more complex. For example, eyestalk ablation does not shorten the molting cycle in females undergoing vitellogenesis (Lachaise et al., 1992) and some species show continued fluctuation of ecdysteroid titer during the molt cycle in ESA animals (Chang, 1985; Hopkins, 1983). In addition, the other neuropeptide hormones, including crustacean

hyperglycemic hormone, gonad-inhibiting hormone (GIH), and mandibular organ-inhibiting hormone (MOIH) are also expressed in the X-organ and other regions of the nervous system (Borst et al., 2002; Chung et al., 1999; Cooper and Ruffner, 1998; Cromarty and Kass-Simon, 1998; De Kleijn and Van Herp, 1995; Dircksen et al., 2001), eyestalk ablation may cause imbalances in other physiological processes. While the XO/SG complex is central in the regulation of molting, experiments on ESA animals indicate that peripheral tissue factors can directly inhibit the Y-organ. In lobsters, ESA stimulates either molting or reproduction, depending on whichever process is dominant at that time (Waddy et al., 1995), indicating that there is an interaction between growth and reproduction that does not require the ES ganglia. Molting and limb regeneration are tightly coupled processes. Regeneration occurs during premolt and precocious molts are induced by MLA (multiple leg autotomy) (Yu et al., 1999; Yu et al., 2001; Yu et al., 2002; Yu and Mykles, 1997; Yu and Mykles, 1998). LBA (Limb bud autotomy) interrupts premolt in ESA animals (Schmiege et al., 1992), indicating that factors produced by the X-organ are not required. These data challenge the central paradigm in crustacean endocrinology that all premolt processes are coordinated by the ES neurosecretory center, and suggest that peripheral tissues may produce factors, such as LAF_{pro} which is MIH-like peptide found in 2° limb buds in land crab, that have direct effects on the Y-organs. Thus, regulation of the molting cycle is not simply a suppression of the Y-organ by MIH. It involves a complex interaction between reproduction, growth, and environmental factors.

Proteomics is a multidisciplinary technology which is based on the proteome, or proteins expressed from a genome. Since genomics cannot always predict the dynamics

or structure of proteins, protein-level analysis is necessary to identify total protein expression profiles, protein-protein interactions, and post-translational modifications. Most regulatory processes occur at the protein level, where most diseases primarily happen and where most drug targets can be selected. Therefore, proteomics has most commonly been used in protein investigations involved with specific physiological or disease states. The main purpose of cell-map proteomics is to define proteins in each organ and their functions and relationships (Blackstock and Weir, 1999). By using this approach, protein-protein interactions and certain cell signaling mechanisms can be determined. For these studies, specific antibodies or resins are commonly applied.

Even though ecdysteroidogenesis in the Y-organ is initially regulated by MIH, there is still little information about the first step of MIH action. It may be binding of MIH to a MIH receptor(s) or other regulator(s). For example, Insulin-like Growth Factor Binding Proteins (IGFBPs) have been shown to modulate the actions of IGFs in either positive or negative ways. In serum and other biological fluids, IGFBPs modulate the endocrine actions of IGFs by regulating the bioavailability of IGFs for their receptors (Cesi et al., 2004; Kajimura et al., 2005; Marshman and Streuli, 2002; Mazerbourg et al., 2004; Nilsson-Ehle et al., 2005; Rosenzweig, 2004; Zhou et al., 2003).

In this chapter, we attempt to identify MIH-binding proteins (MIHBPs) by cell-map proteomics using immunoprecipitation and mass spectrometry. Since blue crab MIH antibody (Lee and Watson, 2002) cross-reacts with land crab MIH, the experiments were done with this antibody.

Materials and Methods

Measurement of hemolymph ecdysteroids

Hemolymph samples (100 µl) were mixed with 300 µl of methanol and centrifuged. Supernatants were then dried under vacuum and assayed for ecdysteroids by radioimmunoassay (Chang and O'Connor, 1979; Yu et al., 2002). Values were reported as picograms of ecdysteroid per microliter of hemolymph.

Immunoprecipitation of MIH and MIHBPs

Total extract of YO, 1° LB and 2° LB were prepared in RIPA (Radioimmunoprecipitation assay) low salt buffer (50 mM Tris-HCl, pH 7.4, 1% NP-40, 0.25% Na-deoxycholate, 150 mM NaCl, 1 mM ethylenediaminetetraacetic acid (EDTA), 1 mM phenylmethylsulphonyl fluoride (PMSF), 1 µg/ml each of aprotinin, leupeptin and pepstatin, 1 mM Na_3VO_4, 1 mM NaF). Briefly, 20 Y-organs were ground in 2 ml RIPA buffer with tissue homogenizer, followed by centrifugation (8,000g, 10 min). The supernatant was recovered and protein concentration was determined by Bradford reagent (Bio-Rad). Total extract (3 mg) was precleared using 10 µl Protein A-Sepharose 4B fast flow (Sigma). The supernatant after preclearing step was recovered and subjected to immunoprecipitation. Blue crab MIH antiserum, against peptide #2 (amino acids #5-18 of the *Callinectes sapidus* MIH sequence), was kindly provided by R. Douglas Watson (University of Alabama at Birmingham). The antiserum (20 µl) was added to the supernatant and incubated for 6 hrs to overnight at 4°C. Protein A-Sepharose 4B fast flow (20 µl) was added and incubated for 3 hrs at 4°C. The beads were collected by a brief

centrifugation and washed 4 times with ice-cold RIPA buffer. Sample lysis buffer {7 M urea, 2 M thiourea, 4% 3-[(3-Cholamidopropyl)dimethylammonio]-1-propanesulfonate (CHAPS), 66 mM dithiothreitol, 1x protease inhibitor cocktail [2 mM 4-(2-Aminoethyl-benzensulfonyl fluoride hydrochloride (AEBSF), 1 mM EDTA, 130 μM bestatin, 14 μM E-64, 1 μM leupeptin, and 0.3 μM aprotinin], and 1 mM benzamidine-HCl} was directly added to the resin and incubated 2 hrs at room temperature. The supernatant was directly used for gel electrophoresis.

Two-dimensional gel electrophoresis

To separate the immunoprecipitated (IP) samples, immobilized pH-gradient (IPG) strips were used for the first-dimensional separation (Bjellqvist et al., 1982; Gorg et al., 1988). Immobiline^{TM} DryStrip was commercially purchased (Amersham Biosciences), and IPGphor system (Amersham Biosciences) was used. IP samples were applied on 7 cm IPG dry strips (3-10NL) by an in-gel rehydration method (Rabilloud et al., 1994; Sanchez et al., 1997). The electrophoretic conditions during isoelectrofocusing (IEF) were as follows: 1 h at 500 V, 1 h at 1,000 V, and to total 17 kVh at 5,000 V at 20°C. After IEF, the strips were equilibrated in equilibration buffer (30% glycerol, 6 M urea, 2% SDS, 0.05 M Tris-base, pH 6.8) containing 10 mg/ml dithiothreitol (DTT) for 15 min and additional 15 min in equilibration buffer containing 42.5 mg/ml iodoacetamide (IAA) instead of DTT. The strips were then sealed onto the 12% mini slab gels with 0.5% agarose in Laemmli electrophoresis buffer (50 mM Tris, 384 mM glycine, 0.1% SDS). The second-dimensional separation was performed in Laemmli electrophoresis buffer at 150 V at room temperature.

Western blot analysis

Hybond-P PVDF membrane (Amersham Biosciences) was washed in methanol for 5 min followed by rinsing in transfer buffer (50 mM Tris, 384 mM glycine, 20% methanol). 2-D gels were blotted at 100 V for 1 hr. After overnight incubation at 4°C in blocking buffer [20 mM Tris-HCl, pH 7.5, 140 mM NaCl, 0.05% Tween-20, 3% bovine serum albumin (BSA)], the membrane was probed with blue crab MIH anti serum (1:5,000, v/v in blocking buffer) and incubated for 2 hrs at room temperature. After washing in Tween-Tris Buffered Saline (TTBS: 20 mM Tris-HCl, pH 7.5, 140 mM NaCl, 0.05% Tween-20) 3 x 10 min each, the membrane was incubated for 1 hr with alkaline phosphatase-conjugated secondary antibody (Sigma, 1:10,000, v/v in blocking buffer), and then washed in TTBS 3 x 10 min each. Finally the blot was developed with 5-bromo-4-chloro-3-indolyl phosphate (BCIP) and p-nitro blue tetrazolium (NBT).

Silver staining

After fixation in 40% ethanol and 10% acetic acid for 1 hr and rehydration in 5% ethanol and 5% acetic acid for 2 hrs, sensitization of the gel was performed using 0.05% (w/v) 2,7-naphtalenedisulfonic acid (NDS) for 30 min followed by three 5 min washes in double-distilled water. The gels were then stained in a freshly made ammoniacal silver nitrate solution for 30 min. To prepare 100 ml of this solution, 0.4 g of silver nitrate was dissolved in 4 ml of deionized water, which was slowly mixed into a solution containing 16 ml of water, 700 µl of concentrated ammonia (25%) and 100 µl of sodium hydroxide (10 N). After staining, the gels were washed 3 times in deionized water for 5 min. The

images were developed in a solution containing citric acid (0.05% w/v) and formaldehyde (0.05% v/v) for 5 to 10 min.

In-gel trypsin digestion

Protein spots were excised from silver-stained 2-D gels and the gel plugs were silver-oxidized. Removal of silver ions prior to tryptic digestion was carried out as described (Gharahdaghi et al., 1999). Briefly, gel plugs were subjected to a 1:1 solution of potassium ferricyanide (30 mM) and sodium thiosulfate (100 mM) and incubated until the dark color disappears. The spots were then washed 3 times with distilled deionized water to stop the oxidation reaction. After discarding the water, the spots were then saturated with 100 mM ammonium bicarbonate, pH 7.8 for about 30 min. The gel plugs were then transferred to acetonitrile, and dried in a speed vac. Proteins were digested overnight with 25 ng of modified sequencing-grade trypsin (Promega) in 50 mM ammonium bicarbonate, pH 7.8 at 37°C. The reaction was stopped by adding 0.5% trifluoroacetic acid and was kept on ice.

Mass spectrometry

MS/MS analyses were performed with an Agilent 1100 series LC/MSD XCT+ ion trap and with the Agilent LC/MSD TOF (Agilent Technologies, Santa Clara, CA), which was equipped with a dual sprayer source for the simultaneous but separate infusion of the reference mass solution with LC eluent. The LC system used was an Agilent 1100 series capillary LC system (Agilent Technologies, Waldbronn, Germany) consisting of a capillary pump with a micro vacuum degasser, a temperature controlled micro well-plate

autosampler and a column compartment. The column used was a Zorbax SB Aq, 0.3 mm x 150 mm, 3.5 μm. The software used for instrument control was Agilent ChemStation A10.02 (Agilent Technologies, Wilmington, DE), ion trap software 5.2, and TOF software A01. Data analysis was performed using ion trap data analysis software LCMSD Trap. The Agilent 1100 capillary pump was operated under the following conditions (Solvent A: water, 10 mM ammonium formate, pH 4.1; Solvent B: ACN. Column flow: 8 μl/min, primary flow: 500–800 μl/min. Gradient: 0 min 0% B, 1 min 0% B, 13 min 25% B, 23 min 25% B. Stop time: 23 min. Post time: 15 min). The Agilent 1100 autosampler was used to make injections of 1 μl and the samples were maintained at 4°C. The sample loop was switched to bypass after 1 min to reduce delay volume. The mass spectrometers were operated under the following conditions (Source: ESI in positive mode; drying gas: 5.0 L/min; gas temperature: 300 °C; nebulizer: 15 psi; ion current control: 150,000; maximum accumulation time: 50 ms; scan: 200–600). For the acquisition of MS/MS and MS^3 the automated data dependent acquisition functionality was used.

Results

ES ablation and ecdysteroid

Eyestalks are the main endocrine system to produce MIH in crustaceans, and eyestalk ablation (ESA) caused significant increases in hemolymph ecdysteroid of land crabs (Fig. 2-1). The corresponding 20 YOs were dissected and combined for sample preparation from each group of the day post ES ablation.

Immunoprecipitation of MIHBPs

MIH peptide in each YO was immunoprecipitated and the enriched peptides were detected in a western blot analysis using blue crab MIH antibody (Fig. 2-2). The MIH signal was specifically shown in IP lanes, whereas it was not present in preclearing and post-IP lanes. This step was absolutely necessary because any non-specific interactions must be identified to confirm the specific interaction between MIH and beads.

The immunoprecipitated samples were separated in 2-D gels and analyzed by western blots by probing anti MIH antibody (Fig. 2-3). MIH was present in ES ganglia and YOs, locating around pI 4.0 and 10 kDa. The amount of MIH decreased in day 1 post ES ablation, but recovered in day 3. The same samples were run again in 2-D gels and silver-stained (Fig. 2-4). More interestingly, two major spots were identified only in YO-intact (in red-dot circle, right upper gel), but not in other YOs. The immuno heavy and light chains were dominantly shown, that were carried over during immunoprecipitations. These two protein spots, which probably represent MIH binding proteins showed a range of pI 7.5-8.0 and 25-37 kDa.

Fig. 2-1. Effect of eyestalk ablation on hemolymph ecdysteroid level. The hemolymph ecdysteroid concentrations of land crab were measured by RIA (radioimmuno assay) in intact (0 Day), 1 day post ES-ablated, and 3 days post ES-ablated animals.

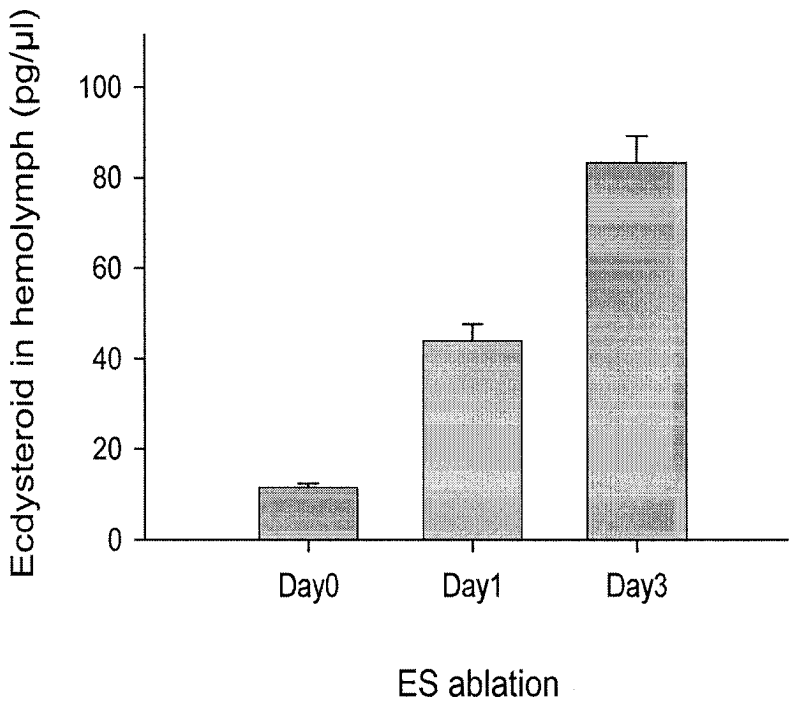

Fig. 2-2. Identification of MIH in the Y-organs by immunoprecipitation. Two sets of samples were analyzed. Preclearing was done by adding protein A-Sepharose to the extracts to remove proteins binding to the bead complex non-specifically. IP was done by adding both MIH antibody and protein A-Sepharose to the precleared supernatant. After IP, post-preclearing was carried out by adding protein A-sepharose to the supernatant from IP, followed by post-IP using protein A-Sepharose and MIH antibody. If the interaction between MIH and its antibody is specific, there should be no MIH signal in post-IP. The samples were resolved on a 16% gel. The gel was then blotted to a PVDF membrane, and western blot analysis was done to show MIH-immunoreactive signals using the blue crab MIH antibody (1:5,000), followed by alkaline phosphatase-conjugated anti-rabbit IgG. The color development was done by BCIP/NBT detection system. Duplicate samples for each step were loaded on the gel.

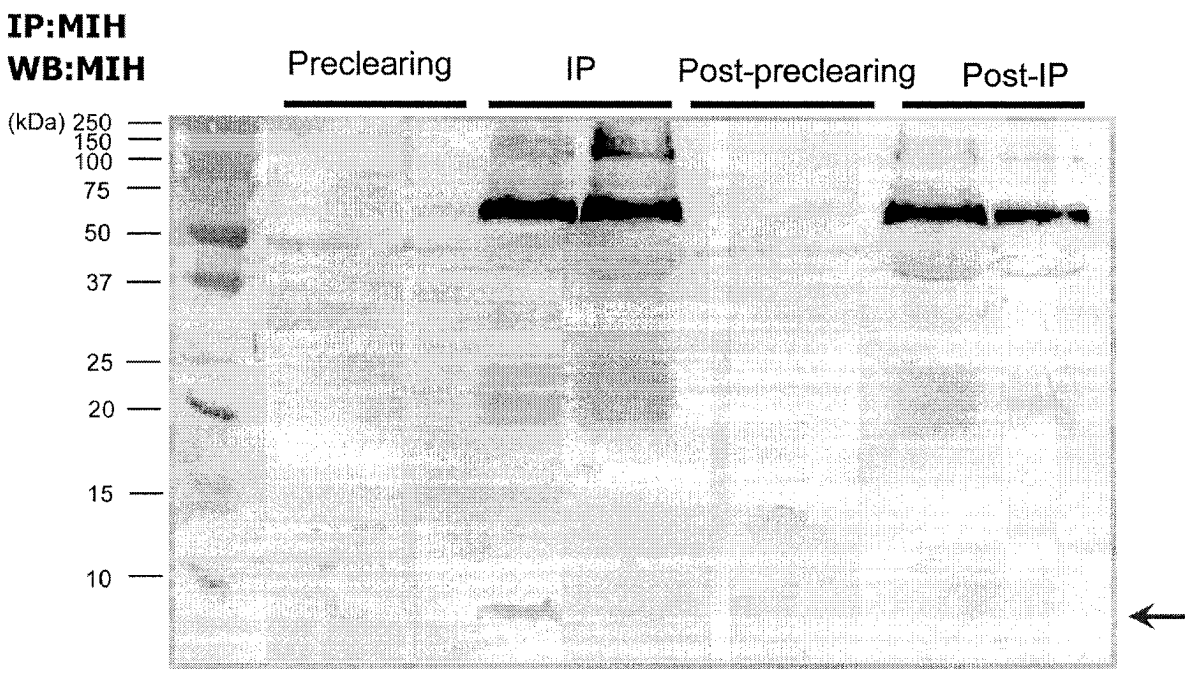

Fig. 2-3. 2-D blots of immunoprecipitation for MIH in eyestalk ganglia and the Y-organs. The immunoprecipitated samples were isoelectrofocused on Drystrips (3-10NL, 7 cm, Amersham Biosciences) for total 19 kVh using IPGphor (Amersham Biosciences). The focused strips were loaded on 15% slab gels, and resolved. The gels were then transferred to PVDF membrane for western blot analysis by MIH antibody with 1:5,000 dilution of primary antiserum and 1:10,000 dilution of secondary antibody. The membranes were developed by ABC-alkaline phosphatase-conjugate kit (Vectastatin). The MIH is indicated by red circles on the lower left side. The MIH was present in all the membranes and the signal was lower in 1 day post ES ablated YO, followed by recovery after 3 days post ES ablation.

IP:MIH

WB:MIH

ES Ganglia

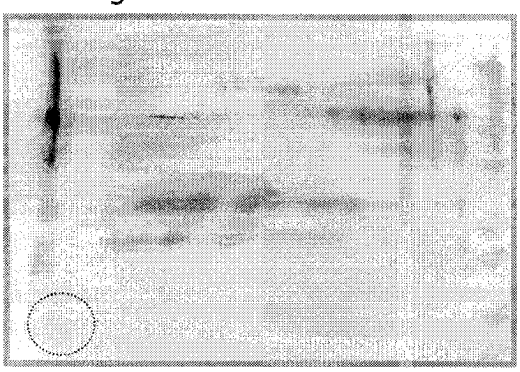

YO-intact

YO-day1 ES ablation

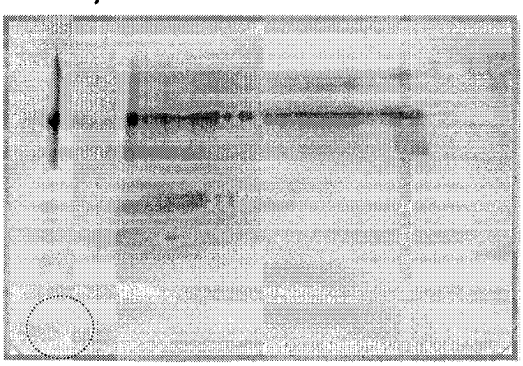

YO-day3 ES ablation

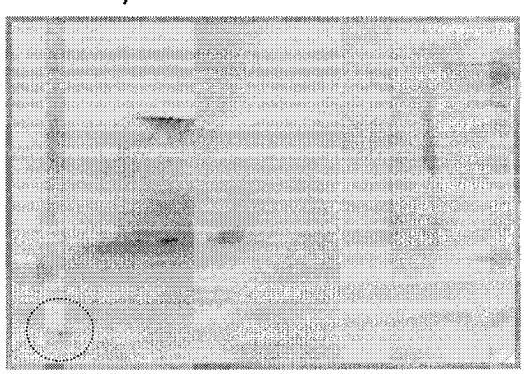

Fig. 2-4. 2-DE analysis of immunoprecipitation for MIH in eyestalk ganglia and the Y-organs. The immunoprecipitated samples were isoelectrofocused on Drystrips (3-10NL, 7 cm, Amersham Biosciences) for total 19 kVh using IPGphor (Amersham Biosciences). The focused strips were loaded on 15% slab gels, and resolved. The gels were then subjected to silver staining. The binding proteins to MIH were present only in intact YO (upper right, in circle).

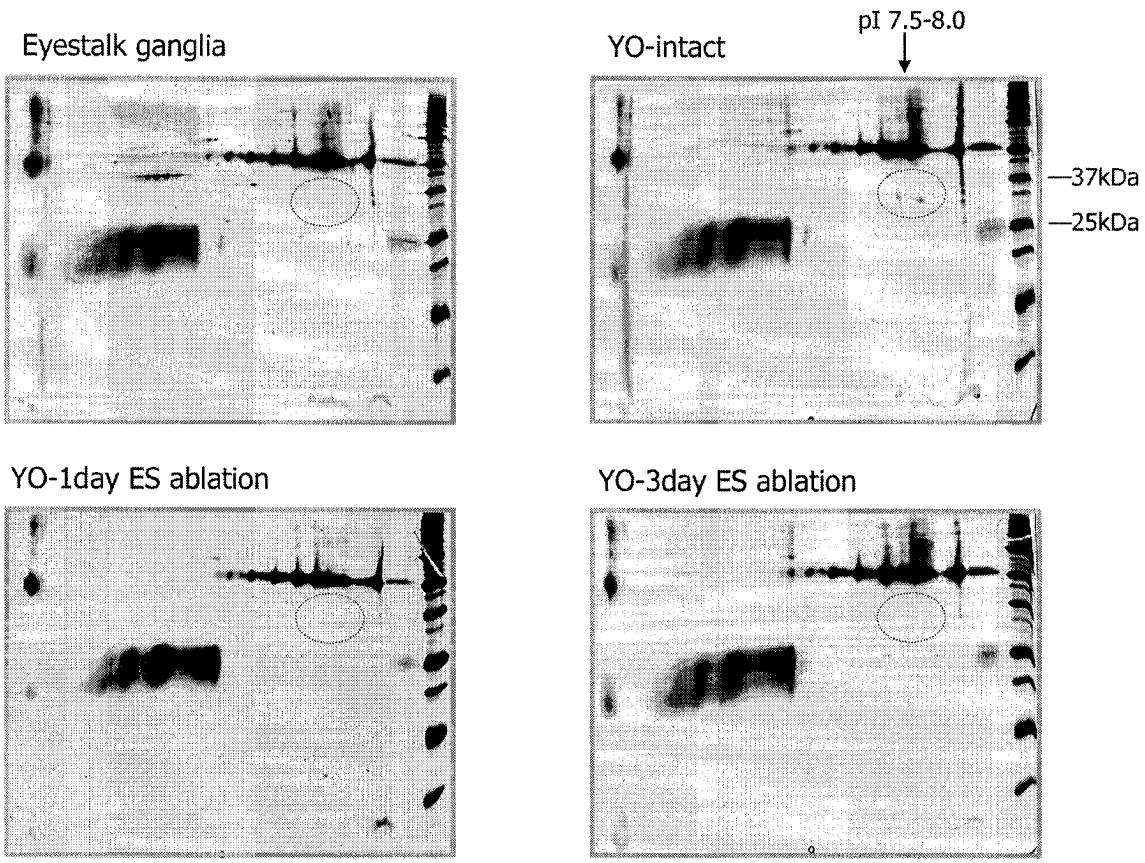

Since 2° LB contains MIH-like factor (LAF_{pro}), which suspends land crab molting by causing decrease of hemolymph ecdysteroid secretion (Yu et al., 1999; Yu et al., 2001; Yu et al., 2002; Yu and Mykles, 1997; Yu and Mykles, 1998), 1° and 2° LBs were used to confirm the presence of MIH-interacting proteins. As a result, similar protein spots to those found in intact YO (Fig. 2-4) were detected in 2° LB but not in 1° LB's (Fig. 2-5, upper panel). The western blots were shown and the MIH immuno-reactive signal was present only in 2° LB blot (Fig. 2-5, lower panel).

Internal peptide sequencing by tandem MS/MS

The spots shown in both intact YO and 2° LB were excised from the gels and analyzed for peptide sequencing after in-gel trypsin digestion. Tandem MS/MS was used for internal peptide sequencing (see Materials and Methods). Mass spectrometry results are shown as well as partial peptide sequences determined by mass difference between peaks (Appendix V, A - R). The partial peptide sequences are arranged in Table 2-1. The mother ions were selected for fragmentation to generate daughter ions for this peptide fragment sequencing. As a result, the same peptides [GGGVA(L/I), (L/I)(L/I)TEG, GGMG(L/I)(L/I)D] were obtained from YO and 2° LB (Table 2-1), indicating that these peptides were obtained from the same protein.

Cloning of the MIHBP(s) failed by using deduced primer set (Table 2-2). These primers amplified some distinct PCR products, but contained too many stop codons.

Fig. 2-5. 2-DE analysis of immunoprecipitation for MIH in limb buds. Secondary limb buds (2° LB) of land crab, *Gecarcinus lateralis* inhibit molting, indicating that they contain MIH or an MIH-like peptide (LAFpro). Both 1° LB (A) and 2° LB (B) from the same crab were used for immunoprecipitation. The immunoprecipitated samples were resolved by 2-DE system using 7 cm drystrip (3-10NL) and 8-16% gel, and analyzed by western blot using MIH antibody. MIH-like peptide binding proteins were present in 2° LB (B, red circle), in which the MIH-immunoreactive signal is present (B, red arrow). Neither MIPBPs nor MIH-immunoreactive signal was detected in 1° LB.

1°-LB(#156) IP:MIH-silver stain

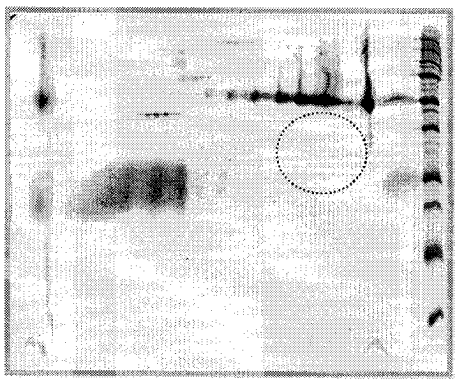

2°-LB(#166) IP:MIH-silver stain

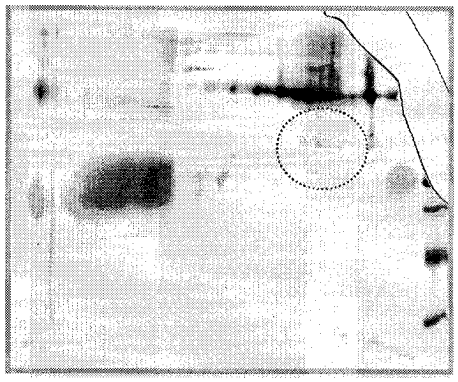

1°-LB(#156) IP&western:MIH

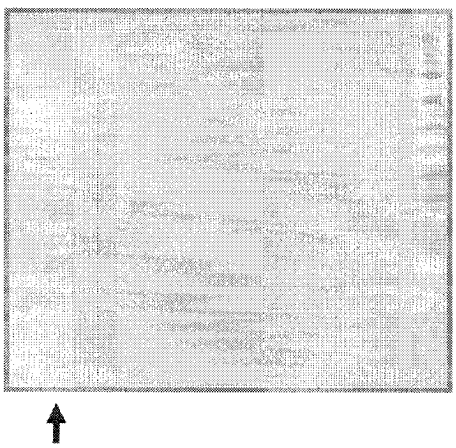

2°-LB(#166) IP&western:MIH

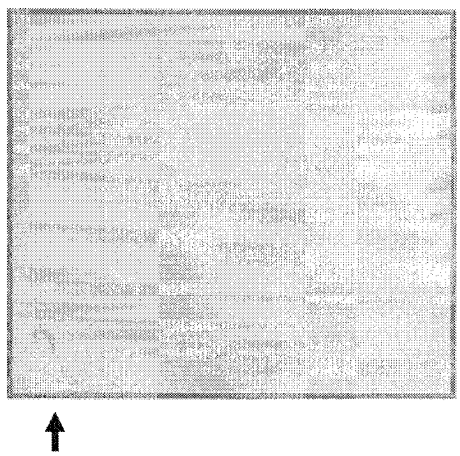

Table 2-1. Internal peptide sequences of MIHBPs. The internal peptide sequences from tandem MS/MS spectrometry analysis were arranged in a table. Molecular weight (Mw) and p*I* are shown for each binding protein, followed by mother ions, daughter ions shown in m/z (mass in dalton/charge). The peptide fragment sequences are shown in the right side of the table.

MIHBPs	MW	pI	Mother ions (m/z)	Daughter ions (m/z)	Sequence (ms/ms)
2'-LB high	35	7.6	746.5	610.5, 539.5, 392.5, 278.3	HAFN
			785.1	742.6, 685.6, 628.6, 571.7, 472.5, 401.5, 288.3	GGGVA(L/I)
			802	773.6, 660.5, 547.5, 446.4, 317.4, 260.3	(L/I)(L/I)TEG
			990.7	933.0, 874.6, 743.6, 686.6, 573.5, 460.4, 345.3	GGMG(L/I)(L/I)D
YO Low	32	8	785.2	742.5, 685.5, 628.5, 571.7, 472.5, 401.3, 288.2	GGGVA(L/I)
			801.2	744.2, 615.4, 544.3, 473.3, 360.3, 232.1	GEAA(L/I)K
			802.2	773.6, 660.5, 547.4, 446.4, 317.3	(L/I)(L/I)TE
			892	794.4, 722.1, 573.4, 472.4, 357.3	PAFTD
			927	822.2, 706.4, 649.3, 518.4, 389.3	DGME
			951.9	947.7, 882.5, 753.4, 696.3, 565.4, 437.3, 290.2	EGMKF
			965.5	955.9, 885.4, 799.4, 728.4, 600.3, 487.2, 372.2, 301.2	ASAK(L/I)DA
			990.1	933.3, 874.5, 743.5, 686.4, 573.4, 460.3, 345.3	GGMG(L/I)(L/I)D
YO high	35	7.6	524	472.3, 401.3, 288.2, 175	A(L/I)(L/I)
			785	742.5, 685.5, 628.5, 571.5, 472.4, 401.4, 288.3	GGGVA(L/I)
			802	773.6, 660.5, 547.4, 446.3, 317.3	(L/I)(L/I)TE
			891.4	808.8, 672.6, 573.3, 472.4, 357.4	HVTD
			909.5	854.8, 719.5, 620.5, 521.4, 407.3, 306.2	HVVNT
			1003.8	983.0, 882.4, 753.4, 696.5, 565.4, 437.3, 290.1	TEGMKF

Table 2-2. Degenerate primers for MIHBP cloning. Three peptides [GEAA(L/I)K, ASAK(L/I)DA, and TEGMKF] were selected for degenerate primers. These primers were used according to the strategy shown in Fig. 2-7.

Primers	Degenerate sequences	Descriptions
MIHBP F12	GGN GAR GCY GCY HTS AAR	Forward of GEAA(L/I)K
MIHBP R12	YTT SAD RGC RGC YTC NCC	Reverse of GEAA(L/I)K
MIHBP F13	GCY WSY GCY AAR HTS GAY GCN	Forward of ASAK(L/I)DA
MIHBP R13	NGC RTC SAD YTT RGC VCT RGC	Reverse of ASAK(L/I)DA
MIHBP F14	GC ACN GAR GGN ATG AAR TTY	Forward of TEGMKF
MIHBP R14	GC RAA YTT CAT NCC YTC NGT	Reverse of TEGMKF

Discussion

To identify MIH receptor or the binding proteins, the presence of MIH itself should be detectable first. However, the amount of MIH in crustaceans is very low, so it has not been possible to detect MIH in tissue extracts by Western blots without enrichment. Therefore, immunoprecipitation using MIH antibody was applied to enrich the low MIH amount from the molting glands (Fig. 2-6).

The XO/SG complex is necessary for the production and secretion of MIH, as well as other neuropeptides, including crustacean hyperglycemic hormone (CHH), gonad-inhibiting hormone (GIH), and mandibular organ-inhibiting hormone (MOIH) (Borst et al., 2002; Chung et al., 1999; Cooper and Ruffner, 1998; Cromarty and Kass-Simon, 1998; De Kleijn and Van Herp, 1995; Dircksen et al., 2001). The land crab MIH should decrease after ES ablation. The MIH immuno-reactive signal was decreased at 1 day post-ES ablation, but obviously recovered at 3 days post-ES ablation. Overall MIH signal was not definitely decreased after ES ablation (Fig. 2-3). Since the circulating peptide hormone is known to be degraded readily (Chung and Webster, 2005), this result implies that there may be alternative source for MIH synthesis or possibly the inhibitory action of MIH in ecdysteroidogenesis is triggered not exclusively by MIH (Yu et al., 1999; Yu et al., 2001; Yu et al., 2002; Yu and Mykles, 1997; Yu and Mykles, 1998). Also, there are some reports showing another sources of ES neuropeptides; for example, CHH synthesis was found other than the eyestalk, such as the pericardial organs and the gut (Chang et al., 1999; Chung et al., 1999; Dircksen and Soyez, 1998).

Fig. 2-6. Schematic flow of the experiment on MIHBP identification.

Immunoprecipitation (IP) was used to enrich the low amounts of MIH in the Y-organ. A blue crab MIH mouse polyclonal antibody was applied for the IP. Post IP was carried out to confirm if the IP was specific. The IP samples were then analyzed by western blots and gel staining. Finally, the MIHBP(s) was/were analyzed by tandem MS/MS spectrometry.

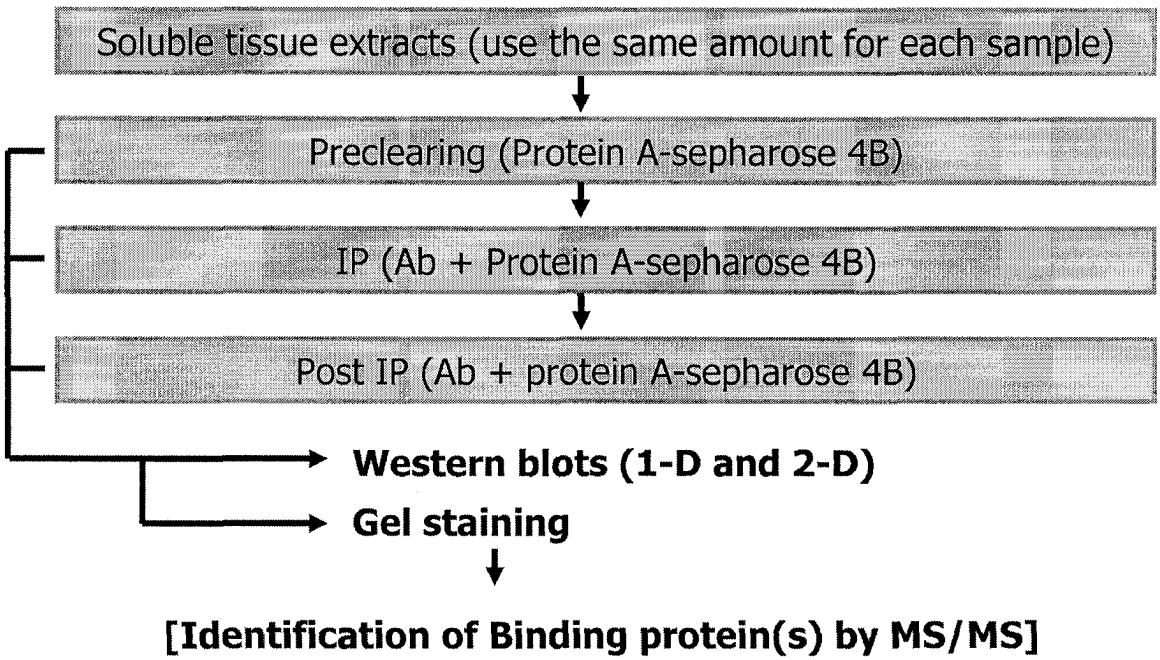

Whether or not the MIH is recovered after ES ablation the result conflicts with the ecdysteroid data after ES ablations (Fig. 2-1). The ecdysteroid titers increased following ES ablation even at 3 days post-ES ablation, where the MIH signal is present (Fig. 2-1, 2-3). Therefore, these results imply that additional factor(s) would be involved in regulating MIH action.

We hypothesized that if there are any binding proteins to MIH, the proteins should interact and be pulled down with MIH peptide from immunoprecipitation. The MIH-immunoprecipitated samples were subjected to 2-D gel electrophoresis, and then silver-stained (Fig. 2-4). As a result, putative MIHBPs (MIH-binding proteins) were observed only in intact YO, suggesting that MIHBPs could be critical regulators for ecdysteroidogenesis in crustaceans. These data are very interesting because of an example of a well known similar regulation in IGF signaling, in which IGF binding proteins regulate IGF binding to their receptors (Awede et al., 1999; Awede et al., 2002; Bayol et al., 2004; Crown et al., 2002; Lang et al., 1996; Oddy and Owens, 1996; Pampusch et al., 2003; Svanberg et al., 2000; White et al., 2003). The discovery of MIH binding proteins is promising since it has been suggested that molt control is not regulated simply by release of MIH, for there is a massive and unprecedented release of MIH during late premolt (Chung and Webster, 2005). Thus, there has been a critical missing link between secreted MIH in hemolymph and the binding to receptor on the YO or MIH activation. In a recent study, it was shown that ES ablation induced a large increase in Gl-GC-Iβ and Gl-GC-III mRNAs in YOs, suggesting that NOS/GC signaling plays a major role in modulating ecdysteroidogenesis in crustacean molting gland (Lee et

al., 2005; Lee et al., 2006). Thus, MIH may stimulate soluble guanylyl cyclase (GC-I) by activating NOS (Kim et al., 2004; Lee and Mykles, 2006).

These MIHBPs remain to be identified, but also raise some additional questions: What is their source? What mechanism induces the MIHBP expression? Are MIHBPs down-regulated by ecdysteroid? How do the MIHBPs interact with MIH? The first step to investigate MIHBPs is to obtain their gene sequences. We propose a schematic diagram for the cloning by nested PCR using three different peptide fragments (Fig. 2-7). Degenerate PCR primers can be designed based on the peptide sequences. Our data suggest that the currently accepted molting control model should be reconsidered. The determination of MIHBP sequences would provide insight into crustacean molting regulation mechanisms.

Fig. 2-7. Schematic diagram for MIHBP cloning strategy. Three fragments of tandem peptide sequence were aligned in different combinations for nested PCR. Blue arrows represent first round PCR and red arrows show second round nested PCR to clone partial fragment of MIHBP gene.

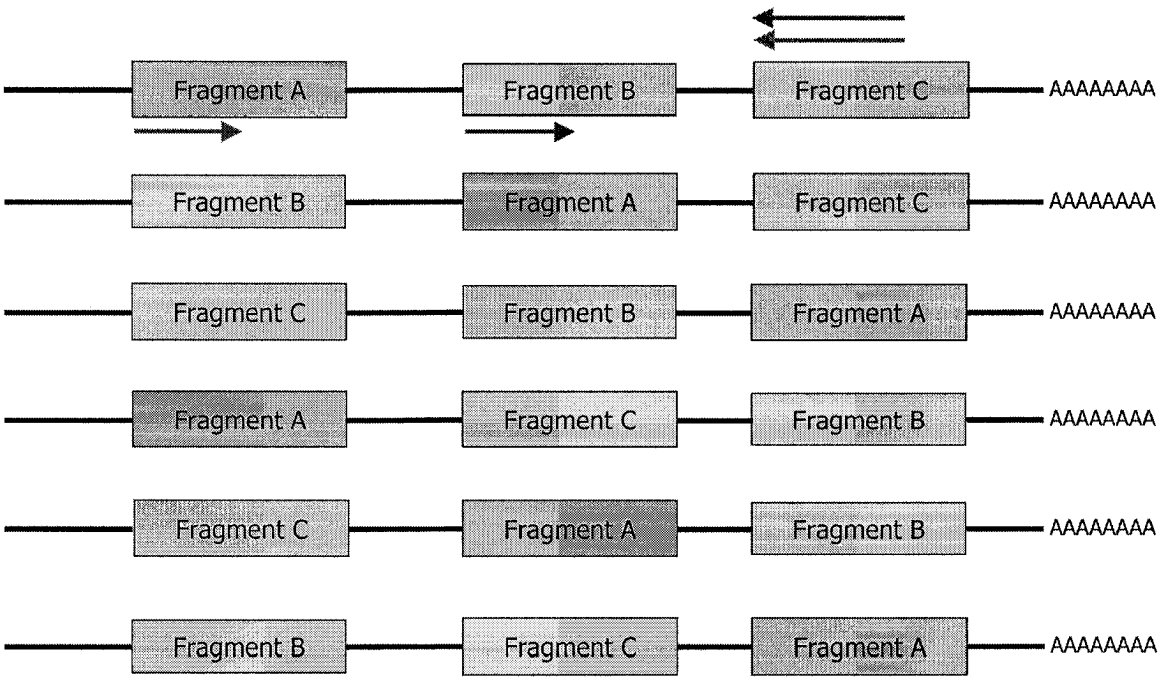

CHAPTER THREE*

THREE GUANYLYL CYCLASES IN TROPICAL LAND CRAB, *GECARCINUS LATERALIS*: CLONING AND TISSUE EXPRESSION IN RESPONSE TO ELEVATED ECDYSTEROID

Abstract

Two eyestalk (ES) neuropeptides, molt-inhibiting hormone (MIH) and crustacean hyperglycemic hormone (CHH), increase intracellular cGMP levels in target tissues. MIH inhibits ecdysteroid secretion by the crustacean molting gland or Y-organ (YO). A nitric oxide synthase is expressed in the YO, suggesting that a NO-sensitive guanylyl cyclase (GC) is a component of the MIH signaling pathway. CHH binds to a membrane receptor GC. cDNAs encoding three GCs, which catalyze the production cGMP from GTP, were cloned from the blackback land crab, *Gecarcinus lateralis*: the β subunit of a NO-sensitive GC (Gl-GC-Iβ; 2,380 bp; 603 amino acids; 68,435 kDa), a membrane receptor GC (Gl-GC-II; 4,609 bp; 1,349 amino acids; 150,999 kDa), and a NO-insensitive GC (Gl-GC-III; 785 bp; >219 amino acids; >25,022 kDa). Two Gl-GC-Iβ isoforms differing in the absence (Δ32N) or presence (Δ0N) of a 32-amino acid sequence at the N-terminus and Gl-GC-III were expressed at higher mRNA levels in ES ganglia, gill, hepatopancreas, ovary, and testis and at lower levels in YO, heart, and skeletal muscle. Three Gl-GC-II isoforms varied in length within the N-terminal ligand-binding domain (+18, +9, and +0

amino acid insertions). Gl-GC-II(+18) was expressed highly in striated muscle (skeletal and cardiac muscles); Gl-GC-II(+9) was expressed in all tissues examined (ES ganglia, YO, gill, hepatopancreas, striated muscles, and gonads), which is consistent with its role as a CHH receptor. Gl-GC-II(+0) was expressed in most tissues and was the dominant isoform in ES ganglia. ES ablation, which increased hemolymph ecdysteroid, had no significant effect on GC expression in most tissues, although Gl-GC-II(+18) mRNA level was positively correlated with ecdysteroid concentration in claw muscle. ES ablation also increased Gl-GC-Iβ and Gl-GC-III mRNA levels in the YO. A single injection of 20-hydroxyecdysone into intact animals transiently lowered Gl-GC-Iβ in hepatopancreas, testis, and skeletal muscle and certain Gl-GC-II isoforms in some of the tissues. These data suggest that GC signaling plays a major role in modulating gene expression by ecdysteroids in crustacean tissues.

---

*This chapter has been submitted to *Journal of Experimental Biology* as follow:

Three guanylyl cyclases in the tropical land crab, *Gecarcinus lateralis*: cloning and tissue expression in response to elevated ecdysteroid

Sung Gu Lee[1], Hyun-Woo Kim[2], Brandon D. Bader[1], Ernest S. Chang[3], and Donald L. Mykles[1,*]

[1]Department of Biology, Colorado State University, Fort Collins, CO 80523, USA; [2]Department of Marine Biology, Pukyong National University, Busan, South Korea; and [3]Bodega Marine Lab, University of California, Bodega Bay, CA 94923, USA

Introduction

Guanylyl cyclases (GCs) catalyze the production of the second messenger 3',5'-cyclic guanosine monophosphate (cGMP) in response to various signals, such as nitric oxide (NO), peptide ligands, and fluxes in intracellular Ca^{2+}. Intracellular cGMP regulates cellular physiology by activating protein kinases, directly gating specific ion channels, or altering intracellular cyclic nucleotide concentrations through phosphodiesterase regulation (Lucas et al., 2000; Padayatti et al., 2004; Potter, 2005; Pyriochou and Papapetropoulos, 2005). GCs can be organized into four classes. GC-I and GC-II classes occur widely, while the GC-III and GC-IV classes occur in insects (Morton, 2004). GC-I is a NO-sensitive soluble GC that forms a heterodimer of α and β subunits (Buechler et al., 1991; Harteneck et al., 1991). GC-II is a homodimeric membrane receptor GC that is either activated by extracellular ligands or intracellular GC-activating proteins (Padayatti et al., 2004). Members of the GC-III and GC-IV classes were first described in the hawk moth, *Manduca sexta*, and were designated Ms-GC-I and Ms-GC-β3, respectively (Nighorn et al., 1999; Simpson et al., 1999). Ms-GC-I is a NO-insensitive soluble GC that is most similar to GC-II (Simpson et al., 1999). Ms-GC-β3 is also a NO-insensitive soluble GC that is most similar to GC-Iβ, although it has a unique 315-amino acid extension at the C-terminus and homodimerizes to form the native protein (Morton, 2004; Nighorn et al., 1999). Ms-GC-β3 mediates the action of eclosion hormone, which coordinates the stereotypic behavior in pupal ecdysis (Morton and Simpson, 2002).

In crustaceans NO-sensitive GC (GC-I) and membrane receptor GC (GC-II) are implicated in the signaling pathways for two neuropeptide hormones, molt-inhibiting hormone (MIH) and crustacean hyperglycemic hormone (CHH), respectively. Both hormones are produced and released from the X-organ/sinus gland complex in the ES ganglia (Skinner, 1985). MIH inhibits ecdysteroid synthesis and secretion in the molting glands, or Y-organs (YOs), which are a pair of epithelioid glands located in the anterior cephalothorax (Lachaise et al., 1993; Skinner, 1985). MIH induces a large increase in cGMP in the YOs (Chung and Webster, 2003; Saidi et al., 1994; Sedlmeier and Fenrich, 1993). A NO synthase (NOS) is phosphorylated in activated YOs, which suggests that a NO-sensitive GC mediates the MIH-induced increase in cGMP (Kim et al., 2004; Lee and Mykles, 2006). CHH binds to a GC-II membrane receptor, which increases cGMP levels in various lobster tissues (Chung and Webster, 2003; Goy, 1990; Goy et al., 1987; Pavloff and Goy, 1990; Sedlmeier and Keller, 1981). cDNAs encoding receptor GCs have been cloned from crayfish (Liu et al., 2004) and blue crab (Zheng et al., 2006).

Crustacean tissues express several different GCs, but only cDNAs encoding membrane receptor GCs have been cloned (Liu et al., 2004; Zheng et al., 2006). Membrane and cytosolic GCs occur in lobster skeletal muscle (Goy, 1990) and a membrane GC occurs in crayfish hepatopancreas (Riediger et al., 1989). Crustacean tissues also express a NO-sensitive GC (GC-I), as NO stimulates GC activity in neurons and muscle and NO synthase (NOS) is expressed in various tissues (Aonuma, 2002; Goy, 2005; Kim et al., 2004; Prabhakar et al., 1997; Scholz et al., 1998; Scholz et al., 2001; Scholz et al., 1996; Scholz et al., 2002; Schuppe et al., 2001). In addition, a cytoplasmic NO-insensitive GC activity has been reported in lobster ventral nerve cord (Prabhakar et

al., 1997). In order to better understand the diversity and functions of crustacean GCs, cDNAs encoding three GCs were cloned: the catalytic β unit of a NO-sensitive soluble GC, which occurs in two alternatively spliced isoforms; a NO-insensitive membrane receptor GC, which occurs in three alternatively spliced isoforms; and a NO-insensitive soluble form. The tissue distribution and effects of ES ablation and ecdysteroid injection on GC mRNA levels were determined.

Materials and Methods

Animals

Blackback land crabs (*Gecarcinus lateralis*) were collected from Puerto Rico or the Dominican Republic. They were kept in covered plastic cages with aspen bedding moistened with tap water at 27 °C and 50% humidity and were fed raisins, carrots, and lettuce twice a week. A 12 h dark/12 light cycle was used. Two methods were used to increase hemolymph ecdysteroid levels *in vivo*: ES ablation (ESA) and injection of intact animals with 20-hydroxyecdysone (20E). ESA removes the primary source of MIH, thus stimulating YO ecdysteroidogenesis (Skinner, 1985); wounds were cauterized with a heated spatula. A 20E (Sigma-Aldrich) stock solution (10 mg/ml) in 10% ethanol was injected into the hemolymph through the arthrodial membrane at the base of a walking leg at 0.41 μg 20E per g body weight. Control animals received the same volume of 10% ethanol.

Cloning of guanylyl cyclases

Partial guanylyl cyclase cDNAs were initially obtained by nested RT-PCR using degenerate primers directed to highly conserved sequences in the catalytic domain of a wide variety of GCs in the GenBank database (http://www.ncbi.nlm.nih.gov), including those from *Manduca sexta* (AAC61264) and *Drosophila melanogaster* (AAA87941) for GC-Iβ; *Manduca sexta* (AAN16469) and *Procambarus clarkii* (AAQ74970) for GC-II; and *Manduca sexta* (AAC62238) for GC-III. Conserved sequences were identified by

aligning proteins using the ClustalW program (http://www.ebi.ac.uk/clustalw/index.html). Two sets of nested degenerate primers were designed to anneal to DNA sequences encoding VKVETIGD and MPRYCLF: cGC F1, 5'-GTN TAY AAR GTN GAR AC-3'; cGC R1, 5'-CCR AAN ARR CAR TAN CKN G-3'; cGC F2, 5'-AAR GTN GAR CAN RTN GGN G-3'; cGC R2, 5'-AAN ARR CAR TAN CKN GGC A-3'. To obtain more of the 5' sequence in the GC-Iβ open reading frame (ORF), a second round of nested PCR was done using two sequence-specific reverse primers (cGC-Iβ R3, 5'-GCG AGG CGA AAC ATT CAT TTC CTT CC-3'; cGC-Iβ R2, CTG TCC GAT CAC TCC CGT CAC CAC TTC-3') and two degenerate forward primers to highly conserved sequences (MYGFVNYAI and VNYAIEQLV) in the N-terminus (cGC-Iβ F90, 5'-ATG TAY GGY TTY GTB AAC YAC GCD YT-3'; cGC-Iβ F91, GTB AAC YAC GCD YTG GAR CTK CTR GT-3'). To obtain more of the 5' sequence in the GC-II ORF, second round of nested PCR was done using two sequence-specific reverse primers (cGC-II R5, 5'-ATG TGC GGA AGT TAC TAC TGA GGC AG-3'; cGC-II R50, 5'-GGA CGG TGG TGG ATA ACG AAC TTG TGT T-3') and four degenerate forward primers to highly conserved sequences (ILVLCLFI, NQMDLTMSN, DLLCRNVSA, and VSAVFGPE) in the ligand-binding domain (cGC-II F90, 5'-ATY YCC GGT GCC YTS ACT WWS GCS ST-3'; cGC-II F91, 5'-ACT WWS GCS STK GAK RAS GTC AAC AA-3'; cGC-II F92, 5'-GAS ATG MTR TGY RAK GGC RTC KCC RC-3'; cGC-II F93, 5'-GCR TCK CCR CYA TYT TYG GSC CRG AA-3'). All primers were synthesized and purified by Integrated DNA Technologies, Inc. (Des Moines, Iowa, USA).

Total RNA was isolated from pooled tissues (Y-organ, ovary, testis, hepatopancreas, and claw muscle) using a Qiagen RNeasy mini kit. cDNA was synthesized according to

the manufacturer's protocol using the Superscript III RNase H- reverse transcriptase first strand synthesis system (Invitrogen, Inc.). Briefly, 12 μl of a mixture containing 1 μl oligo $(dT)_{12-18}$ (500 μg/ml), 1 μg total RNA, and 1 μl 10 mM dNTPs was heated to 65 °C for 5 min and chilled on ice for 1 min. 5X First-Strand Buffer (4 μl), 2 μl 0.1 M DTT, and 1 μl RNaseOUT recombinant ribonuclease inhibitor (40 units/μl) were added. The reaction was initiated by the addition of 1 μl (200 units) of Superscript III reverse transcriptase and incubated at 50 °C for 60 min. The reaction was inactivated at 70 °C for 15 min.

PCR was performed using an ABI 9600 cycler (Perkin-Elmer, Inc.). The reactions contained 2 μl cDNA mixture, 3 μl 10X Takara EX Taq buffer, 2 μl 250 μM dNTPs, 1 μl 10 mM forward degenerate primer, 1 μl 10 mM reverse degenerate primer, 0.2 μl Takara EX HS Taq DNA polymerase (5 units/μl), and 18.8 μl PCR grade deionized water. Initial denaturation (96 °C for 5 min) was followed by 35 amplifying cycles (96 °C for 30 sec, 62 °C for 30 sec, and 72 °C for 3 min) and final extension at 72 °C for 7 min. For the second PCR reaction, 0.01 μl of the first PCR reaction and the nested degenerate primers were used. Other reaction components and PCR conditions were same as those in the first reaction.

The PCR products were separated with agarose (1.5 %) gel electrophoresis and stained with ethidium bromide. The PCR products were purified from the gel slices using the Qiaquick Gel Extraction kit (Qiagen, Inc.), ligated into TA cloning vector with TOPO TA Cloning Kit (Invitrogen, Inc.), and transformed into OneShot TOP 10 *E. coli* strain (Invitrogen, Inc.). Transformants were first selected by blue-white colony selection on LB agar plates containing 100 μg/ml ampicillin (Sigma-Aldrich, Inc.) and subjected to

PCR with T7 and M13-reverse vector primers to verify sizes of inserts. Plasmids were purified using the Qiagen spin mini prep kit and sequenced using T7 and M13-reverse vector primers (Davis Sequencing, Inc., Davis, CA USA).

RACE (Rapid Amplification of cDNA Ends) of mRNA was used to obtain full-length sequences. Poly (A^+) RNA was isolated from total claw muscle RNA using Oligotex mRNA kit (Qiagen). For the 3' sequence, the Invitrogen 3' RACE System was used. Briefly, first-strand cDNA synthesis reactions contained 200 ng poly(A^+) RNA isolated from pooled tissues (Y-organ, ovary, testis, hepatopancreas, and claw muscle), and 1 µl adaptor primer (10 µM, 5'-GGCCACGCGTCGACTAGTACTTTTTTTTTTTTTTTT-3') was incubated at 70 °C for 10 min. After chilling the reaction for 1 min on ice, 2 µl 10X PCR buffer [200 mM Tris-HCl (pH 8.4), 500 mM KCl], 2 µl 25 mM $MgCl_2$, 1 µl 10 mM dNTP mix, and 2 µl 0.1 M DTT were added and the mixture was equilibrated to 42 °C for 5 min. SuperScript™ II RT (1 µl) was added and incubated at 42 °C for 50 min. The reaction was terminated at 70 °C for 15 min, treated with *E. coli* RNase H (2 units), and used for first-round PCR. First-round PCR on the cDNA (20 ng) included a universal amplification primer (5'-CUACUACUACUAGGCCACGCGTCGACTAGTAC-3') and gene-specific forward primer (Table 3-1) under the following conditions: denaturation at 96 °C for 5 min, 35 amplification cycles (96 °C for 30 sec, 62 °C for 30 sec, and 72 °C for 2 min), and extension at 72 °C for 10 min.

Table 3-1. Primers used for 3' and 5' RACE to clone cDNAs encoding land crab guanylyl cyclases.

Name	Sequence	Tm (°C)	Description
cGC-Iβ R97	5'-CGG CCA CGA TGT TGT ACG TGA TCT CA-3'	62.4	GC-Iβ first round 5' RACE RP
cGC-Iβ R98	5'-CAT CCT CGT AGG TGA GTC TGA CGA GG-3'	61.4	GC-Iβ nested 5' RACE RP
cGC-Iβ F1	5'-GTG AGT GGT CTG CCA GAG GCC TGT GAT C-3'	65.5	GC-Iβ first round 3' RACE FP
cGC-Iβ F2	5'-AGT GCA AAT CAC CAT CGG TAT CCA TCG-3'	60.7	GC-Iβ nested 3' RACE FP
cGC-II R94	5'-GTC ATG TTG GAT CGC TCA GCC TCC CAC-3'	64.6	GC-II first round 5' RACE-1 RP
cGC-II R95	5'-TGT GTC CTT TGT GCT CTC CTG GT-3'	60.5	GC-II nested 5' RACE-1 RP
cGC-II R96	5'-ATG GTT CCC TCC ACG AAG CAG GTG TGT TCT-5'	65.9	GC-II first round 5' RACE-2 RP
cGC-II R97	5'-TGA AGG CGC CAG GTA TCT TGA TG-3'	59.2	GC-II nested 5' RACE-2 RP
cGC-II F1	5'-CAA CGG TAG ACA CGC TGG GGA G-3'	61.9	GC-II first round 3' RACE FP
cGC-II F2	5'-CAC ACT GGG CCT GTC ATT GCT GGA G-3'	63.8	GC-II nested 3' RACE FP
cGC-III R50	5'-GAC GCA AGG ACC CGT GTG TAA CCC GAT C-3'	65.8	GC-III first round 5' RACE RP
cGC-III R51	5'-GAT CTC CCG TGT GTG TGT GGT G-3'	60.0	GC-III nested 5' RACE RP

Abbreviations: FP, forward primer; GC, guanylyl cyclase; RP, reverse primer

Nested PCR of each reaction was conducted with gene-specific primers (Table 3-1) and abridged universal amplification primer (5'-GGCCACGCGTCGACTAGTAC-3') using the same conditions as the first-round PCR (total reaction volume 30 μl). PCR products were separated by agarose gel electrophoresis and stained with ethidium bromide.

SMART™ RACE cDNA Amplification Kit (BD Biosciences, Inc.) was used to obtain the 5' sequences. The first-strand cDNA synthesis reaction contained 3 μl poly(A^+) RNA (100 ng) isolated from pooled tissues (Y-organ, ovary, testis, hepatopancreas, and claw muscle), 1 μl 5' CDS primer [10 mM, 5'-(T)25N-IN-3'], and 1 μl SMART II A oligo (10 mM, 5'- AAGCAGTGGTATCAACGCAGAGTACGCGGG-3') was incubated at 68 °C for 2 min. After chilling the reaction for 2 min on ice, 2 μl 5X First-Strand buffer [250 mM Tris-HCl (pH 8.3), 375 mM KCl, and 30 mM $MgC1_2$], 1 μl DTT (20 mM), 1 μl dNTPs (10 mM), and 1 μl Powerscript reverse transcriptase were added. The reaction was incubated in 42 °C heat block for 1.5 h in ABI 9600 cycler (Perkin-Elmer). The first-strand reaction was diluted 10-fold with autoclaved deionized water and used for first-round PCR with 10X Universal Primer A Mix (0.4 mM 5'-CTAATACGACT CACTATAGGGCAAGCAGTGGTATCAACGCAGAGT-3' and 2 mM 5'-CTAATACGACTCACTATAGGGC-3') and gene-specific reverse primers (Table 3-1) under the following conditions: denaturation at 96 °C for 5 min, 35 amplification cycles (96 °C for 30 sec, 64 °C for 20 sec, 72 °C for 3 min) and extension at 72 °C for 10 min. Second-round PCR was conducted using nested gene-specific primers (Table 3-1) and nested universal primer A (10 mM, 5'-AAGCAGTGGTATCAACGCAGAGT-3'). The PCR conditions were the same as those used for first-round PCR. PCR products were separated by agarose gel electrophoresis and stained with ethidium bromide.

Phylogenetic analysis was done by using ClustalW and Treeview software. A paired alignment algorithm (http://www.ebi.ac.uk/emboss/align/) was used to determine the sequence similarity of the catalytic domains.

Tissue expression of land crab guanylyl cyclases

Tissues were dissected from 3-5 crabs and immediately placed in RNA*later* RNA Stabilization Reagent (Qiagen) and stored at –20 °C. Total RNA was isolated using either the RNeasy Mini column according to the manufacturer's instructions (Qiagen) and treated with DNase I to remove contaminating genomic DNA. RNA concentration was determined by UV absorbance at 260/280nm and stored at –80 °C. First strand cDNA was synthesized in a reaction (20 µl) containing ~1 µg total RNA, 50 mM Tris-HCl (pH 8.3), 75 mM KCl, 3 mM $MgCl_2$, 10 mM dithiothreitol, 0.5 mM dNTPs, 40 units of RNaseOUT ribonuclease inhibitor, 200-500 ng oligo$(dT)_{12-18}$ primer, and 200 units Superscript™ III reverse transcriptase (Invitrogen). The reaction was incubated for 60 min at 50 °C, inactivated at 70 °C for 15 min, treated with *E. coli* RNase H (2 units), and stored at –20 °C.

PCR was performed in a Perkin Elmer 9600 cycler using TaKaRa Ex Taq HotStart polymerase (Takara, Inc.). Sequence-specific primers to Gl-GCIβ, GC-II, Gl-III, and Gl-EF2 were synthesized by Integrated DNA Technologies, Inc. (Table 3-2). Reactions (30 µl) contained 1 µl first strand cDNA mixture, 3 µl 10X Takara EX Taq buffer, 2 µl 250 µM dNTPs, 0.2 µl Takara EX Taq DNA polymerase (5 units/µl), and 18.8 µl PCR grade deionized water.

Table 3-2. Primers used for semi-quantitative PCR of land crab GC-Iβ, GC-II, GC-III, and EF2

Name	Sequence	Tm (°C)	Description
cGC-Iβ-F4	5'-ACA CTG TCA ACA TCA CTT CGA GGA CG-3'	62.3	GC-Iβ FP, C-terminal
cGC-Iβ-R3	5'-GCG AGG CGA AAC ATT CAT TTC CTT CC-3'	62.4	GC-Iβ RP, C-terminal
cGC-Iβ-F100	5'-ATG TGT TGT GTT CCT CTG TGA GGA CGC-3'	62.4	GC-Iβ FP, 5'UTR
cGC-Iβ-R100	5'-CGA ACA GTT CCA GAA TGG CGT TGG C-3'	62.5	GC-Iβ RP, N-terminal
cGC-II-F83	5'-CCA CGA CAA TAA CGG AAA CAG ACC ACG G-3'	62.8	GC-II FP
cGC-II-R83	5'-CTT GTC CTT GAT AAG CGT GCC GTT GC-3'	62.2	GC-II RP
cGC-III-F60	5'-AAC GAG TCA GGC AAC ATC CTG GAC AA-3'	62.1	GC-III FP
cGC-III-R60	5'-AGT GCT GTG AAC CCG ACA ATA TCG CT-3'	62.1	GC-III RP
cEF2-F1	5'-TTC TAT GCC TTT GGC CGT GTC TTC TC-3'	62.6	EF2 FP
cEF2-R1	5'-TGA TGG TGC CCG TCT TAA CCA GAT AC-3'	62.1	EF2 RP

Abbreviations: EF, elongation factor 2; FP, forward primer; GC, guanylyl cyclase; RP, reverse primer

The PCR conditions were an initial denaturation at 96 °C for 5 min, then 35 cycles of denaturation at 96 °C for 20 sec, annealing at 62 °C for 20 sec, and extension at 72 °C for 30 sec, followed by 5 min at 72 °C as a final extension. Samples (15 µl) were separated on 2% agarose gels with a 100-bp PCR Molecular Ruler DNA size ladder (Bio-Rad) and stained with ethidium bromide. The gel image was reversed and analyzed by Quantity One software (Bio-Rad). All expression data were normalized to an internal positive control (Gl-EF2).

Statistical analyses

Statview 5.0.1 software (SAS Institute, Inc., Cary, NC, USA) was used for statistical analyses. Regression analysis was used to determine the correlations between ecdysteroid concentration and GC mRNA level. One-way analysis of variance (ANOVA) post-hoc tests (Bonferroni/Dunn, Tukey/Kramer, and Fisher's PLSD tests) were used to determine significant differences in GC mRNA levels in response to ES ablation and 20E injection.

Results

Cloning of three guanylyl cyclases

RT-PCR and 3' and 5' RACE were used to clone cDNAs encoding land crab GCs. Initial nested PCR with degenerate primers yielded products of the expected size (~240 bp) from cDNA synthesized from mRNA pooled from YO, ovary, testis, hepatopancreas, and claw muscle. Twenty-two cDNA clones were selected for sequencing. The sequences encoding part of the GC catalytic domain fell into three categories: one was similar to the β subunit of soluble NO-sensitive GC; the second was similar to membrane receptor GC; and the third was similar to *Manduca sexta* NO-insensitive GC (Ms-GC-I). Additional sequence 5' to the catalytic domain of Gl-GC-Iβ and Gl-GC-II (*G. lateralis* guanylyl cyclases Iβ subunit and II, respectively) was obtained by a second round of nested PCR. 5' and 3' RACE using nested sequence-specific primers obtained full-length sequences of Gl-GC-Iβ and Gl-GC-II and a partial sequence of Gl-GC-III. Several attempts at varying the 3' RACE conditions failed to obtain the 3' sequence of the Gl-GC-III.

The domain organization of the three land crab GCs is shown in Figure 3-1. All three GCs have a highly conserved catalytic domain, which is located in the C-terminal region of Gl-GC-Iβ and Gl-GC-II. Gl-GC-Iβ has heme/NO-binding (HNOB) and HNOB-associated (HNOBA) domains, which are characteristic of NO-sensitive GCs in other species. Gl-GC-II has an N-terminal extracellular ligand-binding domain, a transmembrane domain, a kinase homology domain, and a dimerization domain.

Fig. 3-1. Domain organization of three guanylyl cyclases from land crab. The deduced amino acid sequences of Gl-GC-Iβ, Gl-GC-II, and Gl-GC-III are depicted; all have a highly conserved catalytic (GC) domain. Gl-GC-Iβ has heme/NO-binding (HNOB) and heme/NO-binding-associated (HNOBA) domains, which are characteristic of the β subunit of NO-sensitive GCs. Gl-GC-II has signal peptide (Signal), ligand-binding (LB), transmembrane (TM), kinase homology (KH), and dimerization (DD) domains. The partial sequence of Gl-GC-III resembles the Gl-GC-II, but lacks the signal peptide, LB, TM, and most of the KH domain. Amino acid residues, numbered from the N-terminus, indicate the domain boundaries.

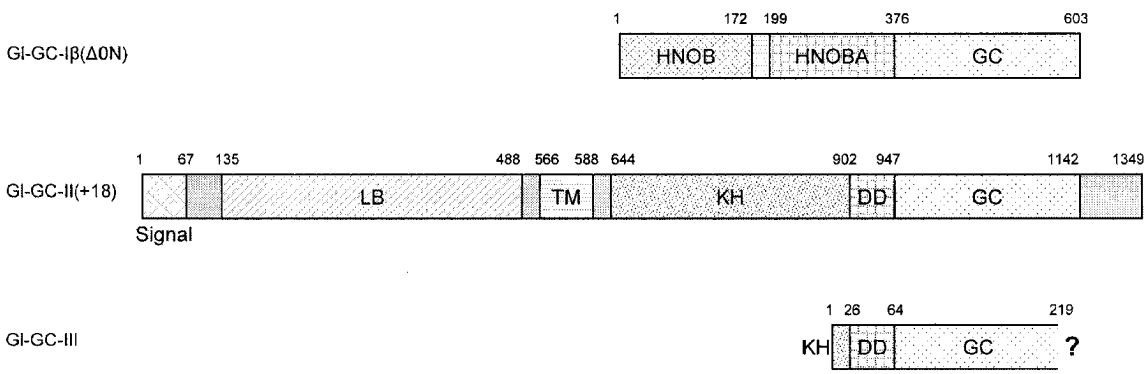

Gl-III has a dimerization domain, but lacks the ligand-binding and transmembrane domains and most of the kinase homology domain.

Two Gl-GC-Iβ isoforms differing in the absence (Δ32N) or presence (Δ0N) of a 32-amino acid sequence at the N-terminus were characterized (Fig. 3-2). The remainder of the open reading frame (ORF) and 3' and 5' untranslated regions (UTRs) of both isoforms were identical. The ORF of the Δ0N isoform encodes a 603- amino acid protein with an estimated mass of ~68.4 kDa (Table 3-3). Alignment of the deduced amino acid sequence of Gl-GC-Iβ with insect GC-Iβ sequences showed a high degree of identity in the HNOB, HNOBA, and catalytic domains (Fig. 3-3). The *Drosophila* GC-Iβ has a 119-amino acid insertion in the HNOB domain and a 29-amino acid Gly-rich C-terminal extension not present in the *G. lateralis* and *M. sexta* sequences. An α-helical span in the HNOBA domain mediates dimerization with the α subunit to form the active protein (Iyer et al., 2003). All three arthropod sequences have highly-conserved amino acids involved in heme/NO binding (C78, H105, Y135, R139, and C212) and GTP binding (E466, R532, and C534) (Figs. 3-2, 3-3).

Three Gl-GC-II isoforms that varied in length within the ligand-binding domain (+18, +9, and +0 amino acid insertions) were found (Fig. 3-4). Other than the insertions, the nucleotide sequences of the three cDNAs were identical. The ORF of the +9 isoform cDNA encodes a 1,340-amino acid protein with an estimated mass of ~150 kDa (Table 3-3). Alignment of the Gl-GC-II(+18) deduced sequence with GC-IIs from crayfish (Pc-GC-II-M2) and blue crab (Cs-GC-YO1) showed highest sequence identities in the transmembrane, kinase homology, amphipathic α-helical dimerization, and catalytic domains (Fig. 3-5). The glycine-rich subdomain, which is critical for ATP-binding, was

Table 3-3. Summary of Gl-GC isoforms and Gl-GC-III consensus sequences obtained from 3' and 5' RACE

Name	Splice variant	cDNA (bp)	Protein (aa)	Mass (Da)	GenBank #
Gl-GC-Iβ(Δ0N)	Full length (no deletion at N-terminus)	2,380	603	68,435	DQ355433
Gl-GC-Iβ(Δ32N)	32-aa deletion at N-terminus	2,283	571	64,596	DQ355434
Gl-GC-II(+0)	No insert in ligand-binding domain	4,555	1,331	149,229	DQ355435
Gl-GC-II(+9)	9-aa insert in ligand-binding domain	4,582	1,340	150,097	DQ355436
Gl-GC-II(+18)	18-aa insert in ligand-binding domain	4,609	1,349	150,999	DQ355437
Gl-GC-III	Single isoform; partial cDNA	785	>219	>25,022	DQ355438

Abbreviations: aa, amino acids; bp, base pairs; Da, Daltons.

Fig. 3-2. The full-length cDNA sequence of NO-sensitive soluble guanylyl cyclase β subunit from land crab (Gl-GC-Iß). Two isoforms differ in the absence (Gl-GC-IβΔ32N) or presence (Gl-GC-IβΔ0N) of a 32-amino acid sequence at the N-terminus; the ORFs specify proteins of 571 and 603 amino acids, respectively. The start codons (ATG) are underlined and the stop codon is indicated with an asterisk. Amino acids essential for heme/NO binding and catalytic activity are boxed. The locations of conserved amino acid sequences (YKVETVGD and MPRYCLF) in the catalytic domain for initial nested PCR are in bold; the locations and directions of degenerate primers are indicated by the dashed lines with solid arrowhead. A second round of nested PCR used degenerate forward primers to a highly conserved amino acid sequence at the N-terminus (MYGFVNYAIEQLVV) and sequence-specific reverse primers (DNA sequences in bold; locations and directions indicated with double lines with solid arrowhead). 3' RACE used sequence-specific nested forward primers in the catalytic domain (DNA sequences indicated in bold; direction indicated with a dashed line with open arrowhead). 5' RACE used sequence-specific nested reverse primers in the N-terminal region (DNA sequences indicated in bold; direction indicated with a solid line with solid arrowhead).

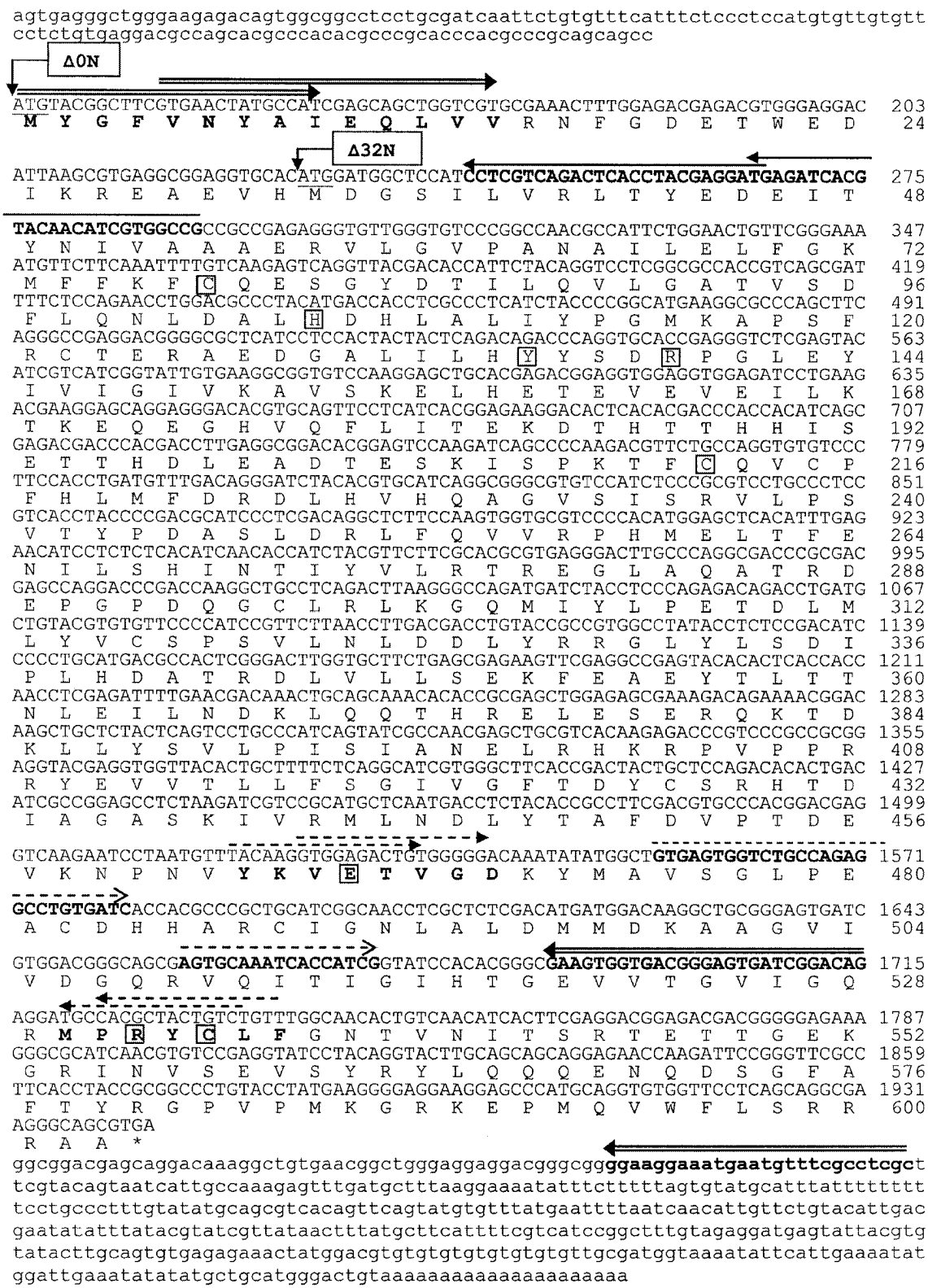

Fig. 3-3. Comparison of deduced amino acid sequences of NO-sensitive soluble guanylyl cyclase cDNAs from crustacean and insects. Amino acid sequence of land crab GC-Iβ (#DQ355434) was aligned with NO-sensitive GCs from *Drosophila* (Dm-GC-Iβ, #AAA87941) and *Manduca* (Ms-GC-Iβ, #AAC61264), using ClustalW software. Broken lines indicate gaps for optimizing alignment. Amino acid residues that are identical or similar between all three sequences are highlighted in black; residues identical or similar in two of the three sequences highlighted in gray. There was a high degree of sequence identity in the heme/NO-binding domain (HNOB; box with dotted line), heme/NO-binding associated domain (HNOBA; box with dashed/dotted line), and catalytic GC domain (GC; box with dashed line). The Dm-GC-Iβ had a 119-amino acid insertion at the C-terminal end of the HNOB domain and a 29-amino acid Gly-rich C-terminal extension not present in the *G. lateralis* or *M. sexta* cDNAs. Residues with essential functions in the HNOB, HNOBA, and GC domains are identified by inverted triangles. The locations of secondary structures (α4, β2, β3, and β4) that form the GTP-binding pocket in GC domain are indicated. The N-terminal 32-amino acid deletion in the truncated isoform is indicated (Δ32N).

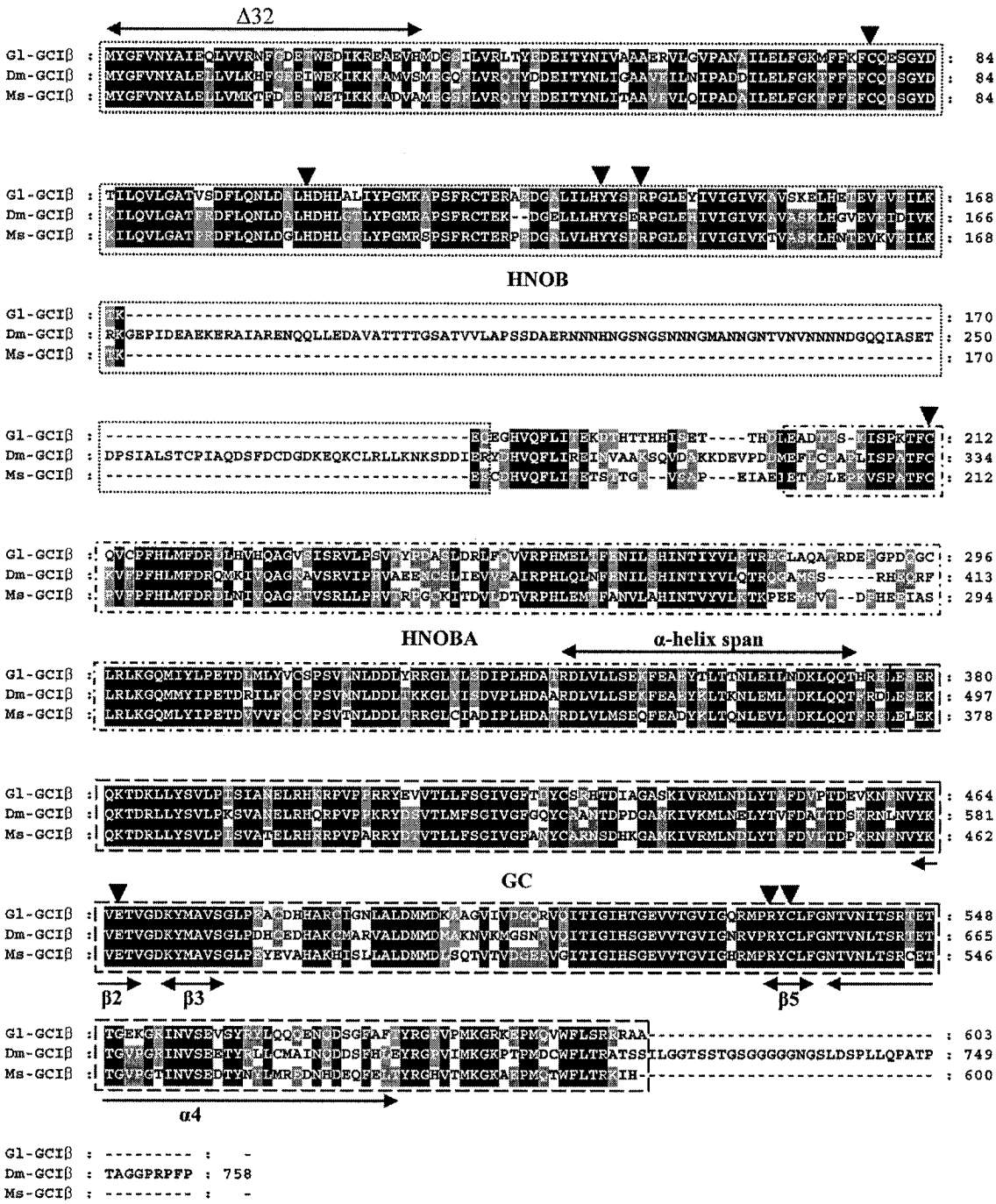

Fig. 3-4. The complete cDNA sequence of membrane receptor guanylyl cyclase from land crab (Gl-GC-II). Three isoforms differed in the length of insertions (0, 9, or 18 amino acids) after D412 in the ligand-binding domain; the ORFs specify proteins of 1331, 1340, and 1349 amino acids, respectively. The start codon (ATG) is underlined and the stop codon is indicated with an asterisk. The signal peptide cleavage site after A67 is indicated by the vertical arrow. In the extracellular region, 8 conserved cysteine residues are boxed and 13 putative N-glycosylation sites are highlighted. Conserved residues in the catalytic domain are boxed. The locations of conserved amino acid sequences (YKVETVGD and MPRYCLF) in the catalytic domain for initial nested PCR are in bold; the locations and directions of degenerate primers are indicated by the dashed lines with solid arrowhead. A second round of nested PCR used degenerate forward primers to a highly conserved amino acid sequence at the ligand-binding domain (DLLCRNVSAVFGPE) and sequence-specific reverse primers (DNA sequences in bold; locations and directions indicated with double lines with solid arrowhead). 3' RACE used sequence-specific nested forward primers in the catalytic domain (DNA sequences indicated in bold; direction indicated with a dashed line with open arrowhead). 5' RACE used sequence-specific nested reverse primers in the ligand-binding domain (DNA sequences indicated in bold; direction indicated with a solid line with solid arrowhead).

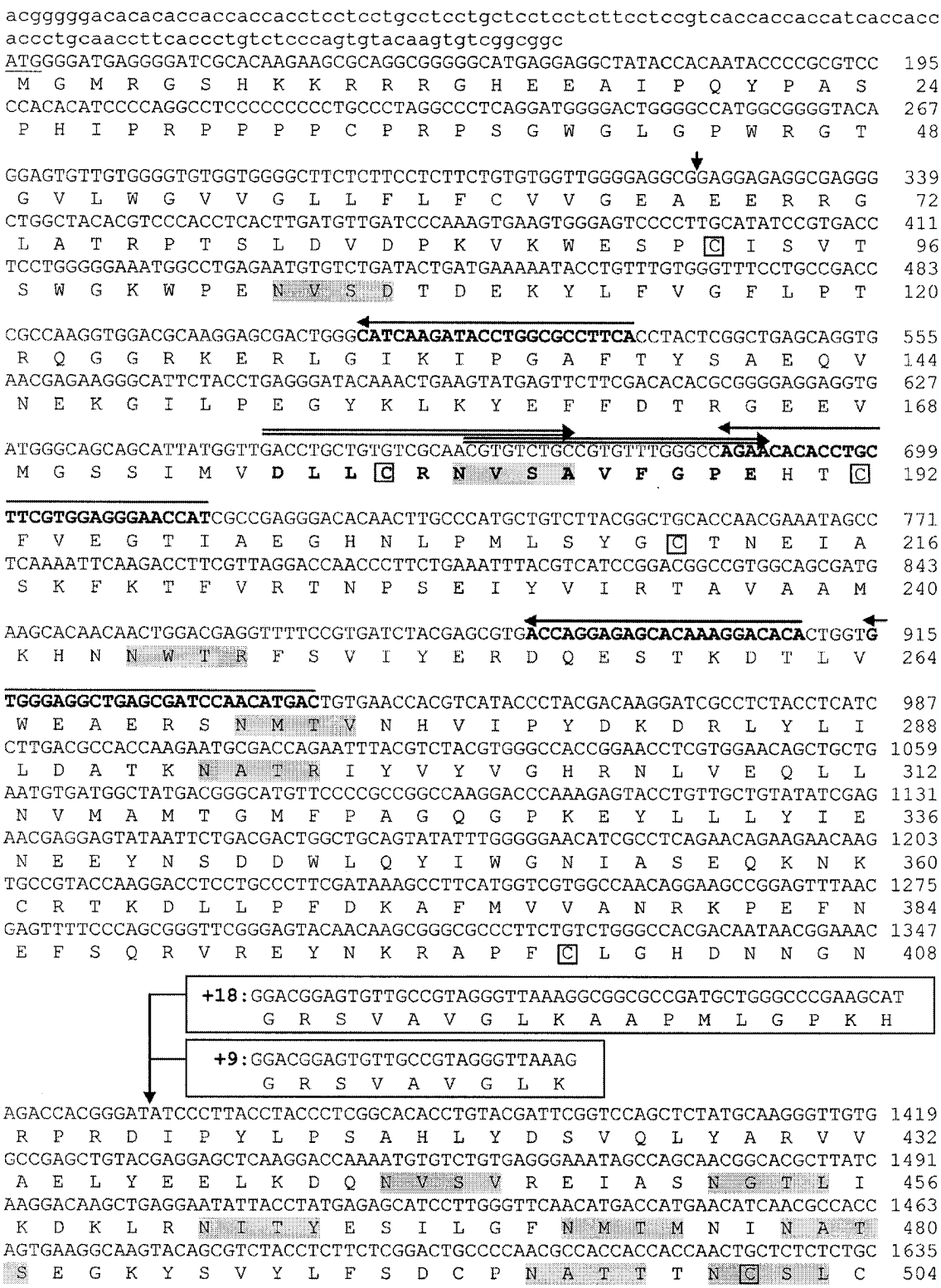

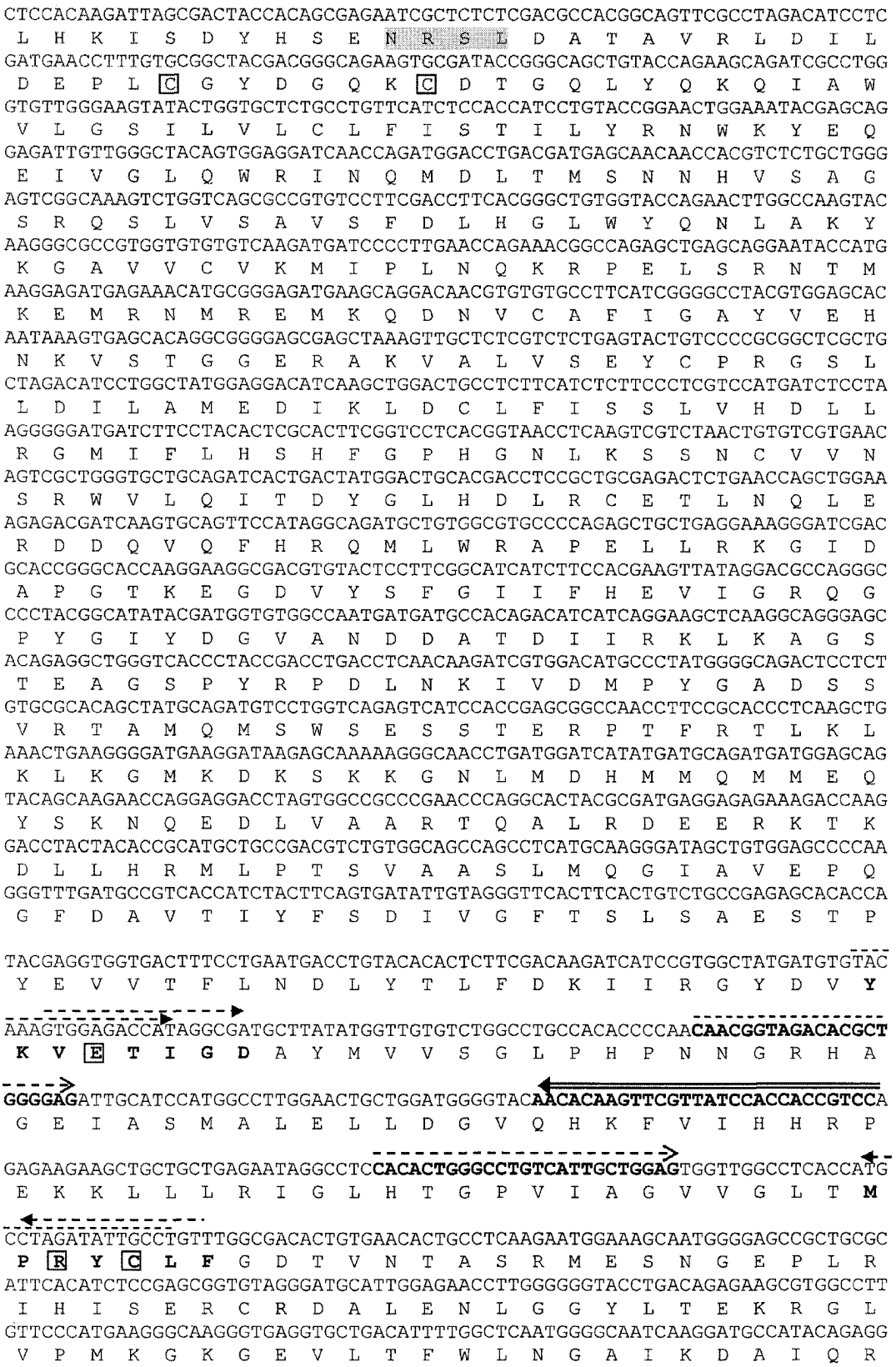

CTCCACAAGATTAGCGACTACCACAGCGAGAATCGCTCTCTCGACGCCACGGCAGTTCGCCTAGACATCCTC 1707
L H K I S D Y H S E N R S L D A T A V R L D I L 528
GATGAACCTTTGTGCGGCTACGACGGGCAGAAGTGCGATACCGGGCAGCTGTACCAGAAGCAGATCGCCTGG 1779
D E P L C G Y D G Q K C D T G Q L Y Q K Q I A W 552
GTGTTGGGAAGTATACTGGTGCTCTGCCTGTTCATCTCCACCATCCTGTACCGGAACTGGAAATACGAGCAG 1851
V L G S I L V L C L F I S T I L Y R N W K Y E Q 576
GAGATTGTTGGGCTACAGTGGAGGATCAACCAGATGGACCTGACGATGAGCAACAACCACGTCTCTGCTGGG 1923
E I V G L Q W R I N Q M D L T M S N N H V S A G 600
AGTCGGCAAAGTCTGGTCAGCGCCGTGTCCTTCGACCTTCACGGGCTGTGGTACCAGAACTTGGCCAAGTAC 1995
S R Q S L V S A V S F D L H G L W Y Q N L A K Y 624
AAGGGCGCCGTGGTGTGTGTCAAGATGATCCCCTTGAACCAGAAACGGCCAGAGCTGAGCAGGAATACCATG 2067
K G A V V C V K M I P L N Q K R P E L S R N T M 648
AAGGAGATGAGAAACATGCGGGAGATGAAGCAGGACAACGTGTGTGCCTTCATCGGGGCCTACGTGGAGCAC 2139
K E M R N M R E M K Q D N V C A F I G A Y V E H 672
AATAAAGTGAGCACAGGCGGGGAGCGAGCTAAAGTTGCTCTCGTCTCTGAGTACTGTCCCCGCGGCTCGCTG 2211
N K V S T G G E R A K V A L V S E Y C P R G S L 696
CTAGACATCCTGGCTATGGAGGACATCAAGCTGGACTGCCTCTTCATCTCTTCCCTCGTCCATGATCTCCTA 2283
L D I L A M E D I K L D C L F I S S L V H D L L 720
AGGGGGATGATCTTCCTACACTCGCACTTCGGTCCTCACGGTAACCTCAAGTCGTCTAACTGTGTCGTGAAC 2355
R G M I F L H S H F G P H G N L K S S N C V V N 744
AGTCGCTGGGTGCTGCAGATCACTGACTATGGACTGCACGACCTCCGCTGCGAGACTCTGAACCAGCTGGAA 2427
S R W V L Q I T D Y G L H D L R C E T L N Q L E 768
AGAGACGATCAAGTGCAGTTCCATAGGCAGATGCTGTGGCGTGCCCCAGAGCTGCTGAGGAAAGGGATCGAC 2489
R D D Q V Q F H R Q M L W R A P E L L R K G I D 792
GCACCGGGCACCAAGGAAGGCGACGTGTACTCCTTCGGCATCATCTTCCACGAAGTTATAGGACGCCAGGGC 2571
A P G T K E G D V Y S F G I I F H E V I G R Q G 816
CCCTACGGCATATACGATGGTGTGGCCAATGATGATGCCACAGACATCATCAGGAAGCTCAAGGCAGGGAGC 2653
P Y G I Y D G V A N D D A T D I I R K L K A G S 840
ACAGAGGCTGGGTCACCCTACCGACCTGACCTCAACAAGATCGTGGACATGCCCTATGGGGCAGACTCCTCT 2715
T E A G S P Y R P D L N K I V D M P Y G A D S S 864
GTGCGCACAGCTATGCAGATGTCCTGGTCAGAGTCATCCACCGAGCGGCCAACCTTCCGCACCCTCAAGCTG 2787
V R T A M Q M S W S E S S T E R P T F R T L K L 888
AAACTGAAGGGGATGAAGGATAAGAGCAAAAAGGGCAACCTGATGGATCATATGATGCAGATGATGGAGCAG 2859
K L K G M K D K S K K G N L M D H M M Q M M E Q 912
TACAGCAAGAACCAGGAGGACCTAGTGGCCGCCCGAACCCAGGCACTACGCGATGAGGAGAGAAAGACCAAG 2931
Y S K N Q E D L V A A R T Q A L R D E E R K T K 936
GACCTACTACACCGCATGCTGCCGACGTCTGTGGCAGCCAGCCTCATGCAAGGGATAGCTGTGGAGCCCCAA 3003
D L L H R M L P T S V A A S L M Q G I A V E P Q 960
GGGTTTGATGCCGTCACCATCTACTTCAGTGATATTGTAGGGTTCACTTCACTGTCTGCCGAGAGCACACCA 3075
G F D A V T I Y F S D I V G F T S L S A E S T P 984

TACGAGGTGGTGACTTTCCTGAATGACCTGTACACACTCTTCGACAAGATCATCCGTGGCTATGATGTGTAC 3147
Y E V V T F L N D L Y T L F D K I I R G Y D V **Y** 1008

AAAGTGGAGACCATAGGCGATGCTTATATGGTTGTGTCTGGCCTGCCACACCCCAA**CAACGGTAGACACGCT** 3219
K V E T I G D A Y M V V S G L P H P N N G R H A 1032

GGGGAGATTGCATCCATGGCCTTGGAACTGCTGGATGGGGTAC**AACACAAGTTCGTTATCCACCACCGTCC**A 3291
G E I A S M A L E L L D G V Q H K F V I H H R P 1056

GAGAAGAAGCTGCTGCTGAGAATAGGCCTC**CACACTGGGCCTGTCATTGCTGGAG**TGGTTGGCCTCACCATG 3363
E K K L L L R I G L H T G P V I A G V V G L T **M** 1080

CCTAGATATTGCCTGTTTGGCGACACTGTGAACACTGCCTCAAGAATGGAAAGCAATGGGGAGCCGCTGCGC 3435
P R Y C L F G D T V N T A S R M E S N G E P L R 1104
ATTCACATCTCCGAGCGGTGTAGGGATGCATTGGAGAACCTTGGGGGGTACCTGACAGAGAAGCGTGGCCTT 3507
I H I S E R C R D A L E N L G G Y L T E K R G L 1128
GTTCCCATGAAGGGCAAGGGTGAGGTGCTGACATTTTGGCTCAATGGGGCAATCAAGGATGCCATACAGAGG 3579
V P M K G K G E V L T F W L N G A I K D A I Q R 1152

```
AGGGAGGTGAGTGAGTCCCTGCCGCCACTGCTGCAGCTAAGTGACACAGAAGTGGGTGAACTTAGAAAGAGG 3651
 R  E  V  S  E  S  L  P  P  L  L  Q  L  S  D  T  E  V  G  E  L  R  K  R  1176
AGCCCACGACTCAGCTCACTTGGAAACCGCACCTCCAGTGTGCCCAGGAGTATGGAAGATGCTGGGGACCTA 3723
 S  P  R  L  S  S  L  G  N  R  T  S  S  V  P  R  S  M  E  D  A  G  D  L  1200
AACGGGGGACCTGGGGGCCTTGTGGATGACCCCCCCATGAGAGACTCCCCTGGGTCAAAGGTCTTCCGCCGC 3795
 N  G  G  P  G  G  L  V  D  D  P  P  M  R  D  S  P  G  S  K  V  F  R  R  1224

CGCTGCCTCAGTAGTAACTTCCGCACATCCAGCGTTGACAACACACCCAGAGGTAGTTTACTCTGTCCACCA 3867
 R  C  L  S  S  N  F  R  T  S  S  V  D  N  T  P  R  G  S  L  L  C  P  P  1248
GTCACCAACACGACCGAGAGAGGATCAACGCCTGATTCTGTCCCCCAGAGCATCAGTTTAGATGGCCTTAAC 3939
 V  T  N  T  T  E  R  G  S  T  P  D  S  V  P  Q  S  I  S  L  D  G  L  N  1272
CAGTCTGGGCTGAGGCTAGAGGTCCCCGCACTTCAGACCATCACTGCCGCCACCTCCCCATCCTCCTCTGAG 4011
 Q  S  G  L  R  L  E  V  P  A  L  Q  T  I  T  A  A  T  S  P  S  S  S  E  1296
CCTACGCTTCCACTGGAAGATAAAAGAGGTGTTAATTTCTGCCCCACTGCACGCACGGGTGGTGCCTCAGTT 4083
 P  T  L  P  L  E  D  K  R  G  V  N  F  C  P  T  A  R  T  G  G  A  S  V  1320
CCAGCACATGGGAATGGTGAGCGGAACCCATGCTGA
 P  A  H  G  N  G  E  R  N  P  C  *
gtggggaggaggggaagaagcctgggtggaggaggtggggacgagaggggaaggcagccctatcccgggcagtcctg
tagttaaatcaaattccctaaaagcttggttttcaggctttttccgccaccctaaaccacccccaaggatcacatcca
agtttacgctgaatggactacggcgggagaatgcggtgtgagtgtttgtatgtgtgtgtgtgtgtgtgtgtttctt
gggactcaaaacgatacccagggatgctgtagtaatgtcatccagggtttttccttccttcattcactctaatgtggt
tcttttcttgctgctgctgctaaaattttgtatgtatgtgtgtgtatcaatggaacattctgtggcacatctcagaaa
cattgtgatacagacttggatgttctggtgtgttggtgactggtgg
```

Fig. 3-5. Comparison of deduced amino acid sequences of crustacean membrane receptor guanylyl cyclase cDNAs. Amino acid sequence of land crab GC-II (Gl-GC-II+18, #DQ355435) was aligned with receptor GCs from blue crab (Cs-GC-YO1, #AY785292) and crayfish (Pc-GC-II-M2, #AAQ74970) using ClustalW software. Broken lines indicate gaps for optimizing alignment. Amino acid residues that are identical or similar between all the sequences are highlighted in black; residues identical or similar in two of the three sequences are highlighted in gray. The putative signal cleavage site is indicated. There was a high degree of sequence identity in the ligand-binding (LB; box with dotted line), transmembrane (TM; box with solid line), kinase homology (KH; box with dashed/dotted line), dimerization (DD; box with dashed/2 dotted line), and catalytic GC (GC; box with dashed line) domains. The extracellular region had 8 conserved cysteine residues (inverted triangles) and 13 potential N-linked glycosylation sites (****). The location of the isoform insertion sequences (+9 and +18) was in a hypervariable region between two highly conserved sequences in the ligand-binding domain. The glycine-rich subdomain (GPYGLYDG; residues 834-841) in the KH domain is indicated. The three conserved residues (inverted triangles) and the locations of secondary structures (α4, β2, β3, and β4) that form the GTP-binding pocket in the GC domain are indicated.

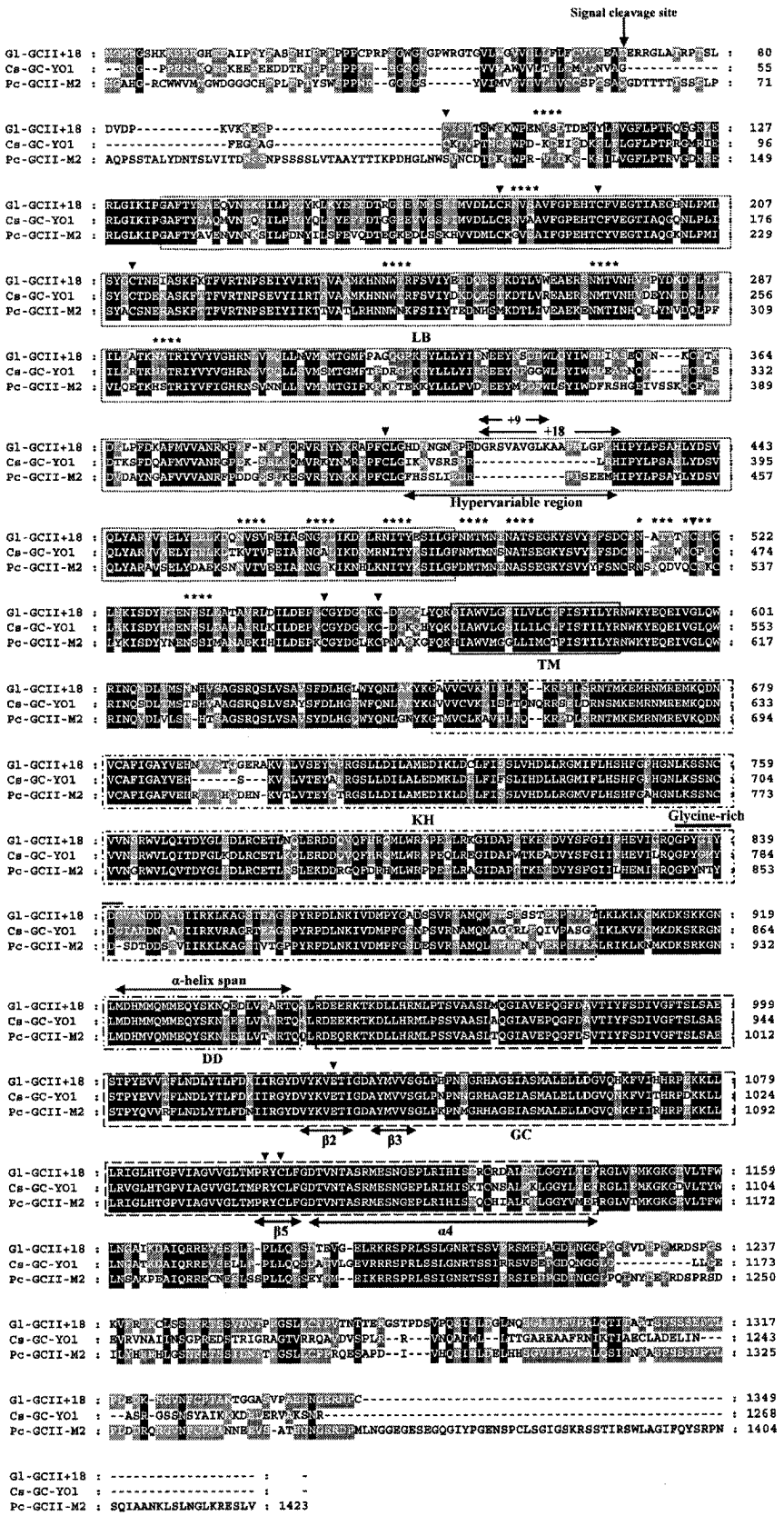

identified in the kinase homology domain (Fig. 3-5). The sequence alignment indicated that the 9- and 18-amino acid insertions were located in a hypervariable region between highly conserved sequences in the ligand-binding domain (Fig. 3-5). The putative signal cleavage site was located at Ala67 (Figs. 3-4, 3-5). The extracellular domain had 8 conserved cysteine residues and 13 putative N-linked glycosylation sites (Figs. 3-4, 3-5). The catalytic domain had the three residues (E1011, R1082, and C1084 in the +0 isoform) involved in GTP binding (Figs. 3-4, 3-5).

A partial cDNA clone of Gl-GC-III (787 bp) was obtained that contains the 5' UTR and part of the ORF including the start codon (Fig. 3-6). The deduced 220-amino acid sequence contained a small part of the kinase homology domain, an amphipathic α-helical dimerization domain, and most of the catalytic domain; the remainder of the ORF and the 3' UTR was missing (Fig. 3-7). Alignment of the Gl-GC-III and Ms-GC-I (Ms-GC-III) sequences showed high identities in the dimerization and catalytic domains (Fig. 3-7). The lengths of the kinase homology domain differed between *G. lateralis* and *M. sexta*; it was 26 amino acids in Gl-GC-III and 90 amino acids in Ms-GC-I (Fig. 3-7). The residues (E146, R216, and C218) essential for GTP binding were present (Figs. 3-6, 3-7).

In order to better understand the relationships between the various GCs, a phylogenetic analysis was carried out based on the deduced amino acid sequences of the catalytic domains from crustaceans, insects, and human (Fig. 3-8). The arthropod NO-sensitive soluble GCs (Gl-GC-Iβ, Ms-GC-β1, and Dm-GC-Iβ) clustered as a distinct group. The Hs-GC-Iβ diverged from the arthropod GC-Iβs. The Ms-GC-β3, the only member of the GC-IV class, is a NO-insensitive soluble GC that was related to the Hs-GC-Iβ.

Fig. 3-6. The partial cDNA sequence of NO-insensitive soluble guanylyl cyclase from land crab (Gl-GC-III). The cDNA (787 bp) contained the 5' UTR and 660 bp of the ORF with the dimerization and GC catalytic domains. Conserved residues (E146, R216, and C218) in the catalytic domain are boxed. The locations of conserved amino acid sequences (YKVETVGD and MPRYCLF) in the catalytic domain for initial nested PCR are in bold; the locations and directions of degenerate primers are indicated by the dashed lines with solid arrowhead. 5' RACE used sequence-specific nested reverse primers in the catalytic domain (DNA sequences indicated in bold; direction indicated with a solid line with solid arrowhead). 3' RACE was not successful.

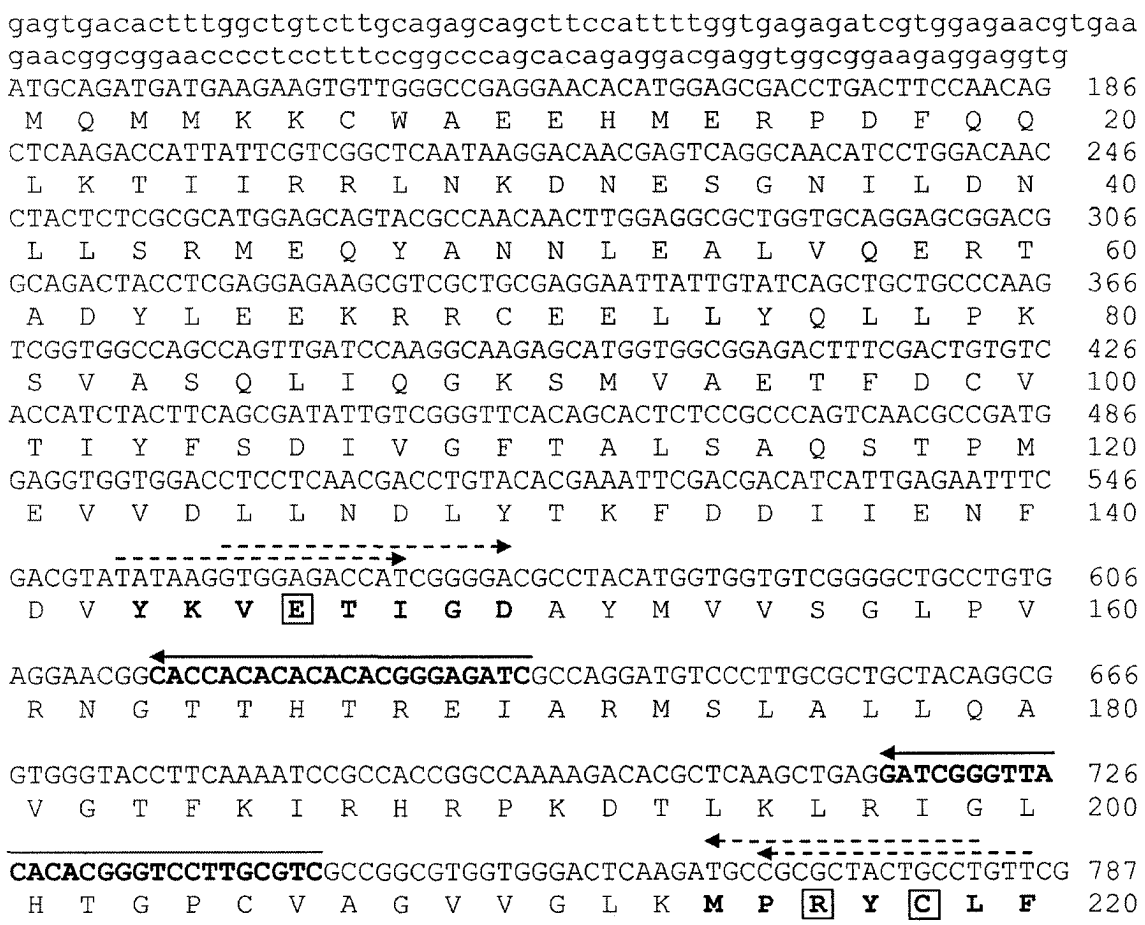

Fig. 3-7. Comparison of deduced amino acid sequences of NO-insensitive soluble guanylyl cyclase cDNAs from crustacean and insect. Amino acid sequence of the partial land crab GC-III (#DQ355438) was aligned with NO-insensitive GC from *Manduca sexta* (Ms-GC-I, #AAC62238) using ClustalW software. Broken lines indicate gaps for optimizing alignment. Amino acid residues that are identical or similar between all the sequences are highlighted in black; residues identical or similar in two of the three sequences are highlighted in gray. There was a high sequence identity in the dimerization (DD; box with dashed/2 dotted line) and catalytic GC (GC; box with dashed line) domains. Conserved residues in the GC domain are indicated with inverted triangles. The sequences in the kinase homology domain (KH; box with dashed/dotted line) were divergent between the Ms-GC-III and Gl-GC-III. The locations of secondary structures (α4, β2, β3, and β4) that form the GTP-binding pocket in GC domain are indicated.

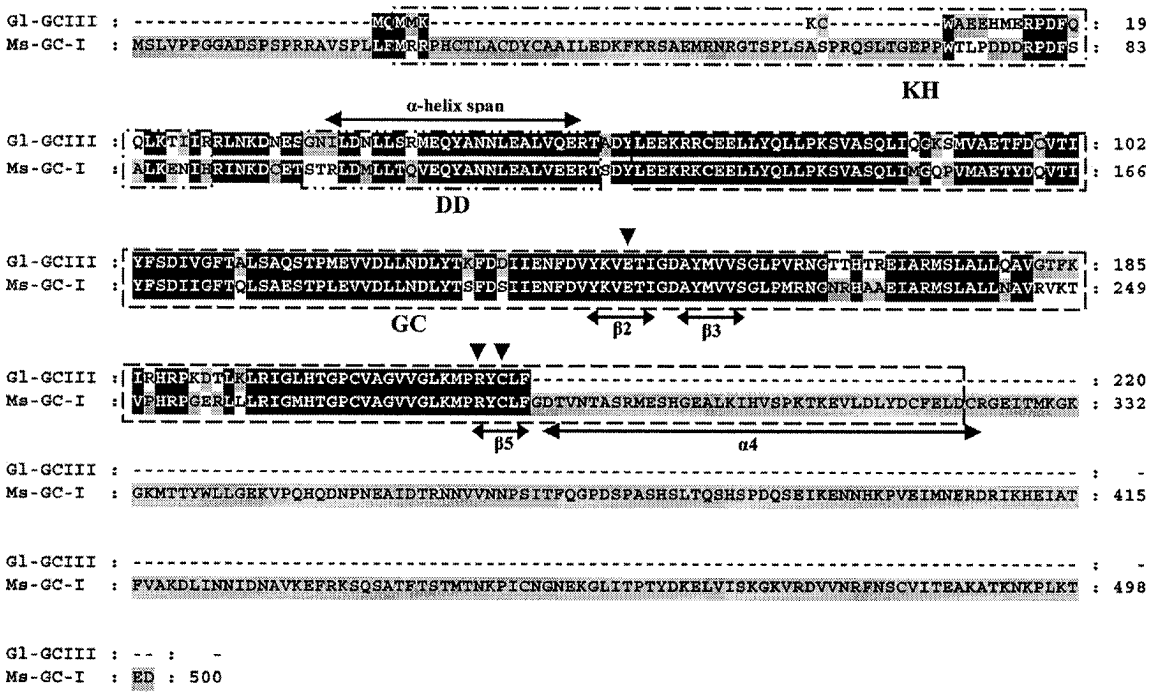

Fig. 3-8. Phylogenetic relationships of catalytic domain of guanylyl cyclases from arthropods and human. The deduced amino acid sequences of the catalytic domain segregate into four classes: GC-Iβ, GC-II, GC-III, and GC-IV. Gl-GC-Iβ grouped with the insect GC-Iβs; human GC-Iβ diverged from the arthropod GC-Iβs. Gl-GC-II grouped with membrane receptors GCs from insects and other crustaceans. Two isoforms of human membrane GCs, a ligand-binding GC-II (Hs-GC-A) and a GC-activating protein binding GC-II (Hs-RetGC-2 or Hs-GC-F) are included for comparison. Gl-GC-III grouped with *Manduca* GC-I. *Manduca* GC-β3, the only member of the GC IV class, was most similar to Hs-GC-Iβ. Abbreviations: Ag (mosquito, *Anopheles gambiae*); Cs (blue crab, *Callinectes sapidus*); Dm (fruit fly, *Drosophila melanogaster*); Gl (land crab, *Gecarcinus lateralis*); Hs (human, *Homo sapiens*); Ms (Tobacco hornworm, *Manduca sexta*); and Pc (crayfish, *Procambarus clarkii*). GenBank accession numbers for the arthropod sequences are given in Table 3-5. Accession numbers for the human sequences are NP004120 for Hs-GC-Iβ, NM000906 for Hs-GC-A, and L37378 for Hs-GC-RetGC-2. Scale represents proportion of amino acid differences between sequences.

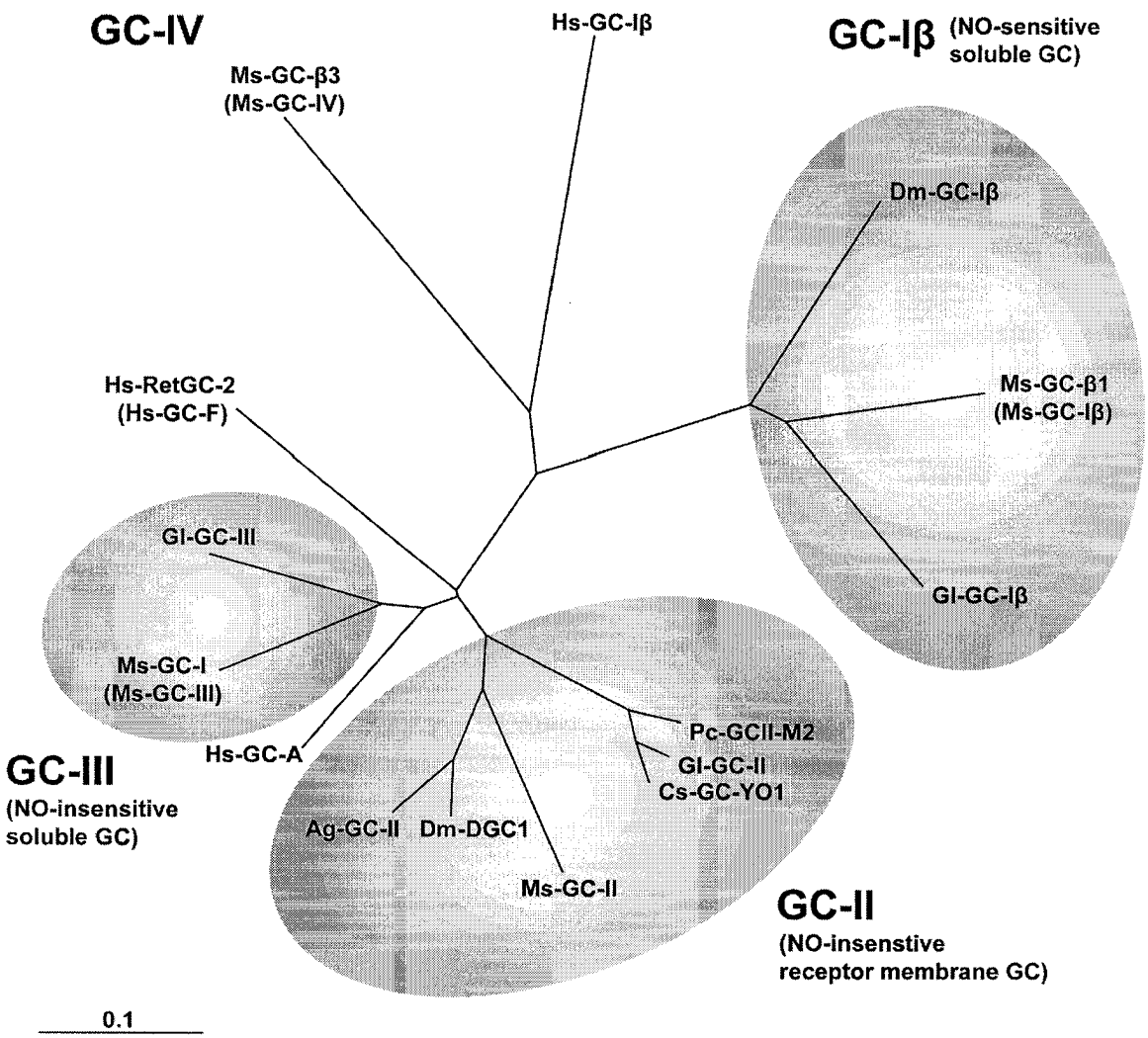

As expected, GC-II and GC-III formed a supercluster distinct from the GC-Iβs and Ms-GC-β3; the human GC A (Hs-GC-A) and F (Hs-RetGC-2) isoforms were related to the arthropod GC-II and GC-III classes. The arthropod membrane receptor GCs (Gl-GC-II, Pc-GC-II-M2, Cs-GC-YO1, Ag-GC-II, Dm-DGC1, and Ms-GC-II) formed a single group. Gl-GC-III was clustered with Ms-GC-I, indicating that both are members of the GC-III class.

The overall similarities were determined by comparing the sequences of the deduced amino acid sequences of the three land crab GCs with those of other arthropod GCs. Gl-GC-Iβ showed 79.9% and 62.4% similarity to *M. sexta* GC-Iβ (#AAC61264) and *D. melanogaster* GC-Iβ (#AAA87941), respectively. The GC-IIs from blue crab (*C. sapidus*; #AY785292) and crayfish (*P. clakii*; #AAQ74970) were 75.8% and 72.1% similar, respectively, to *G. lateralis* GC-II. *D. melanogaster* GC-II (Dm-DGC1; #AAA74408) and *M. sexta* GC-II (#AAN16469) showed 44.9% and 35.3% similarity to Gl-GC-II, respectively. The partial sequence of Gl-GC-III was 36.4% similar to the comparable sequence of *M. sexta* Ms-GC-I (#AAC62238).

Expression of guanylyl cyclases

Most tissues expressed the three guanylyl cyclases, although the levels of expression varied among tissues in intact animals (Fig. 3-9). RT-PCR was used with primers that amplified the same product from both Gl-GC-Iβ isoforms. Gl-GC-Iβ was expressed at higher levels in ES ganglia (EG), gill (Gi), hepatopancreas (HP), ovary (Ov), and testis (Ts).

Fig. 3-9. Effects of eyestalk ablation on guanylyl cyclase expression in land crab tissues. Total RNA from intact, 1 day post-ESA, 3 days post-ESA, and 7 days post-ESA animals was DNase-treated, reverse-transcribed, and PCR-amplified using sequence-specific primers (see Materials and Methods). PCR products were resolved on 2% agarose gels (for Gl-GC-Iβ, Gl-GC-III, and Gl-EF2) or 10% polyacrylamide gels (for Gl-GC-II), and stained with ethidium bromide. (A) Reversed images of gels. (B) Quantitative analysis from triplicate measurements for each tissue and condition (mean ±1 S.E; n= 3). Both Gl-GC-1β (ΔON and Δ32N isoforms were not distinguished; primers were direct to a common sequence in the C-terminus) and Gl-GC-III were expressed at high levels in ES ganglia (EG), gill (Gi), ovary (Ov), and testis (Ts) from intact animals. Tissues from intact animals differed in relative expression of the three Gl-GC-II isoforms. Gl-GC-II(+9) was expressed at varying levels in all tissues and was the dominant isoform in Y-organ (YO), gill, hepatopancreas (HP), and gonad (Ov and Ts). Gl-GC-II(+18) was expressed at highest levels in heart (Ht), claw muscle (CM), and thoracic muscle (TM). Gl-GC-II(+0) was expressed at low levels in most tissues except ES ganglia, in which it was the major isoform. ES ablation had no significant effect on Gl-GC-Iβ (GC1), Gl-GC-II (GC2), and Gl-GC-III (GC3) expression in most tissues (B). The only exception was the increased expression of the Gl-GC-II(+18) isoform in claw muscles from 3 days and 7 days post-ESA animals. Gl-EF2 was expressed at similar levels in all tissues. Significant differences between means were determined by one-way ANOVA post-hoc test (Fisher's PLSD); P values indicated with brackets (a, $P < 0.034$; b, $P < 0.013$; c, $P < 0.023$).

3-9A

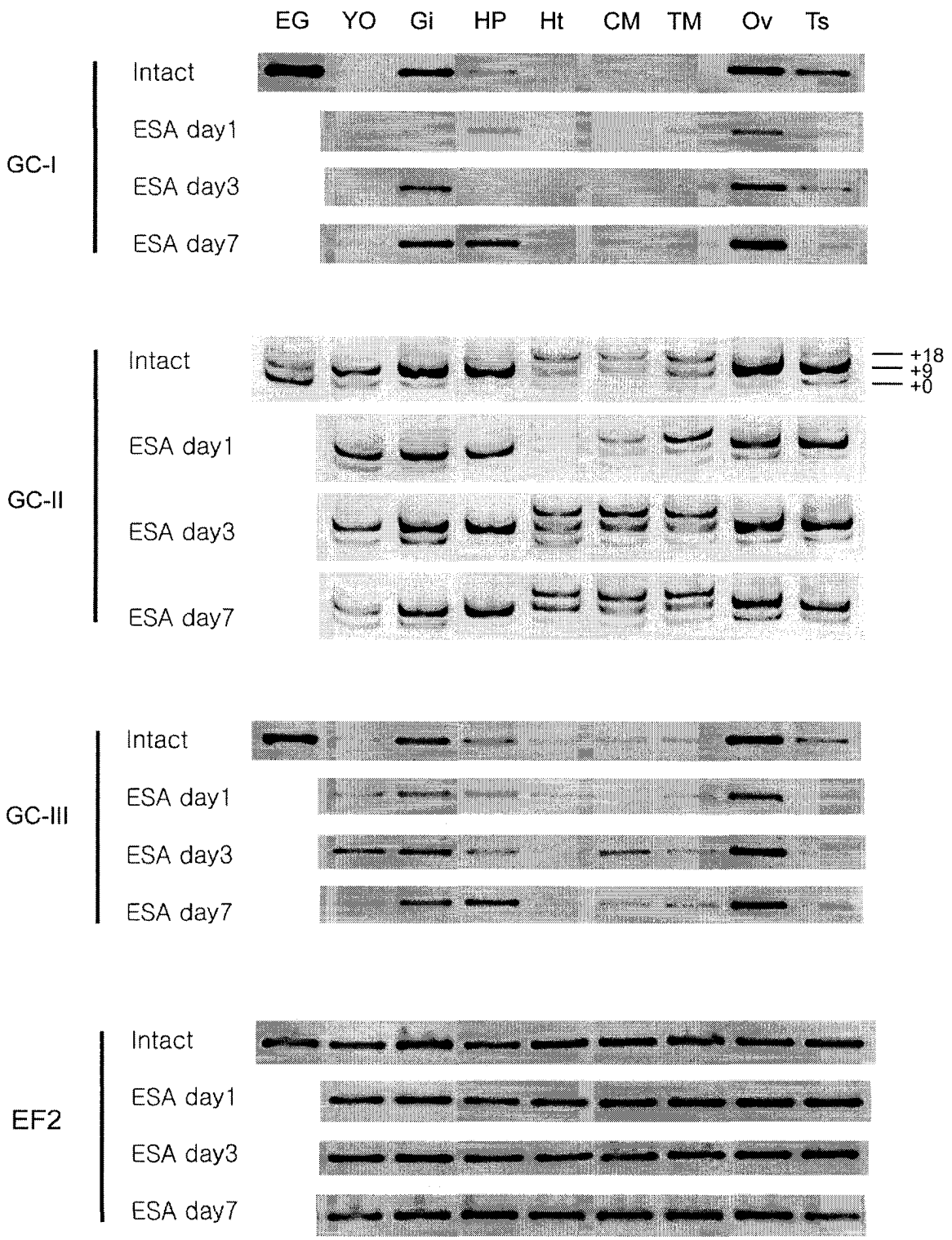

3-9B

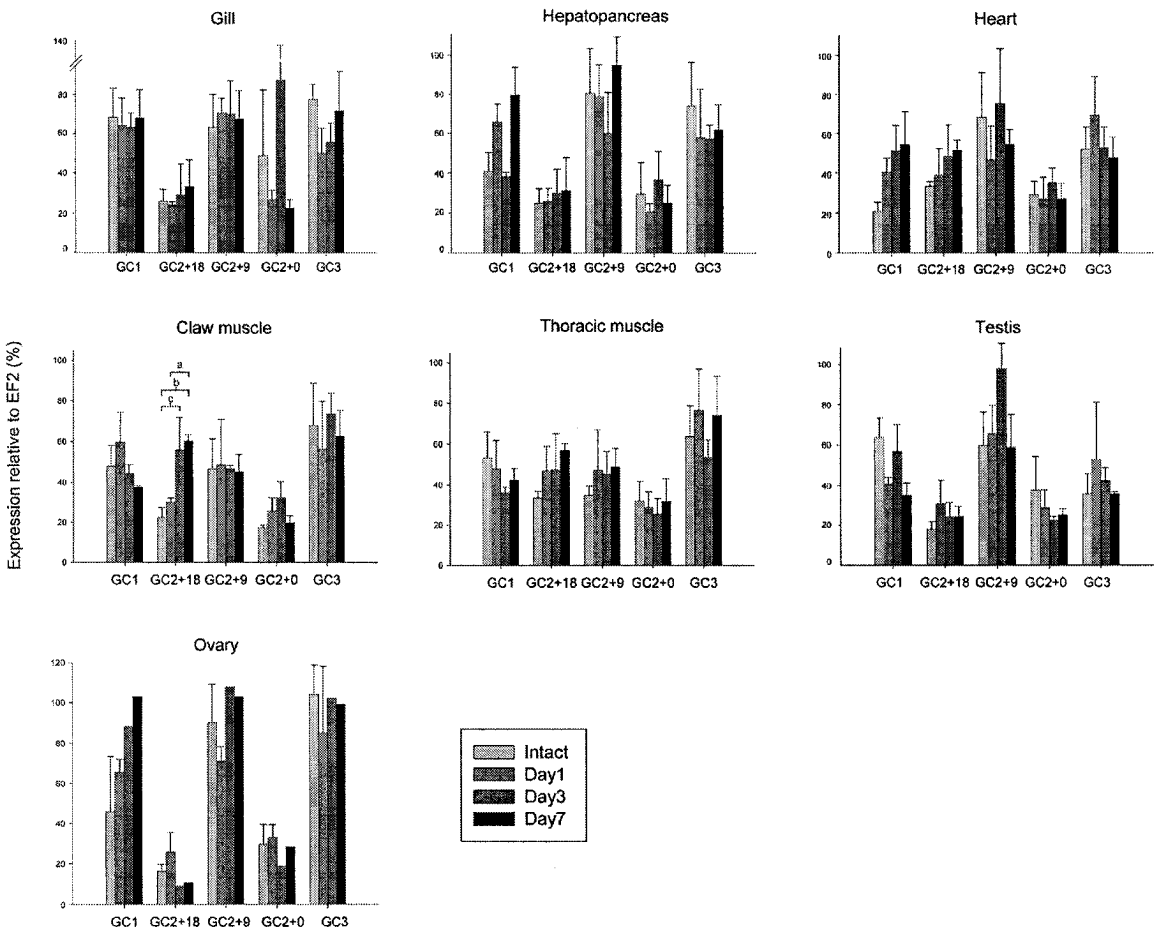

Expression was lower in YO, heart (Ht), claw muscle (CM), and thoracic muscle (TM). RT-PCR with primers that flanked the insertion in the ligand-binding domain quantified the expression of the three Gl-GC-II isoforms (+18, +9, and +0). The reactions were separated on a polyacrylamide gel to distinguish the three products. Gl-GC-II(+18) was expressed at highest levels in heart and skeletal muscle; Gl-GC-II(+9) was expressed in all tissues, with the highest levels in gill, hepatopancreas, and gonad; and Gl-GC-II(+0) was expressed at low levels in most tissues, but was the predominant isoform in nervous tissues, including EG (Fig. 3-9) and thoracic ganglion (data not shown). Gl-GC-III showed an expression pattern similar that of Gl-GC-Iβ (Fig. 3-9). Elongation factor 2 (Gl-EF2) was expressed at similar levels in all tissues (Fig. 3-9A).

The effect of ES ablation on each GC was quantified by semi-quantitative RT-PCR analysis after normalizing to Gl-EF2, which was constitutively expressed (Fig. 3-9A). As expected, ES ablation increased ecdysteroid levels in the hemolymph (Table 3-4). RT-PCR from a single set of animals suggested that GC expression was responsive to ES ablation (Fig. 3-9A). However, analysis of tissues from 3 sets of animals (n = 3 for each tissue at each time period) showed no significant effect of ES ablation in most tissues (Fig. 3-9B). The only exception was the expression of the Gl-GC-II(+18) isoform in claw muscle; its expression increased about 3-fold in 3- and 7-day post-ESA animals. Moreover, Gl-GC-II(+18) mRNA level was significantly correlated with ecdysteroid concentration in claw muscle, but not in heart or thoracic muscle (Fig. 3-10). The expression of the Gl-GC-Iβ Δ0N and Δ32N isoforms and Gl-GC-III in YO increased in response to ES ablation, while the expression of the Gl-GC-II(+0) and Gl-GC-II(+9) isoforms remained unchanged (Fig. 3-11).

Table 3-4. Effect of eyestalk ablation (ESA) on hemolymph ecdysteroid levels. Ecdysteroid was quantified with radioimmunoassay (mean ± 1 S.E.).

Treatment	Hemolymph Edysteroid (pg/µl)
Intact (Control)	11.45 ± 0.86 (n = 29)
1 Day post-ESA	44.06 ± 3.68 (n = 20)
3 Days post-ESA	83.35 ± 5.98 (n = 20)
7 Days post-ESA	132. ± 11.20 (n = 20)

Fig. 3-10. Regression analysis of Gl-GC-II(+18) isoform expression in striated muscles as a function of ecdysteroid concentration. Gl-GC-II(+18) was significantly correlated with hemolymph ecdysteroid concentration in claw muscle, but not in thoracic muscle or heart.

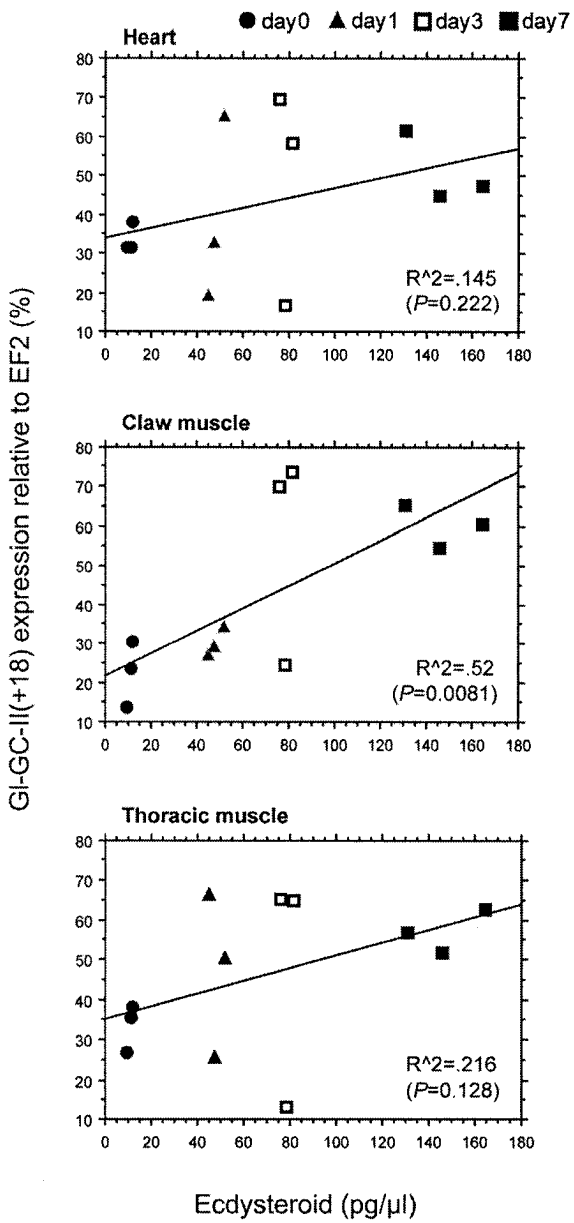

Fig. 3-11. Effects of eyestalk ablation on guanylyl cyclase expression in Y-organ. Total RNA from intact, 1 day post-ESA, and 3 days post-ESA animals was DNase-treated, reverse-transcribed, and PCR-amplified using sequence-specific primers (see Materials and Methods). PCR products were resolved on 2% agarose gels (for Gl-GC-Iβ, Gl-GC-III, and Gl-EF2) or 10% polyacrylamide gels (for Gl-GC-II) and stained with ethidium bromide (reversed images). ES ablation increased mRNA levels of the two Gl-GC-Iβ isoforms (Δ0N and Δ32N) and Gl-GC-III, but had no effect on mRNA levels of Gl-GC-II(+9), Gl-GC-II(+0), and Gl-EF2.

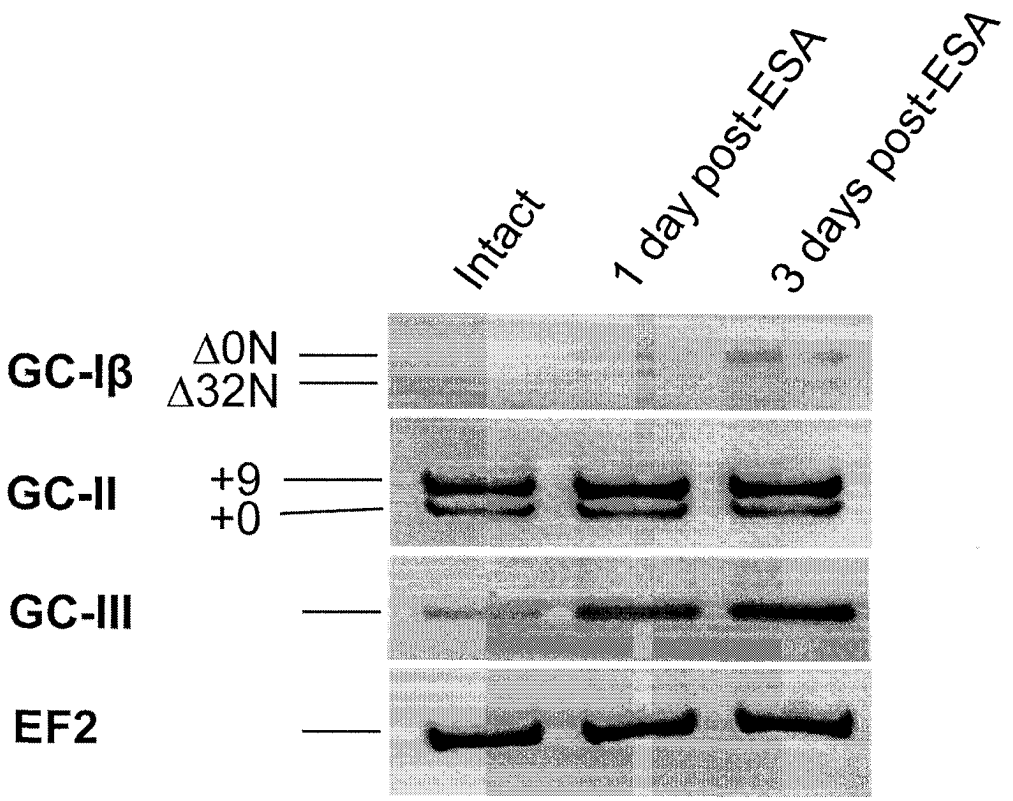

ES ablation removes the primary source of MIH, CHH, and other neuropeptides; the increase in hemolymph ecdysteroid is a secondary response to reduced MIH level. Therefore, an injection of a single dose of 20E was used to determine the direct effects of ecdysteroid in intact animals. Animals were injected with 20E or vehicle (10% ethanol) and tissues were collected at 4 h, 8 h, and 12 h after injection. The 20E injection caused a transient elevation of ecdysteroid levels in the hemolymph, whereas the vehicle had no effect (Fig. 3-12). GC mRNA levels in hepatopancreas, testis, claw muscle, and thoracic muscle were determined by semi-quantitative RT-PCR analysis. Injection of 20E did affect GC expression in the four tissues (Fig. 3-13). In general, if there was an effect on a particular GC, it was usually an initial reduction in mRNA level at high hemolymph 20E concentrations (4 h post-20E injection) followed by a return to preinjection levels at 8 h and 12 h post-injection. The only exceptions were a significant increase in GC-Iβ mRNA in hepatopancreas 12 h post-injection and continued suppression of Gl-GC-II(+0) m RNA in claw muscle at 8 h and 12 h post-injection (Fig. 3-13). The level of Gl-GC-Iβ mRNA was lowered or remained low at 4 h post-20E injection in hepatopancreas, testis, claw muscle, and thoracic muscle. There were significant decreases in Gl-GC-II(+9) mRNA at 4 h in the testis and in Gl-GC-II(+0) mRNA at 4 h in hepatopancreas and thoracic muscle. The response of Gl-GC-II(+18) to 20E injection was similar in claw and thoracic muscles, although the decrease at 4 h post-injection was only significant in claw muscle. There was no significant effect of 20E on Gl-GC-III expression in all four tissues (Fig. 3-13).

Fig. 3-12. Effect of 20-hydroxyecdysone injection on hemolymph ecdysteroid concentration. Intact animals were injected with 20E or vehicle (10% ethanol) and sampled at 4 h, 8 h, 12 h, and 24 h after injection. Ecdysteroid was quantified with radioimmunoassay. 20E caused a large, transient increase in ecdysteroid concentration in the hemolymph (mean ± 1 S.E; n = 10).

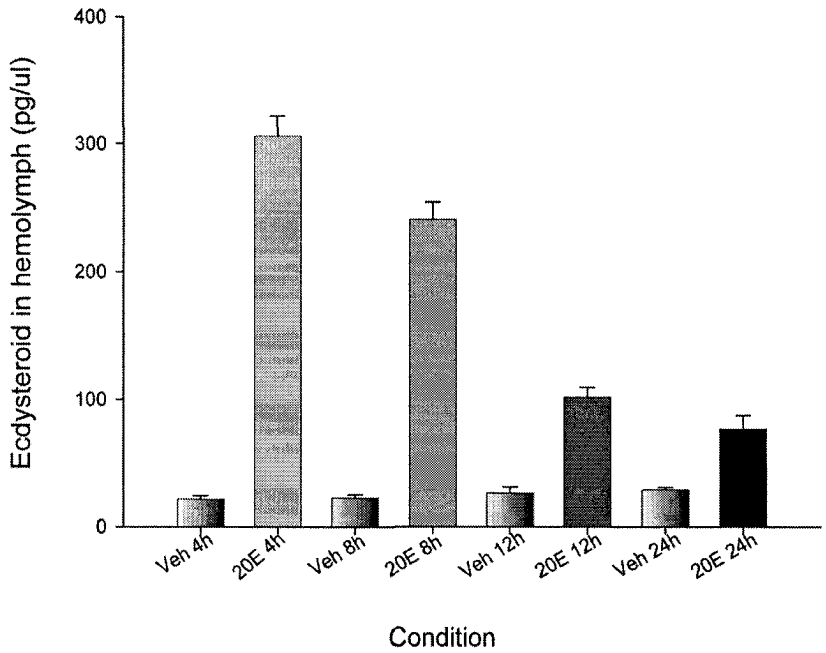

Fig. 3-13. Effects of 20E injection on expression of guanylyl cyclases in hepatopancreas, testis, claw muscle, and thoracic muscle. Intact animals were injected with 20E or vehicle (10% ethanol) and tissues collected at 4 h, 8 h, and 12 h after injection. Total RNA was DNase-treated, reverse-transcribed, and PCR-amplified using sequence-specific primers (see Materials and Methods). PCR products were resolved on 2% agarose gels (for Gl-GC-Iβ, Gl-GC-III, and Gl-EF2) or 10% polyacrylamide gels (for Gl-GC-II), stained with ethdium bromide, and quantified by scanning densitomethry. GC expression was normalized to Gl-EF2 (mean ± 1 S.E.; n = 3). Significant differences between means, obtained by one-way ANOVA post-hoc test (Bonferroni/Dunn), are indicated with brackets (a, $P < 0.05$; b, $P < 0.01$; c, $P < 0.002$).

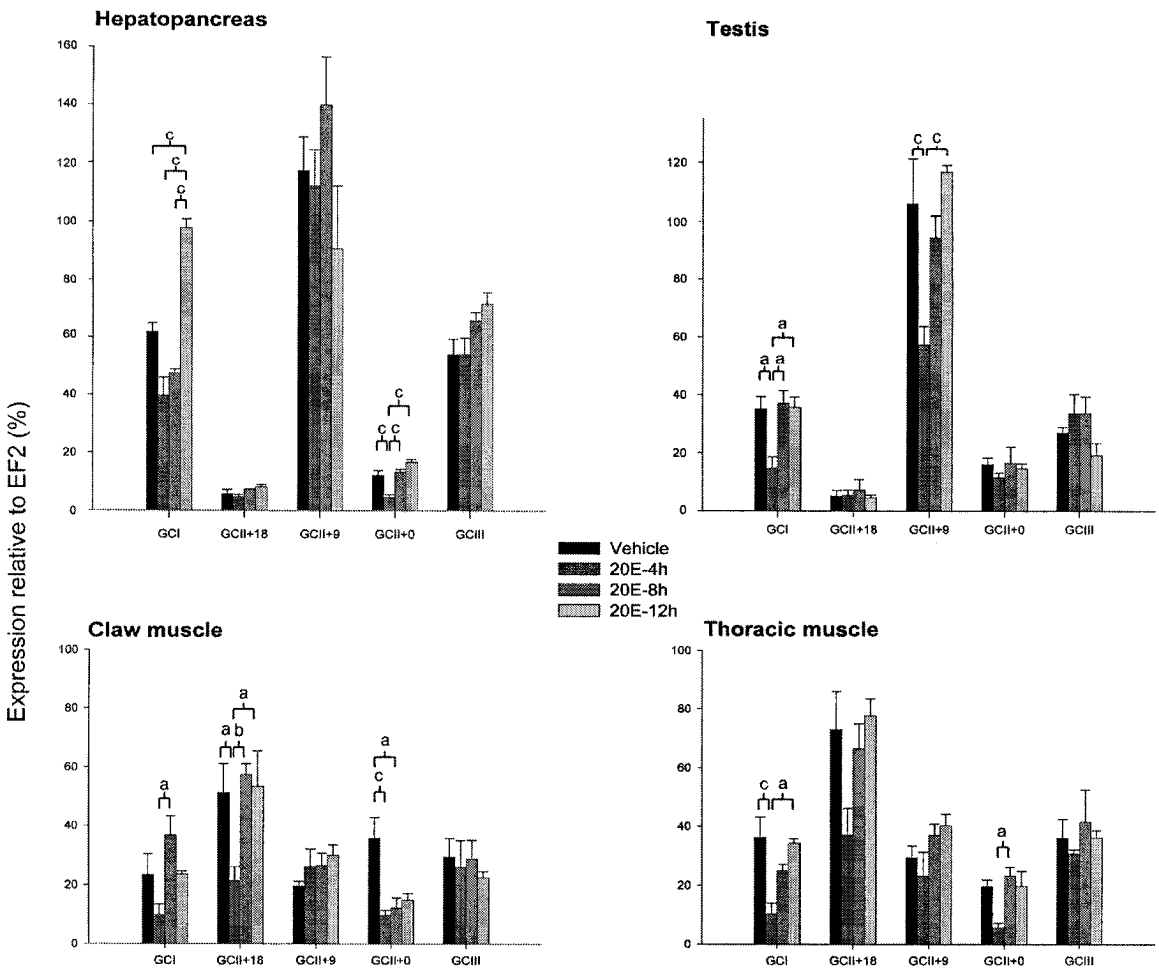

Discussion

GCs can be grouped into four major classes based on sequence identities and domain organization; all animal GCs have highly conserved catalytic domains (Fig. 3-8). As the nomenclature for arthropod GCs is inconsistent, we propose a standardized classification summarized in Table 3-5. GC-I and GC-II are the most thoroughly characterized, as both occur in mammals (Padayatti et al., 2004). GC-I is a NO-sensitive GC with highly conserved HNOB and HNOBA domains in the catalytic subunit (Pyriochou and Papapetropoulos, 2005). GC-II is a NO-insensitive membrane receptor GC with ligand binding, a single-pass transmembrane, kinase homology, and dimerization domains (Potter, 2005). There are two types of receptors in mammals: one type is activated by extracellular ligands, such as atrial natriuretic peptide; the other is activated by intracellular GC activating proteins (Potter, 2005). Arthropods appear to have only the extracellular ligand-binding type (Morton, 2004). The other two classes, GC-III and GC-IV, have only been found in invertebrates (Morton, 2004). GC-III is a NO-insensitive GC related to membrane GCs (Nighorn et al., 2001; Simpson et al., 1999). GC-IV is a NO-insensitive GC related to GC-Iβ (Nighorn et al., 1999). Unlike GC-Iβ and GC-II, in which the catalytic domain is located near the C-terminus, GC-III and GC-IV have long extensions C-terminal to the catalytic domain (Nighorn et al., 1999; Simpson et al., 1999). The three land crab GCs segregate into the GC-I, GC-II, and GC-III classes (Table 3-5; Fig. 3-8); RT-PCR cloning failed to obtain a cDNA encoding a land crab GC-IV.

This is the first report of the cloning of a cDNA encoding the catalytic subunit of a crustacean NO-sensitive GC.

Table 3-5. Proposed classification of cDNAs encoding arthropod guanylyl cyclases.

Class	Crustacean	Insect	Properties & Structure
GC-I	Gl-GC-Iβ[1]	Dm-GC-Iβ[6] Ms-GC-β1[7]	Soluble; NO-sensitive; α, β heterodimer; heme-binding domain at N-terminus; catalytic domain at C-terminus; two isoforms in land crab.
GC-II	Gl-GC-II[2] Cs-GC-YO1[3] Pc-GC-II-M2[4]	Ag- GC-II[8] Dm-DGC1[9] Ms-GC-II[10]	Membrane; NO-insensitive; homodimer; ligand-binding, transmembrane, kinase-homology, dimerization, and catalytic domains; catalytic domain at C-terminus; three isoforms in land crab.
GC-III	Gl-GC-III[5]	Ms-GC-I[11]	Soluble; NO-insensitive; similar to GC-II; homodimer; dimerization and catalytic domains only; novel sequence C-terminal to catalytic domain.
GC-IV	Not detected	Ms-GC-β3[12]	Soluble; NO-insensitive; involved in eclosion hormone action in insect; homodimer; atypical regulatory and catalytic domains only; novel sequence C-terminal to catalytic domain.

Abbreviations: Ag, *Anopheles gambiae*; Cs, *Callinectes sapidus*; Dm, *Drosophila melanogaster*; Gl, *Gecarcinus lateralis*; Ms, *Manduca sexta*; Pc, *Procambarus clarkii.*

GenBank accession numbers: [1]DQ355433 (Gl-GC-Iβ Δ 0N); DQ355434 (Gl-GC-Iβ Δ 32N), [2]DQ355435 (Gl-GC-II+18); DQ355436 (Gl-GC-II+9); DQ355437 (Gl-GC-II+0), [3]AY785292, [4]AAQ74970, [5]DQ355438, [6]AAA87941, [7]AAC61264, [8]XP320371, [9]AAA74408, [10]AAN16469, [11]AAC62238, [12]AAD09836

The catalytic domain of Gl-GC-Iβ (Fig. 3-3) has conserved secondary structures (α-4, β-2, β-3, and β-5) and residues (E466, R532, and C534) in the purine-binding pocket (Sunahara et al., 1998), suggesting that the protein has GC activity. The HNOBA domain (Fig. 3-3) contains an amphipathic α-helical linker region involved in heterodimer formation (Iyer et al., 2003). Two Gl-GC-Iβ isoforms, most likely generated by alternative mRNA splicing, differ in the presence or absence of a 32 amino acid sequence at the N-terminus (Fig. 3-2; Table 3-3). Truncated isoforms of GC-Iβ have not been reported previously. It may be an NO-insensitive protein, as the N-terminal sequence of mammalian NO-sensitive GC is required for NO/heme activation (Foerster et al., 1996; Koglin and Behrends, 2003). Amino acid residues important for heme binding and activation have been identified. Mutations of mammalian GC-Iβ at cysteines 78 and 214 significantly decrease heme-binding affinity (Friebe et al., 1997). Substitution of histidine 105 with phenylalanine, alanine, or glycine produces a heme-deficient apo-enzyme (Foerster et al., 1996; Wedel et al., 1994; Zhao et al., 1998). Tyrosine 135 and arginine 139 are also critical for heme binding and NO activation (Schmidt et al., 2004). Although none of these conserved residues are located in the 32-amino acid N-terminal sequence, a 64 amino acid deletion at the N-terminus of bovine GC-Iβ eliminates NO sensitivity, although it retains basal activity (Foerster et al., 1996). Moreover, a 13-amino acid sequence at the N-terminus (MYGFVNYAIEQLV) is highly conserved in all GC-Iβ cDNAs (e.g., 12 of the 13 residues are identical between land crab and insect; Fig. 3-3), suggesting this region plays a critical role in heme/NO binding. These data suggest that

the Gl-GC-Iβ(Δ32) isoform would be able to dimerize with the α subunit to form a NO-insensitive protein that is constitutively active.

NO-sensitive GC has a more restricted tissue distribution than receptor GCs. As NO is rapidly metabolized, it must be produced at or near the target tissue. Thus, it is not surprising that the tissue expression is similar between NO synthase (NOS) and GC-Iβ. Both NOS and GC-I are highly expressed in nervous tissues of arthropods and mammals (Aonuma, 2002; Collmann et al., 2004; Mahadevan et al., 2004; Nighorn et al., 1998; Prabhakar et al., 1997; Scholz et al., 1996; Scholz et al., 2002). Lobster tissues with significant NO-sensitive GC activity are intestine, hepatopancreas, nerve cord, heart, and gill (Prabhakar et al., 1997). In land crab, NOS and GC-Iβ are co-expressed in ES ganglia, thoracic ganglion, gill, ovary, and testis (Kim et al., 2004) (Fig. 3-9). An exception is the YO, in which Gl-NOS is expressed at moderate levels (Kim et al., 2004), whereas Gl-GC-Iβ is expressed at very low levels in intact animals (Fig. 3-9). However, ES ablation induces an increase in GC-Iβ mRNA (Fig. 3-11), suggesting the YO responds to the absence of neuropeptide(s) by increasing its sensitivity to hormone. The YOs of other decapods display altered responses to ecdysteroid and neuropeptides over the molt cycle (Chung and Webster, 2003; Dell et al., 1999; Nakatsuji and Sonobe, 2004). These data suggest that altered YO sensitivity during the molt cycle is mediated in part through NO-sensitive GC.

Gl-GC-II is a member of a large family of membrane receptor GCs that bind a variety of ligands. In mammals, seven membrane GCs differ in ligand-binding properties and physiological functions: GC-A binds atrial natriuretic peptide and brain natriuretic peptide; GC-B binds C-type natriuretic peptide; GC-C binds bacterial heat-stable

enterotoxins and endogenous peptides guanylin, lymphoguanylin, and uroguanylin; GC-E and GC-F are activated by intracellular GC activating proteins in response to decreased Ca^{2+}; and GC-D and GC-G are orphan GCs with no known ligands or functions (Lucas et al., 2000; Padayatti et al., 2004). The crustacean and insect GC-IIs are most similar to the mammalian GC-IIs that bind extracellular ligands. The extracellular region of the three crustacean GC-IIs all have the highly conserved amino acid residues and most of the N-linked glycosylation sites required for ligand binding (Fig. 3-5).

GC-II appears to be the receptor for CHH, an ES neuropeptide that regulates glucose and lipid metabolism, ion transport, and other processes in crustacean tissues (Chung et al., 1999; Dircksen et al., 2001; Santos and Keller, 1993; Santos et al., 1997; Sedlmeier, 1988; Serrano et al., 2003). CHH increases cGMP levels in target tissues by way of a membrane receptor GC (Chung and Webster, 2003; Goy, 1990; Goy et al., 1987; Pavloff and Goy, 1990; Scholz et al., 1996; Sedlmeier and Keller, 1981). Given its pleiotropic effects, one would expect the CHH receptor to be expressed in all tissues. Crayfish, blue crab, and land crab (Gl-GC-II+9) membrane receptor GCs are expressed at varying levels in all tissues examined (Liu et al., 2004; Zheng et al., 2006) (Fig. 3-9). Moreover, the Gl-GC-II(+9) is the dominant isoform in hepatopancreas and YO (Fig. 3-9), both of which have high-affinity CHH receptors (Chung and Webster, 2003; Kummer and Keller, 1993; Webster, 1993).

Three different Gl-GC-II isoforms, which are probably generated by alternative splicing, were identified (Fig. 3-4). Only a single GC-II variant has been described in crayfish and blue crab (Liu et al., 2004; Zheng et al., 2006); these cDNAs are equivalent to the Gl-GC-II(+9) isoform (Fig. 3-5). The Gl-GC-II isoforms varied in length within the

ligand-binding domain (Table 3-3). The insertions occur in a hypervariable region flanked by highly conserved sequences in the three crustacean GC-II cDNAs (Fig. 3-5). This hypervariable region differs in length and sequence between the three species, which suggests that this region contributes to species-specific ligand specificities. Gl-GC-II(+18) was expressed highly in heart and skeletal muscle; Gl-GC-II(+9) was expressed in all tissues; and Gl-GC-II(+0) was expressed in most tissues (Fig. 3-9). The different tissue distributions suggest the Gl-GC-II isoforms have different functions. Many crustacean species express two or more CHH isoforms that differ in biological activities (Bulau et al., 2003; Bulau et al., 2005; Chung et al., 1999; Chung et al., 1998; Dircksen et al., 2001; Gu and Chan, 1998; Marco et al., 2003; Serrano et al., 2003; Soyez et al., 1994; Yang et al., 1997; Yasuda et al., 1994). The three land crab isoforms may differ in CHH isoform binding, thus conferring a specific response of a tissue to hormone(s).

The identity of the MIH receptor remains controversial. YO membranes have distinct receptors for both CHH and MIH (Chung and Webster, 2003; Webster, 1993). As MIH and CHH are members of the same neuropeptide family, it seems reasonable to expect that they would be ligands for related membrane receptors. While there is compelling data supporting the CHH receptor as a GC-II, the data do not support the MIH receptor as another GC-II. Only one GC-II has been isolated in crustacean tissues (Liu et al., 2004; Zheng et al., 2006). Importantly, the wide tissue distribution of the three isoforms is not consistent with the role of GC-II as an MIH receptor. As MIH-binding capacity is highest in YO membranes (Asazuma et al., 2005), a receptor for MIH would be expected to be expressed preferentially in the YO. This is not the case for any GC-II isoform (Fig. 3-9). Moreover, cross-linking prawn ^{125}I-MIH with YO membrane labeled a

~70 kDa protein (Asazuma et al., 2005), which is about one-half the estimated nonglycosylated masses of the membrane GC cDNAs from crayfish, blue crab, and land crab (Liu et al., 2004; Zheng et al., 2006)(Table 3-3). The actual mass of the GC-II is probably larger due to extensive N-linked glycosylation in the extracellular domain, which is necessary for ligand binding and activation (Padayatti et al., 2004). Finally, the up-regulation of Gl-GC-Iβ in YOs of ES-ablated animals (Fig. 3-11) supports the hypothesis that a NO-sensitive GC, and not a membrane receptor GC, mediates MIH signaling. Although these data suggest that the MIH receptor is not a membrane GC, the identity of the MIH receptor will not be resolved until the protein is isolated and characterized fully.

A partial cDNA encoding a NO-insensitive soluble GC was cloned, indicating that members of the GC-III class occur in arthropods other than insects. The only other member, Ms-GC-I, is expressed in the nervous system of *M. sexta* and is associated with membranes *in vivo* (Nighorn et al., 2001; Simpson et al., 1999). It has high catalytic activity that is insensitive to NO (Simpson et al., 1999). The catalytic domains of Gl-GC-III and Ms-GC-I are more similar to the catalytic domains of membrane receptor GCs than NO-sensitive GCs (Fig. 3-8). The members of this class have dimerization and catalytic domains, but lack the ligand-binding, transmembrane, and kinase homology domains found in GC-IIs (Figs. 3-1, 3-7). The tissue distribution of Gl-GC-III is similar to that of Gl-GC-Iβ, as its highest expression is in ES ganglia, gill, hepatopancreas, ovary, and testis (Fig. 3-9). In addition, both Gl-GC-Iβ and Gl-GC-III are up-regulated in YOs in response to ES ablation (Fig. 3-11). These data suggest that there is a functional

interaction between Gl-GC-Iβ and Gl-GC-III such that both play a role in a tissue's response to NO.

Both cAMP and cGMP inhibit YO ecdysteroidogenesis, although cGMP appears to be the principal secondary messenger associated with MIH action on the YO in most species (Baghdassarian et al., 1996; Böcking and Sedlmeier, 1994; Chung and Webster, 2003; Mattson and Spaziani, 1985; Mattson and Spaziani, 1986; Saidi et al., 1994; Sedlmeier and Fenrich, 1993; Spaziani et al., 1999; Von Gliscynski and Sedlmeier, 1993). Any signaling mechanism should account for the action of both cAMP and cGMP. We propose a pathway involving a G protein-coupled MIH receptor, adenylyl cyclase, NO synthase, and GC-I (Kim et al., 2004; Lee et al., 2006). YOs express a trimeric G protein (Han and Watson, 2005), NOS (Kim et al., 2004), and NO-sensitive GC (Fig. 3-9A, 3-11). Activators of adenylyl cyclase inhibit YO ecdysteroidogenesis (Mattson and Spaziani, 1985; Mattson and Spaziani, 1986; Saidi et al., 1994; Sedlmeier and Fenrich, 1993). MIH stimulates cGMP-dependent and cAMP-dependent kinases (PKG and PKA, respectively) (Baghdassarian et al., 1996; Böcking and Sedlmeier, 1994; Spaziani et al., 1999; Von Gliscynski and Sedlmeier, 1993). This pathway is similar to that inhibiting ecdysteroidogenesis in blowfly ovary, except that cAMP and cGMP are antagonists. Stimulation of ecdsteroid secretion by cAMP is blocked by cGMP (Maniere et al., 2003). A cGMP analog and phosphodiesterase inhibitors (IBMX and MDBAMQ) suppress ecdysteroid secretion by previteollogenic and vitellogenic ovaries *in vitro* (Maniere et al., 2003). Moreover, sodium nitroprusside, a NO donor, inhibits ecdysteroid secretion (Maniere et al., 2003). Reduced ecdysteroid secretion results from the activation of PKG, as KT 5823, a specific PKG inhibitor, increases secretion by previteollogenic and

vitellogenic ovaries (Maniere et al., 2003). Taken together these data suggest an inhibitory pathway involving NOS and GC-I in blowfly ovary. Zheng et al. (2006) report unpublished data that sodium nitroprusside has no effect on ecdysteroid secretion on blue crab YOs *in vitro*. However, negative results are difficult to interpret without knowing if the NO donor actually raised intracellular cGMP levels. NO is highly volatile and may have been metabolized before reaching levels needed to activate the GC-I.

The activation of ecdysteroid-responsive genes regulates development, reproduction, growth, and molting in arthropods (Chang, 1993; Kozlova and Thummel, 2000; Skinner, 1985; Truman and Riddiford, 1999). Ecdysteroid regulates crustacean gene expression through a heterodimeric nuclear hormone receptor consisting of ecdysone receptor (EcR) and retinoic-X receptor (RXR) (Durica et al., 2002; Wu et al., 2004). ES ablation, which produces a large sustained increase in ecdysteroid (Table 3-4), had no significant effect on GC expression in most tissues (Fig. 3-9). There were only two exceptions. Gl-GC-II(+18) mRNA increased in claw muscle in response to ES ablation and was correlated with hemolymph ecdysteroid, but not in heart or thoracic muscle (Figs. 3-9B, 3-10). This differential response to ES ablation is consistent with a previous study showing that ES ablation stimulates expression of EcR and calpain T in claw muscle specifically (Kim et al., 2005a). The different sensitivities of claw and thoracic muscles may be due to differences in the expression of RXR isoforms, which dimerize with EcR to form ecdysteroid receptors that differ in ligand and DNA binding properties (Kim et al., 2005b; Wu et al., 2004). ES ablation also induced a large increase in Gl-GC-Iβ and Gl-GC-III mRNAs in YOs without affecting Gl-GCII mRNAs (Fig. 3-11). Except for the YO, neither ES ablation nor 20E injection had any affect on Gl-GC-III mRNA levels in

all other tissues, indicating that its expression is not regulated by ecdysteroid in most tissues (Figs. 3-9B, 3-13).

As ES ablation removes the major site for the synthesis of MIH, CHH, and other neuropeptides, the response of tissues may be due to reduced ES factors, increased ecdysteroid, or a combination of the two. 20E was injected into intact animals to determine the direct effects of ecdysteroid on GC expression in hepatopancreas, testis, claw muscle, and thoracic muscle. A common pattern for those GCs showing significant changes was a reduced or low mRNA level at 4 h post-injection followed by restored or increased levels at 8 h and 12 h post-injection. These data suggest that high ecdsyteroid levels, which were comparable to those at the end of the premolt period (Skinner, 1985), can repress expression of Gl-GC-Iβ in all four tissues and certain Gl-GC-II isoforms in certain tissues (Fig. 3-13).

The GCs constitute a diverse family of enzymes. The discovery of Gl-GC-Iβ and Gl-GC-II isoforms adds further complexity. The truncated Gl-GC-Iβ subunit may form a constitutively active enzyme no longer regulated by NO. The three Gl-GC-II isoforms may differ in ligand binding properties. Not surprisingly, the expression of the three GC classes and NOS (Kim et al., 2004) in crustacean tissues other than the nervous system suggests that cGMP has functions in addition to neuromodulation. Our particular interest is the possible role of cGMP signaling in the crustacean molting gland. The inhibition of YO ecdysteroidogenesis by both MIH and CHH is associated with large increases in intracellular cGMP (Chung and Webster, 2003; Saidi et al., 1994). It appears that the two neuropeptides accomplish this using two different signaling pathways. CHH acts directly via binding to a membrane receptor GC (Goy, 1990). MIH may stimulate GC-I by

activating NOS (Kim et al., 2004; Lee and Mykles, 2006). The two methods (ES ablation and 20E injection) used to increase hemolymph ecdysteroid levels elicited very different responses by tissues. ES ablation induced a three-fold increase of Gl-GC-II(+18) in claw muscle, suggesting it has a role in molt-induced atrophy (Mykles, 1997). ES ablation increased Gl-GC-Iβ and Gl-GC-III expression in the YO, suggesting the tissue is compensating for low MIH levels in the hemolymph. 20E at high doses generally had a transient inhibitory effect on the expression of Gl-GC-Iβ and some Gl-GC-II isoforms, most likely resulting from the rapid clearance of 20E from the hemolymph. These data indicate that there are interactions between ES neuropeptides and ecdysteroids that can affect the expression of GCs in tissues. The three GC classes represent diverse GC signaling mechanisms, all of which may play roles in modulating gene expression during molting.

CHAPTER FOUR*

PROTEOMICS AND SIGNAL TRANSDUCTION IN THE CRUSTACEAN MOLTING GLAND

Abstract

Regulation of the molting cycle in decapod crustaceans involves two endocrine organs: the X-organ/sinus gland (XO/SG) complex located in the eyestalk ganglia and the Y-organ (YO) located in the cephalothorax. At least two neuropeptides (molt-inhibiting hormone or MIH and crustacean hyperglycemic hormone or CHH) are produced in the XO/SG complex and inhibit ecdysteroidogenesis in the YO. Thus, YO activation is induced by eyestalk ablation (ESA), which removes the primary source of MIH and CHH. Cyclic nucleotides (cAMP and cGMP) and nitric oxide (NO) appear to mediate neuropeptide suppression of the YO. Proteomics was used to identify components of signal transduction pathways ("targeted" or cell-map proteomics) as well as assess the magnitude of protein changes in response to activation ("global" or expression proteomics) in the tropical land crab, *Gecarcinus lateralis*. Total proteins in YOs from intact and ES-ablated animals were separated by 2-dimensional gel electrophoresis and expression profiles were assessed by image analysis and gene clustering software. ESA caused a >3-fold increase in the levels of 170 proteins and >3-fold decrease in the levels of 89 proteins; a total of 543 proteins were quantified in total YO extracts. ESA induced

significant changes in the levels of three groups of proteins eluting from a phosphoprotein column and detected with phosphoprotein staining of 2-dimensional gels; ~17 kDa and ~150 kDa phosphoproteins increased in activated YOs, while ~12 kDa phosphoproteins decreased. A ~150 kDa phosphoprotein, which was isolated only from activated YO, was identified as NO synthase by Western blotting and mass spectrometry of trypsin peptides. These data show that phosphorylation of NO synthase is associated with activation of the molting gland.

---

*This Chapter has been submitted to *Integrative Comparative Biology* as follow:

Proteomics and signal transduction in the crustacean molting gland

Sung Gu Lee and Donald L. Mykles*

Department of Biology, Colorado State University, Fort Collins, CO 80523, USA

Introduction

"Proteomics" was coined about 10 years ago and is defined as a "systematic analysis of proteins expressed by a genome" (Dhingra et al., 2005). As many physiological processes are regulated post-transcriptionally, proteomics has become an important tool for examining protein expression profiles, protein-protein interactions, and post-translational modifications associated with physiological states. Proteomics can be divided into two major categories: expression and cell-map proteomics (Blackstock and Weir, 1999). Expression proteomics provides a "global" view by quantifying protein expression profiles in cell or tissue extracts using 2-dimensional gel separation and image analysis. It offers the potential to elucidate interactions within and between metabolic pathways and discover markers for diseases (Blackstock and Weir, 1999). Cell-map proteomics uses specific antibodies and/or chromatography resins to characterize a subset of proteins (e.g. phosphoproteins) (Blackstock and Weir, 1999). This "targeted" approach can elucidate functional interactions, such as cell signaling mechanisms (Collins et al., 2005).

Proteomics is a potential tool for elucidating signal transduction mechanisms in the crustacean molting gland, or Y-organ (YO). The YOs, a pair of epithelioid glands located in the cephalothorax, synthesize ecdysone and related ecdysteroids from cholesterol (Lachaise et al., 1993; Skinner, 1985). The YOs are negatively regulated by a neuropeptide, molt-inhibiting hormone (MIH), which are synthesized and secreted by the X-organ/sinus gland complex in the eyestalks (Chan et al., 2003). Consequently, eyestalk ablation (ESA) induces precocious molting by eliminating the primary source of MIH

(Skinner, 1985). The YOs, no longer repressed, hypertrophy and synthesize new protein before ecdysteroidogenesis begins (Lachaise et al., 1993). However, regulation of ecdysteroidogenesis in the YOs is more complex. Vitellogenesis can inhibit molting (Lachaise et al., 1992) and ES-ablated animals continue to show molt cycle-dependent fluctuations in hemolymph ecdysteroid titers (Chang, 1985; Hopkins, 1983). In addition, the XO produces other neuropeptide hormones, including crustacean hyperglycemic hormone (CHH), gonad-inhibiting hormone (GIH), and mandibular organ-inhibiting hormone (MOIH), which may have direct or indirect effects on the YO (Borst et al., 2002; Chung et al., 1999; Cooper and Ruffner, 1998; Cromarty and Kass-Simon, 1998; De Kleijn and Van Herp, 1995; Dircksen et al., 2001). Both MIH and CHH directly inhibit YO ecdysteroid secretion via high-affinity membrane receptors and cAMP and cGMP as second messengers (Baghdassarian et al., 1996; Böcking and Sedlmeier, 1994; Chung and Webster, 2003; Saidi et al., 1994; Sedlmeier and Fenrich, 1993; Von Gliscynski and Sedlmeier, 1993; Webster, 1993). An optimal intracellular Ca^{2+} concentration is necessary to maintain ecdysteroidogenesis, as extremes in intracellular Ca^{2+} inhibit ecdysteroidogenesis (Spaziani et al., 2001).

Studies showing MIH causes large increases intracellular cGMP led us to examine if NO synthase (NOS) and guanylyl cyclases (GCs) are expressed in the land crab YO. NOS produces NO by converting L-arginine to L-citrulline. NOS is regulated by Ca^{2+}/calmodulin (CaM) and phosphorylation (Bivalacqua et al., 2004; Bredt et al., 1992; Dawson et al., 1998; Ghosh and Salerno, 2003; Kone, 2001; Stasiv et al., 2001; Wang and Marsden, 1995). NO activates a Class I GC (GC-I), which is a heterodimeric protein consisting of α and β subunits. Using RT-PCR, we cloned from the land crab cDNAs

encoding NOS (Gl-NOS) and three classes of GCs, including the β subunit of NO-sensitive GC (Gl-GC-Iβ); all four genes are expressed in the YO (Kim et al., 2004; Lee et al., 2005). The open reading frame of the Gl-NOS cDNA codes for an 1199-amino acid protein with an estimated mass of ~136 kDa. The domain organization is highly conserved, with a CaM-binding domain located between the oxygenase and reductase domains (Kim et al., 2004). All three GCs have highly conserved catalytic domains at the C-terminus (Lee et al., 2005).

Despite intense study, our knowledge of the neuroendocrine regulation of the YO is still incomplete. Few of the components, including the MIH receptor, have been cloned and characterized. We reasoned that proteomics could be applied to quantify time-dependent changes in proteins associated with ecdysteroidogenesis. Proteomic analysis of phosphoproteins was used to identify potential components of the neuropeptide signaling transduction pathways. YO activation is accompanied with large-scale changes in protein levels, including phosphorylation of NOS.

Materials and Methods

Animals

Blackback land crabs, *Gecarcinus lateralis*, were collected from Puerto Rico or the Dominican Republic, shipped via air freight to Colorado, and maintained as described (Kim et al., 2004). All animals were at the intermolt stage. Eyestalk ablation (ESA) was used to activate the YOs by eliminating the primary source of MIH (Skinner, 1985). Wounds were cauterized with a heated spatula to minimize loss of hemolymph.

Sample preparation

For the analysis of global changes in protein composition, 6 YOs were homogenized in 200 µl lysis buffer [7 M urea, 2 M thiourea, 4% CHAPS, 66 mM dithiothreitol, and 1x protease inhibitor cocktail (2 mM AEBSF, 1 mM EDTA, 130 µM bestatin, 14 µM E-64, 1 µM leupeptin, and 0.3 µM aprotinin)] using a Dounce homogenizer. The lysate was centrifuged at 40,000 xg for 1 h and the protein concentration in the supernatant was determined with the Bradford reagent (Sigma) using BSA as standard. Aliquots were stored at -80°C until analysis.

For the analysis of phosphoproteins, a PhosphoProtein purification kit (Qiagen) was used according to manufacturer's protocol. Briefly, YOs were homogenized in 5 ml phosphoprotein lysis buffer containing 0.25% CHAPS, 1 Protease inhibitor tablet, and 10 µl Benzonase stock solution (the concentration was not provided) using a Dounce homogenizer. After 30 min at 4°C, the lysate was centrifuged at 10,000 xg at 4 °C for 30 min. The supernatant fraction was adjusted to 0.1 mg protein/ml with phosphoprotein

lysis buffer and loaded onto a phosphoprotein purification column equilibrated with lysis buffer. The column was washed with 6 ml lysis buffer and phosphoproteins were eluted with 500 µl elution buffer containing 0.25% CHAPS. The elution step was repeated four times. Eluate fractions were combined and protein was concentrated using Nanosep ultrafiltration columns included with the kit. The final protein concentration was measured by the Bradford method. A typical yield was 80-90 µg phosphoprotein from 5 mg total protein in YO extracts. Aliquots were stored at –80 °C until analysis.

Two-dimensional gel electrophoresis

Immobiline™ DryStrip (Amersham Biosciences) immobilized pH-gradient (IPG) strips were used for the first-dimensional isoelectric separation of proteins using the Amersham IPGphor system (Bjellqvist et al., 1982; Gorg et al., 1988). Before isoelectrofocusing, 0.5% 4-7 or 3-10 IPG buffer (Amersham Biosciences) was added to the protein sample. Protein was loaded onto 7-cm pH 4-7 linear IPG strips using an in-gel rehydration method (Rabilloud et al., 1994; Sanchez et al., 1997). The isoelectrofocusing conditions were as follows: 1 h at 500 V, 1 h at 1,000 V, and at 5,000 V for a total of 17 kVh at 20 °C. After isoelectrofocusing the strips were equilibrated in a buffer containing 30% glycerol, 6 M urea, 2% SDS, 10 mg/ml dithiothreitol, and 0.05 M Tris-HCl (pH 6.8) for 15 min and then for an additional 15 min in equilibration buffer in which 42.5 mg/ml iodoacetamide replaced the dithiothreitol. The strips were positioned at the top of 12.5% polyacrylamide gels with 0.5% agarose containing Laemmli sample buffer (50 mM Tris, 384 mM glycine, and 0.1% SDS). SDS-polyacrylamide gel electrophoresis was performed in Laemmli electrophoresis buffer at 150 V at room temperature.

Proteins were stained with silver or with Pro-Q® Diamond Phosphoprotein Gel Stain kit (Molecular Probes, Eugene, OR, USA). For silver staining, gels were fixed in 40% ethanol and 10% acetic acid for 1 h, rehydrated in 5% ethanol and 5% acetic acid for 2 h, and sensitized in 0.05% (w/v) 2,7-naphthalenedisulfonic acid for 30 min. After three 5-min washes in double-distilled water, the gels were stained in ammoniacal silver nitrate solution for 30 min. To prepare 100 ml of this solution, 0.4 g silver nitrate was dissolved in 4 ml of deionized water, which was slowly mixed into a solution containing 16 ml of water, 700 µl of 25% NH_4OH and 100 µl 10 N NaOH. After staining the gels were washed 3 times in deionized water for 5 min each. The gels were developed in a solution containing 0.05% (w/v) citric acid and 0.05% formaldehyde for 5 to 10 min.

For phosphoprotein staining, gels were fixed in 50% methanol and 10% acetic acid for at least 30 min, rinsed three times with distilled deionized water, stained 60-90 min in the dark with Pro-Q Diamond phosphoprotein gel stain, and rinsed three times for 30 min with destaining solution (20% acetonitrile and 50 mM sodium acetate; pH 4.0). Images were captured with a BioRad Molecular Imager FX at 555 nm excitation.

Image analysis

Digitized images of two-dimensional gels were analyzed using PDQuest v7.3 software (Bio-Rad). Quantified proteome data from intact and ES-ablated animals were selected for clustering analysis (Eisen et al., 1998) using the Cluster program (http://rana.stanford.edu). Hierarchical clustering analysis was performed without the "time zero" mathematical transformation of the data from experiments in which a reference pool was used. The data were weighted according to the overall similarity of

each proteome to others in the data set, which served to under-weight proteomes that were highly similar. K-means clustering was carried out with a K number of 6. The Euclidean distance metric was used for both hierarchical and K-means clustering. The resulting clusters were visualized using TreeView software (http://rana.stanford.edu/software/).

Production of anti-NOS polyclonal serum and Western blot analysis

Antheprot software (http://antheprot-pbil.ibcp.fr) was used to design the antigenic peptide from the N-terminal region of land crab NOS (NH_2-IKRYKSEQHRLRWKQVCREV-COOH) (Kim et al., 2004). Peptide synthesis and antibody production was performed by Macromolecular Resources at Colorado State University. The peptide was conjugated to the C-terminal cysteine of keyhole lympet hemocyanin and used to immunize and boost two rabbits at bi-weekly intervals for 70 days.

After 2-dimensional gel electrophoresis, protein was electrophoretically transferred to Hybond-P PVDF membrane (Amersham Biosciences) in transfer buffer (50 mM Tris base, 384 mM glycine, 20% methanol) for 1 h at 100 V. Blots were blocked overnight at 4 °C in TTBS (20 mM Tris-HCl, pH 7.5; 140 mM NaCl; 0.05% Tween-20; and 3% bovine serum albumin) and incubated with land crab NOS antiserum (1:5,000 dilution in TTBS) for 2 h at room temperature. After washing in TTBS (3 times at10 min each), blots were incubated with alkaline phosphatase-conjugated rabbit immunoglobulin G antibody (Sigma; 1:10,000 in TTBS), washed in TTBS (3 times at 10 min each), and

developed colorimetrically with 5-bromo-4-chloro-3-indolyl phosphate and nitro blue tetrazolium.

Mass spectrometry

Protein was excised from silver-stained gels; silver was removed prior to tryptic digestion as described (Gharahdaghi et al., 1999). Briefly, gel plugs were incubated in a 1:1 solution of 30 mM potassium ferricyanide and 100 mM sodium thiosulfate until the silver was removed. The plugs were washed 3 times with distilled deionized water and incubated with 100 mM ammonium bicarbonate (pH 7.8) for 30 min. The gel plugs were then transferred to acetonitrile and dried in a Speed Vac. Proteins were digested overnight in 5 µl 25 ng/µl modified sequencing-grade trypsin (Promega) in 50 mM ammonium bicarbonate (pH 7.8) at 37 °C.

For MALDI-TOF spectrometry, a sample crystal mixture was prepared by the modified dried-droplet method (Gobom et al., 1999). Briefly, the tryptic digest was directly applied to POROS R2 fast flow C_{18} resin (Applied Biosystem) in a gel loading tip (Eppendorf). The resin was washed with 30 µl 0.5% trifluoroacetic acid (TFA) and peptides were eluted with 1 µl matrix solution (α-cyano-4-hydroxy-cinnamic acid) saturated in 50% acetonitrile and 0.5% TFA. The elution was divided into several spots on a target plate to eliminate matrix-saturated fractions and air-dried. MS spectrum data were acquired on a MALDI TOF/TOF (ultraflex II TOF/TOF, Bruker Daltonics, Germany) in reflectron mode. Reflectron spectra were acquired using the delayed extraction technique in positive ion mode with an acceleration voltage of 1.5 kV. About 100 laser shots were summed to acquire the spectra.

Obtained mass spectra were analyzed by m/z software (Proteometrics), and the spectrum peak list was manually subjected to database search using MASCOT (http://www.matrixscience.com) or ProFound (http://129.85.19.192/profound_bin/WebProFound.exe), or manually analyzed with theoretically digested peak lists of Gl-NOS.

Results

Changes in proteins in the activated Y-organ

Total extracts of Y-organs from intact, 1 day post-ESA, and 3 days post-ESA land crabs were separated by 2-dimensional gel electrophoresis. A master image was built from the digitized images of the three gels; a total of 543 proteins were analyzed with pI's between 4 and 7 using the BioRad PDQuest software (Fig. 4-1). YO activation in response to ESA caused large changes in protein levels, with about half of the proteins showing a change of at least 3-fold by 3 days post-ESA. ESA resulted in more than 3-fold increases of 170 proteins (Fig. 4-1, red circles in the master image) and 3-fold decreases in 89 proteins (Fig. 4-1, green crosses in the master image).

Clustering software was originally designed to analyze expression patterns in DNA microarrays, but it worked well for the analysis of protein expression. The data on the 543 proteins were subjected to clustering analysis to identify proteins with similar expression profiles in response to ESA. Two clustering methods, hierarchical and K-means, were applied to analyze the YO proteome profile (Figs. 4-2, 4-3). Hierarchical clustering organized the 543 proteins into 26 groups, and made relational chains in a single cluster based on the expression profiles after ES ablation (Fig. 4-2). The results are shown as a "heat map" with the levels in intact animals serving as a reference. Increased levels are represented as different intensities of red; decreased levels are represented as different intensities of green. K-means clustering was done by grouping separately the proteins showing the most similar expression profiles in terms of magnitude and direction of changes in response to ESA (Fig. 4-3).

Fig. 4-1. "Global" proteomics: changes in proteins associated with activation of the molting gland (Y-organ). Land crabs were ES-ablated to reduce circulating MIH and stimulate YO ecdysteroidogenesis. Protein (35 μg) in total extracts of YOs from 10 intact (non-stimulated), 10 1-day post-ESA, and 10 3-day post-ESA animals were separated by two-dimensional gel electrophoresis and stained with silver. Gels were scanned and analyzed using Bio-Rad PDQuest software. A master image was built from the three digitized images and protein levels were quantified; red circles indicate proteins that increased >3-fold by ESA and green crosses indicate proteins that decreased >3-fold by ESA.

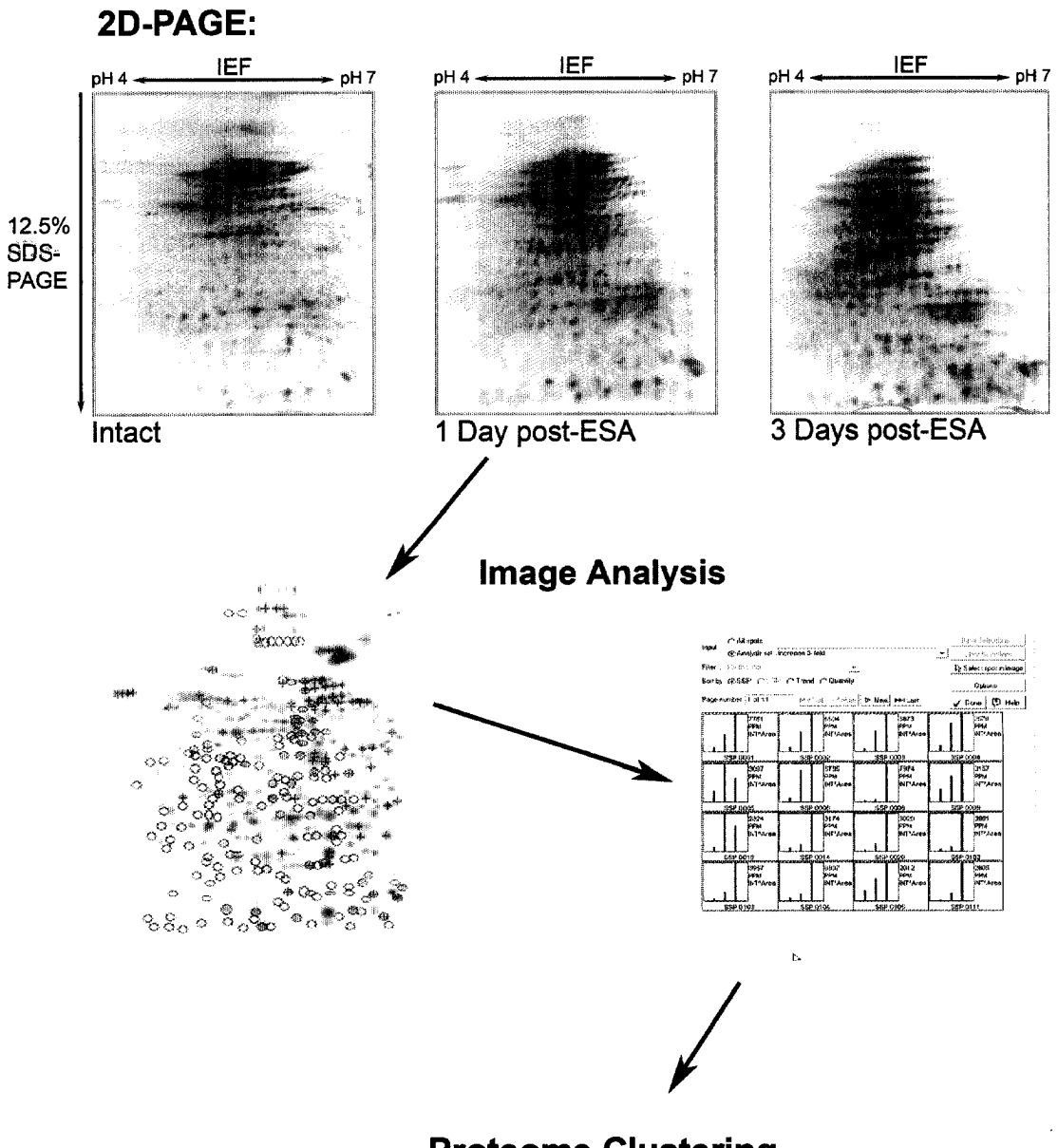

Fig. 4-2. Hierarchical clustering analysis of Y-organ protein expression in response to ES ablation. Hierarchical clustering, displayed as a "heat map", groups proteins responding similarly to ESA and thus may be metabolically linked; green color indicates decreased protein levels with respect to intact control, red indicates increased levels, and black indicates no change in levels.

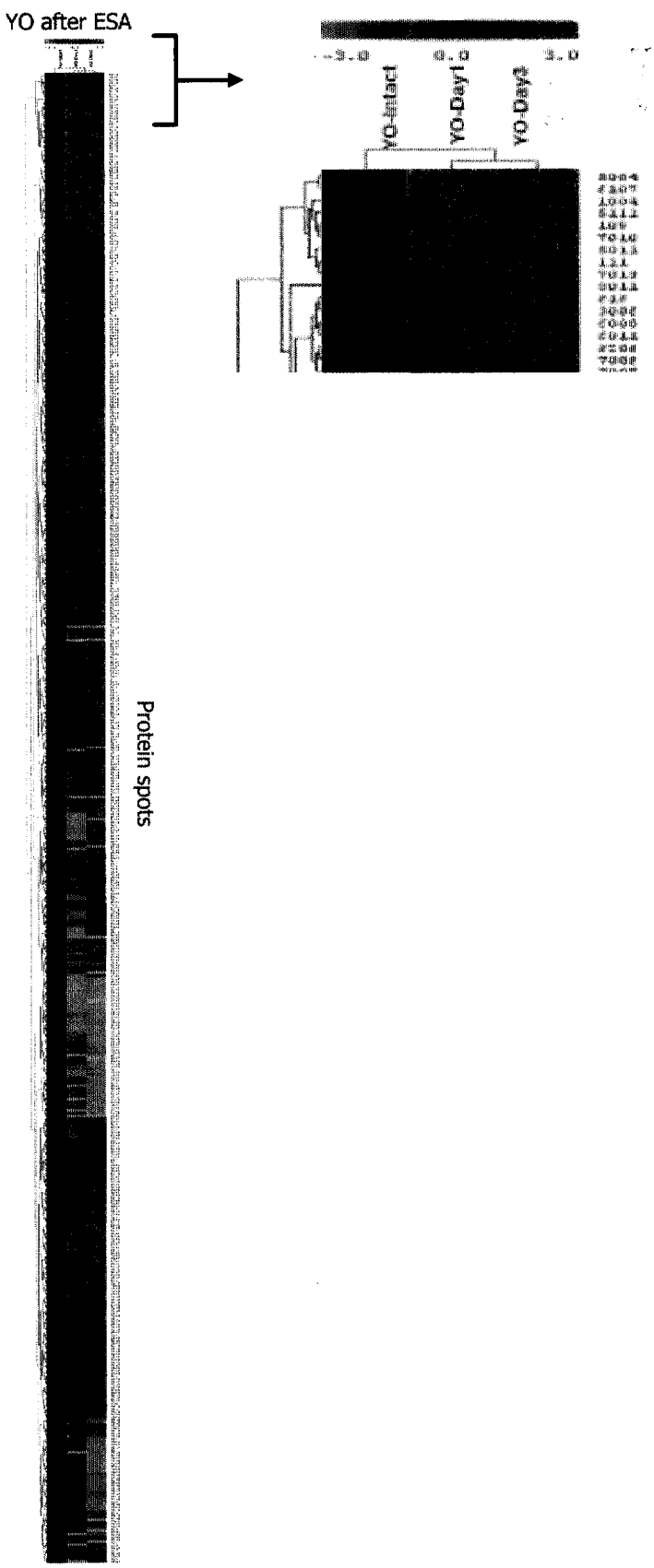

Fig. 4-3. K-means clustering analysis of Y-organ protein expression in response to ES ablation. K-means clustering of the imaging data (A) was converted to centroid graphs that grouped proteins into 6 clusters with similar expression profiles in response to ESA (mean ± 1 S.D.) (B). Clusters differed with respect to magnitude and direction of the response. About 38% (207) of the proteins showed a gradually increasing expression pattern that did not exceed a 3-fold change of mean value (mean ±1 S.D.) in level (cluster #3). Clusters #2, #4, and #5 showed large (>3-fold) changes in levels.

(A)

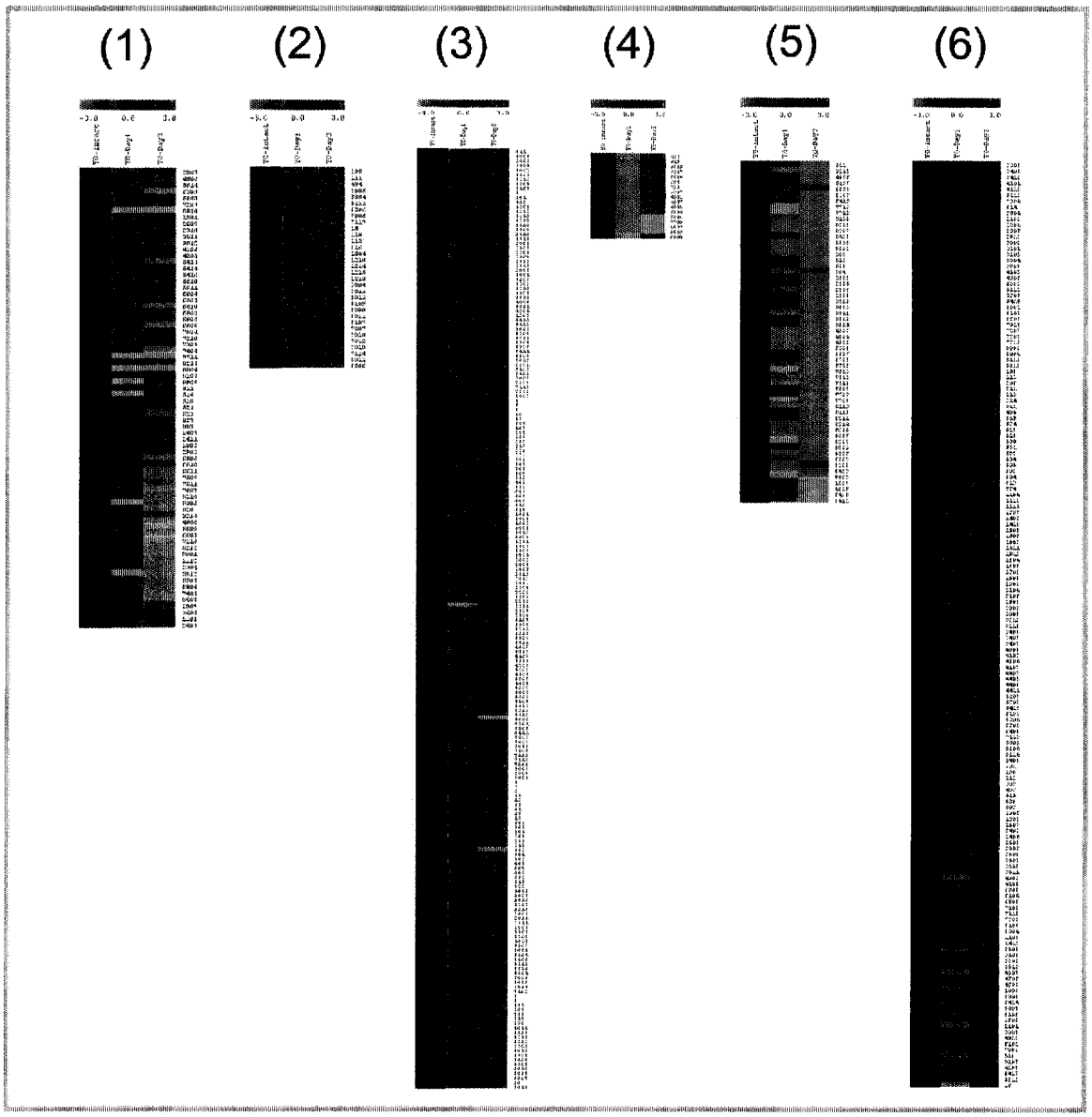

(B)

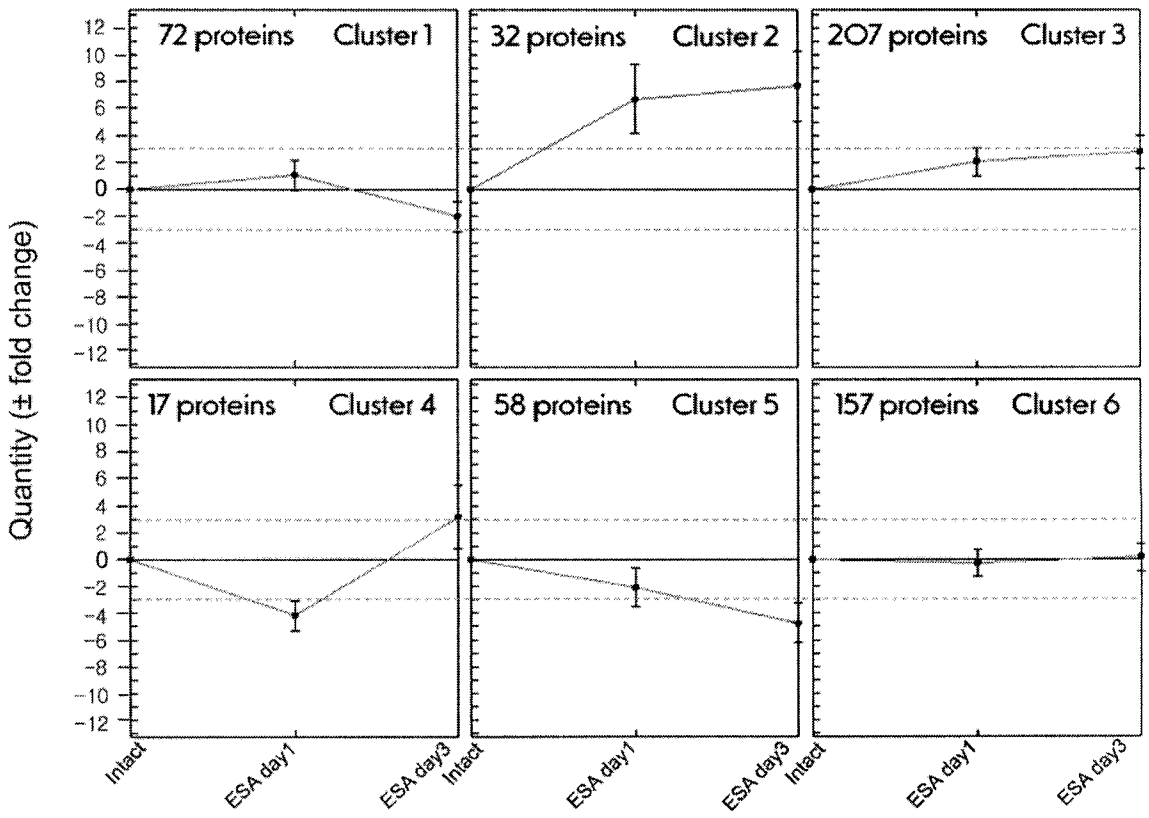

The K-means clustering data (Fig. 4-3A) was converted to centroid graphs (Fig. 4-3B) to show the expression profile for each of the six clusters. About 38% (207 proteins) displayed a gradually increasing expression profile after ESA that did not exceed a 3-fold change (Fig. 4-3B, cluster #3). Other proteins showed large increases or decreases at 1 day post-ESA (Fig. 4-3B, clusters #2, #4, and #5). Only 32 proteins (~6% of the total) showed large sustained increases in response to ESA (Fig. 4-3B, cluster #2). About 29% (157 proteins) showed no change in mean value (Fig. 4-3B, cluster #6).

Changes in phosphoproteins and identification of phosphorylated NO synthase in activated Y-organ

The MIH pathway involves rapid changes in protein phosphorylation (Böcking and Sedlmeier, 1994). Cyclic nucleotide-dependent protein kinases, such as protein kinase A (PKA) and protein kinase G (cGPK), are activated by MIH (Baghdassarian et al., 1996; Von Gliscynski and Sedlmeier, 1993). The activity of NOS is regulated by phosphorylation (Bivalacqua et al., 2004; Bredt et al., 1992; Kone, 2001). Thus, a targeted proteomic analysis of phosphoproteins in the activated YO was used to identify potential signal transduction components of the signaling pathway. Phosphoproteins in YOs from intact and 1 day post-ESA animals were separated by 2-dimensional gel electrophoresis. The phosphoprotein stain revealed 3 groups of proteins that changed in response to ESA (Fig. 4-4). Six ~17-kDa proteins with pI's between 4 and 5 increased after ESA (Fig. 4-4, Box #1). A prominent ~12 kDa phosphoprotein with pI 5.2 in intact YOs decreased dramatically in 1 day ES-ablated YOs (Fig. 4-4, Box #2).

Fig. 4-4. Effect of ES ablation on Y-organ proteins eluting from a phosphoprotein column. Proteins (15 μg) in Y-organs from intact and 1 day ES-ablated animals were separated by two-dimensional electrophoresis and were visualized with phosphoprotein stain (A); the same gels were subsequently stained with silver. Proteins with masses of ~17 kDa and ~150 kDa increased in response to ES ablation, while ~12 kDa proteins decreased (B). Silver staining indicated many other proteins were up-regulated in response to ES ablation; these could be phosphorylated proteins that were not detected with the phosphoprotein stain and/or non-phosphorylated proteins that co-purified with the phosphoproteins. The ~150 kDa proteins were similar in mass and net charge to the Gl-NOS deduced sequence (Kim et al., 2004). The identities of the other proteins are not known. Positions and masses of protein standards indicated on the right of each gel.

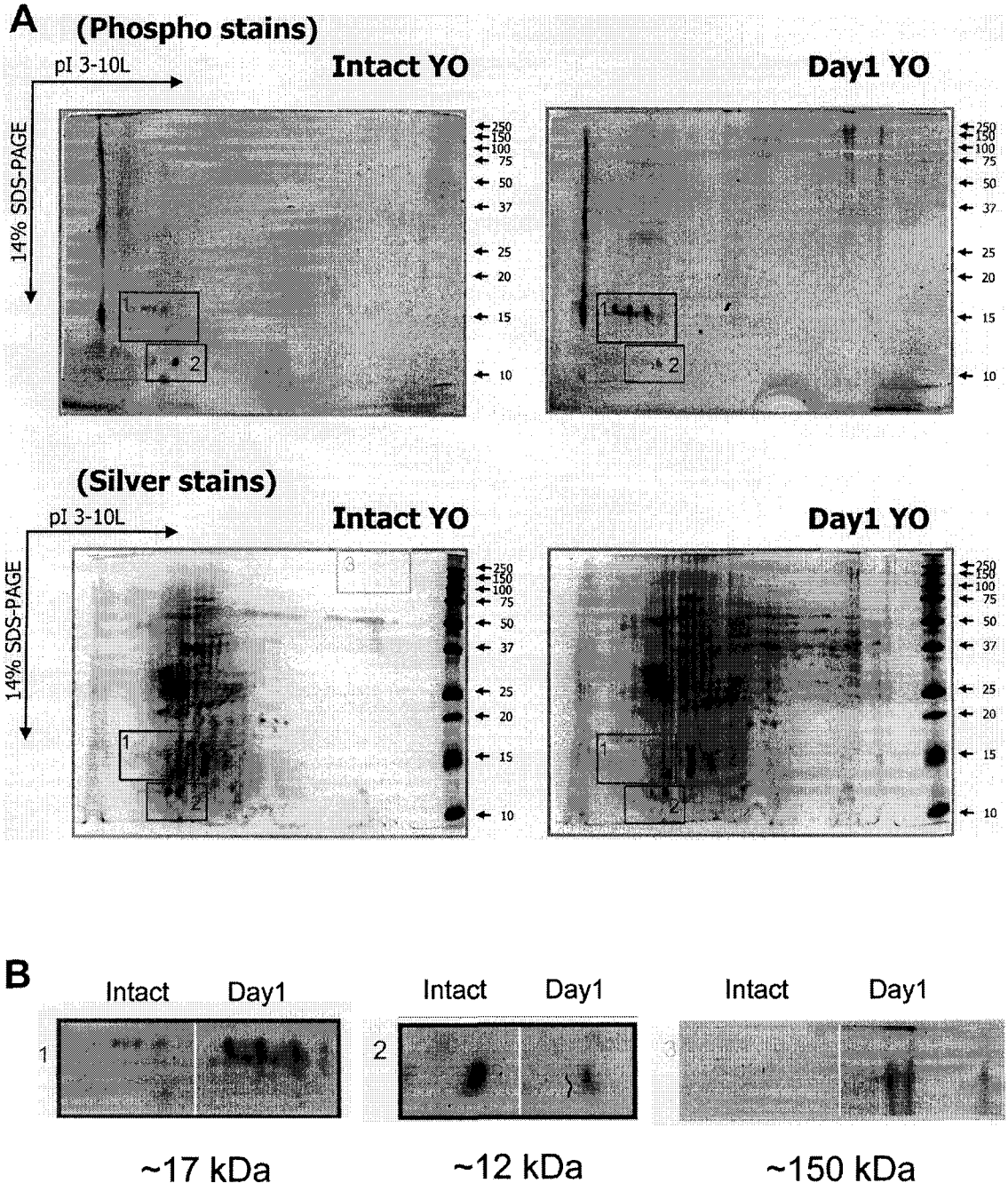

The third group consisted of three ~150-kDa phosphoproteins positioned at pI 7.8-9.5 that were detected only in 1-day post-ESA YOs (Fig. 4-4, Box #3). Silver staining of the same gels revealed additional proteins in the eluates from the phosphoprotein column (Fig. 4-4A, lower panels). The levels of most of these proteins were increased in the activated YO.

The antigenic peptide was designed for land crab NOS antibody production based on antigenicity, hydrophilicity, and solvent accessibility (Fig. 4-6). The location of the peptide was indicated in Fig. 4-5. The antigenic peptide sequence for NOS revealed 50% similarity with other NOS of insects, molluscs, and human (Fig. 4-7).

The electrophoretic mobilities of the ~150 kDa phosphoproteins (Fig. 4-4, Box #3) were similar to those predicted from the deduced amino acid sequence of Gl-NOS cDNA. More importantly, the ~150 kDa phosphoproteins were only present in YOs from ES-ablated animals. Western blot analysis showed that the ~150-kDa phosphoproteins reacted with a Gl-NOS peptide antibody (Fig. 4-8). Tryptic peptides of the major ~150-kDa phosphoprotein were analyzed by MALDI-TOF mass spectrometry (Fig. 4-9A). The major cross-contaminants, including autodigested trypsin fragments, were manually eliminated from the observed peptide mass peaks. A theoretical tryptic peptide mass peak list based on the translated land crab NOS cDNA (Kim et al., 2004) was used for manual matching with the peaks obtained from mass spectrometry. Eleven peptides, which covered 16% of the NOS sequence, matched the theoretical and observed peak lists (Fig. 4-9). A database search for peptide map fingerprints using ProFound software identified land crab NOS as the most probable candidate with a Z score of 1.65 ($P < 0.05$).

Fig. 4-5. Location of antigenic peptide for land crab NOS antibody. The protein sequence was translated from the cDNA sequence. The underlined peptide sequence in red font presents antigenic peptide for antibody generation.

```
   1 MREANHKPQRLHNVSTGNEVYDNLHTRSHTEGLCTRYQCNGALMLPRKSGTEPRSPEEVLKLAREFIDE
  70 YYQSIKRYKSEQHRLRWKQVCREVTERGTYDLTQTELVYGAKLGWRNAPRCIGRIQWSKLQVFDARYVS
 139 TASGMFEALCNHIKYGTNKGNLRSAITIFPQRTDGKHDFRVWNSELISYAGYKQEDGSIVGDPLNVEFT
 208 EVCQRLGWRGKGGRWDVLPLVLSASGHDPEWFDIPPELILTVPITHPEYKWFQELDLQWYGLPGVSSLM
 277 FDCGGLEFPAAPFNGWYMVSEIGTRDLCDPHRYNILETVGRRMGLDTRSPTNLWKDKALVEVNIAVLHS
 346 FQSLNVTIVDHHSAAESFMKHFENEQKLRGGCPADWVWIVPPLSGSITPVFHQEMSLYYLKPSYEYQEP
 415 AWKTHVWKKNKDINRNSIRRTKRKFRFKEIARAVKFTSKLFGKALSKRIKATILYATETGKSEMYAKKL
 484 GEIFGHTFNAQVYCMADYDLINIEHEALVLVVTSTFGNGDPPENGEDFAKNLYAMKVSGTAADIDDVSS
 553 SMHRSLSFMRMNSLTEGAGVSSVAQENGVINSNFRSSITSDIMSEDNFGPLSNVRFAVFALGSSAYPNF
 622 CAFGKYVDNLLAELGGERLMKLTCGDELAGQEQAFKQWAADVFSVGCETFCLDDVVAMKEATAALKTEA
 691 AASADKIKLYPCNRSDNIALGLSRAHGKRVRSCQVLASRNLHGENASSGGGSRGTQQVVLSTSGTNELH
 760 YQPGDHVAILPANRKELVDAVLARLQQCPDPDQPIQVLLLKEIHSLNGITQTWEPHERLPSASVRELLT
 829 RYLDITTPPAPNFLHMLAEYAHDNDQRTRLDQLATDPHEYEEWKHLRYPHLREVLEEFSSVNLDAGLLL
 898 THLPLLGPRFYSISSSPEAHPGQVHVTVAIVQYHTEGGKGPLHYGVCSNFLKEVSPGDHVELFVRSASS
 967 FRLPCDPSVPVIMVGPGTGVAPFRGFWHHRHYSLRHKKPTEKFSQMTLFFGCRTRAMDLYAEEKETMKT
1036 CGVLTHTHLALSREPTLPKTYVQDLLVEVGEQVYQQVVLEKGHFYVCGDCTMAECVYQKLRSIVQEHGR
1105 LSDQEVENFMLQMRDENRYHEDIFGITLRTEEIHRQKRESARVRMSSVVQQGPSTPTQAPANAPNLSTP
1174 PLCPRVPTKPSWPRRYSSRVFRSKLS
```

Properties

Average mass :		135600.0700
Monoiso. mass:		135513.8110
Molar ext. coeff.(280nm):		170280
Molar absorbance:		1.256
Theor. pI (SS/SH):	(1)	7.96 / 7.29
	(2)	8.02 / 7.31
	(3)	8.06 / 8.01

Fig. 4-6. Analytic Plots for determination of antigenic peptide for land crab NOS. N-terminal region of land crab NOS was selected for antigenic peptide to produce NOS antibody by using software Antheprot (http://antheprot-pbil.ibcp.fr). The selected peptide region (bidirectional arrow) was thought to have a good antigenicity based on the analysis plots since the sequence was analyzed as it has good hydrophilicity and solvent accessibility.

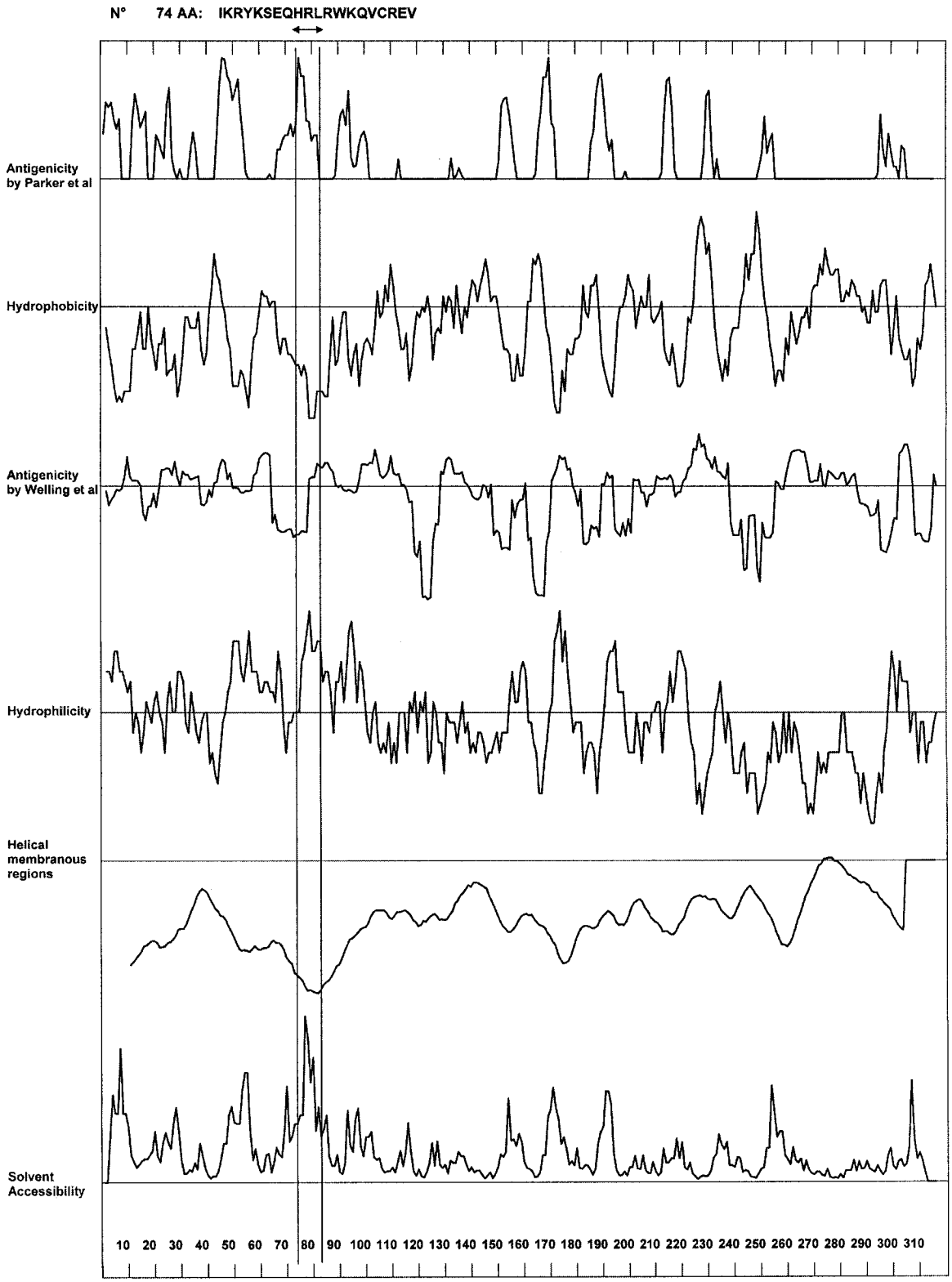

Fig. 4-7. Comparison of antigenic peptide sequence of land crab NOS with insects, molluscs, and human. The peptide sequence shares more than 50% similarity with other NOS.

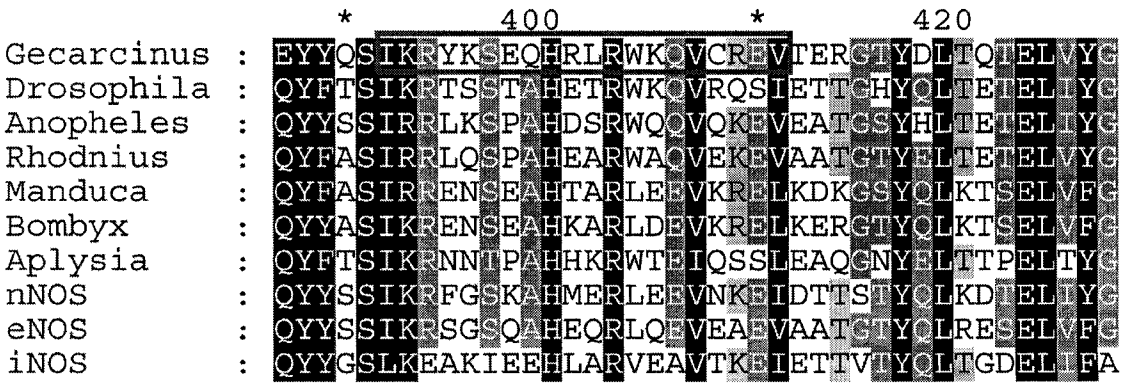

Fig. 4-8. Western blot of land crab NOS in Y-organs from intact and 1 day ES-ablated animals. Proteins eluted from a phosphoprotein column (15 μg) were separated by two-dimensional gel electrophoresis, transferred to PVDF membrane, and probed with land crab NOS peptide antibody. NOS was detected in YOs from 1 day ES-ablated animals but not in YOs from intact animals. Circles indicate the region in the gels where NOS should be located. The secondary antibody reacted nonspecifically with acidic proteins with masses greater than 37 kDa. Positions and masses of protein standards indicated on the right of each blot.

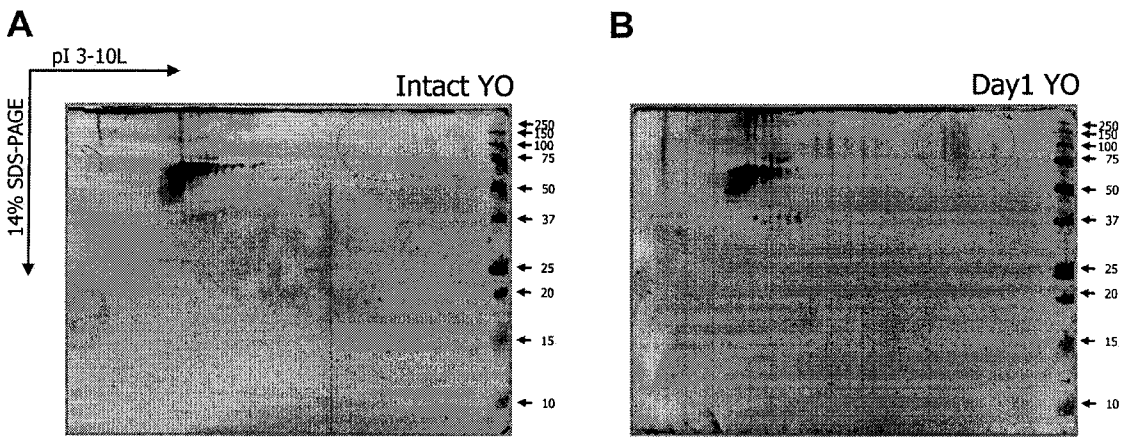

Fig. 4-9. Peptide mapping of putative land crab NOS using MALDI-TOF mass spectrometry. Tryptic peptides of the most abundant ~150 kDa phosphoprotein in YOs from 1 day ES-ablated animals (Fig. 4-3) were analyzed with mass spectrometry (A). The observed masses of eleven peptides (#1 through #11; asterisks) matched the theoretical masses of tryptic peptides based on the deduced Gl-NOS amino acid sequence (B). The peptides are underlined or overlined and identified with the corresponding number in panel A.

(A)

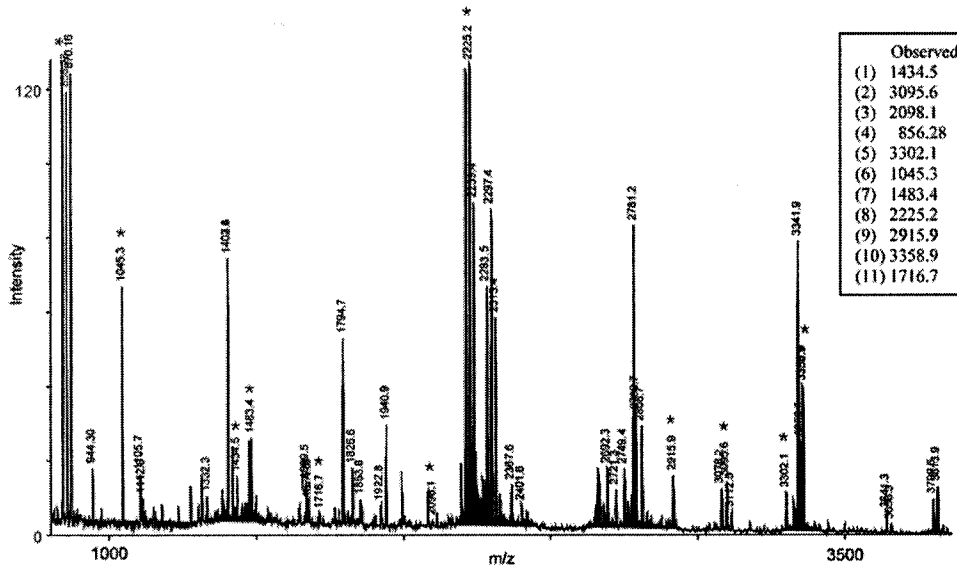

	Observed	Theoretical
(1)	1434.5	1434.68
(2)	3095.6	3095.58
(3)	2098.1	2098.12
(4)	856.28	856.42
(5)	3302.1	3302.59
(6)	1045.3	1045.56
(7)	1483.4	1483.75
(8)	2225.2	2224.89
(9)	2915.9	2915.46
(10)	3358.9	3358.7
(11)	1716.7	1716.93

(B)

```
                                                                    (1)
1    MREANHKPQRLHNVSTGNEVYDNLHTRSHTEGLCTRYQCNGALMLPRKSGTEPRSPEEVLKLARFFIDEYYQSIKRYKSEQHRLRWKQVC
                (2)                    (3)
91   REVTERGTYDLTQTELVYGAKLGWRNAPRCTGRIQWSKLQVFDARYVSTASGMFEALCNHIKYGTNKGNLRSAITIFPQRTDGKHDFRVW
181  NSELISYAGYKQEDGSIVGDPLNVEFTEVCQRLGWRGKGGRWDVLPLVLSASGHDPEWFDIPPELILTVPITHPEYKWFQELDLQWYGLP
271  GVSSLMFDCGGLEFPAAPFNGWYMVSEIGTRDLCDPHRYNILETVGRRMGLDTRSPTNLWKDKALVEVNIAVLHSFQSLNVTIVDHHSAA
361  ESFMKHFENEQKLRGGCPADWVWIVPPLSGSITPVFHQEMSLYYLKPSYEYQEPAWKTHVWKKNKDINRNSIRRTKRKFRFKEIARAVKF
                       (4)
451  TSKLFGKALSKRIKATILYATETGKSEMYAKKLGEIFGHTFNAQVYCMADYDLINIEHEALVLVVTSTFGNGDPPENGEDFAKNLYAMKV
                                (5)
541  SGTAADIDDVSSSMHRSLSFMRMNSLTEGAGVSSVAQENGVINSNFRSSITSDIMSEDNFGPLSNVRFAVFALGSSAYPNFCAFGKYVDN
                                                                    (6)
631  LLAELGGERLMKLTCGDELAGQEQAFKQWAADVFSVGCETFCLDDVVAMKEATAALKTEAAASADKIKLYPCNRSDNIALGLSRAHGKRV
721  RSCQVLASRNLHGENASSGGGSRGTQQVVLSTSGTNELHYQPGDHVAILPANRKELVDAVLARLQQCPDPDQPIQVLLLKEIHSLNGITQ
811  TWEPHERLPSASVRELLTRYLDITTPPAPNFLHMLAEYAHDNDQRTRLDQLATDPHEYEEWKHLRYPHLREVLEEFSSVNLDAGLLLTHL
                                                                    (7)
901  PLLGPRFYSISSSPEAHPGQVHVTVAIVQYHTEGGKGPLHYGVCSNFLKEVSPGDHVKLFVRSASSFRLPCDPSVPVIMVGPGTGVAPFR

991  GFWHHRHYSLRHKKPTEKFSQMTLFFGCRTRAMDLYAEEKETMKTCGVLTHTHLALSREPTLPKTYVQDLLVEVGEQVYQQVVLEKGHFY
          (8)                    (9)                                                    (10)
1081 VCGDCTMAECVYQKLRSIVQSHGRLSDQEVENFMLQMRDENRYHEDIFGITLRTEEIHRQKRESARVRMSSVVQQGPSTPTQAPANAPNL
                          (11)
1171 STPPLCPRVPTKPSWPRRYSSRVPRSKLS
```

Further analysis of YO cell fractions indicated that the NOS was present in the cytosolic fraction and absent in the membrane fraction (Fig. 4-10).

Fig. 4-10. The phospho-NOS is present in cytosol fraction. 2-DE comparisons of phosphoproteins in cytosol and membrane fraction of the Y-organs after phosphocolumn purification. Cytosol and membrane fractions were prepared by using an ultracentrifugation (100,000 xg, 1 h at 4 °C). Each cytosolic and membrane phosphoprotein (80~90 μg, each) was purified by PhosphoProtein Purification kit (Qiagen) from 5 mg total Y-organ extracts. 15 μg of purified phosphoproteins was subjected to 7 cm Drystrip (3-10L) for 1-D isoelectrofocusing and resolved on mini slab gel system (Bio-Rad). The proteins were visualized with Pro-Q Diamond phosphoprotein stain kit (Molecular Probes), and the image was captured by Molecular imager FX (Bio-Rad). Silver staining was done after phosphoprotein images were obtained. The phosphoprotein was present in cytosol fraction (indicated by red dot-box).

[Cytosol fraction from ESA YO] **[Membrane fraction from ESA YO]**

Phosphostains

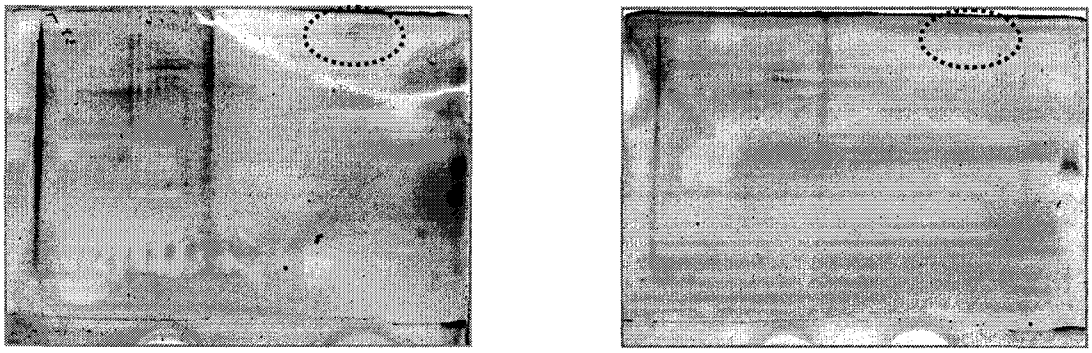

Silver stains

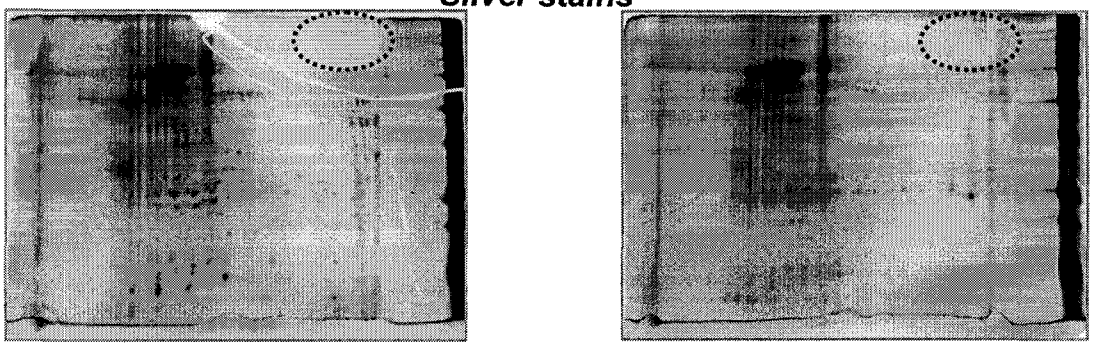

Discussion

"Global" proteomics of the activated molting gland

In this study proteome matching PDQuest software (Bio-Rad) and gene clustering Cluster and TreeView software (Eisen et al., 1998) were used to quantify changes in protein composition associated with activation of the Y-organ. Clustering tools use various algorithms to identify genes with similar expression profiles (Jagota, 2000; Jain et al., 1999; Janin and Dubes, 1988). Hierarchical clustering generates a series of successive mergence or splits of a data set until a final number of clusters are obtained (Fig. 4-2). This clustering method provides a more comprehensive view of expressional relationships within each cluster, which contains proteins with similar expression profiles. K-means clustering is a non-hierarchical clustering algorithm to classify or group objects based on attributes/features into a K number of groups (Fig. 4-3). A K number of 6 was selected for this study. Grouping is performed by minimizing the sum of the squares of distances between the data and the corresponding cluster centroid, which is a weighted average in a two-dimensional space. Thus the purpose of K-means clustering is to classify proteins into discrete expression groups, which can be used to select proteins for use as diagnostic markers. Therefore, as hierarchical clustering sorts data out into previously unknown clusters, K-means actually assigns data between predefined partitions. Both clustering methods provide a global view of the expressional profile, and organize all the proteome data into relatively homogeneous groups with similar expression profiles. This enables investigators to quickly identify proteins that may share physiological function. This approach must be validated by subsequent identification of

the proteins in a cluster to determine whether they are associated with a particular physiological process, such as cholesterol uptake and metabolism or a signal transduction pathway.

Activation of the YO results in dramatic changes in protein expression (Fig. 4-1). Of the 543 proteins analyzed, more than 100 proteins (~20% of the total) increased or decreased at least 3-fold in response to ESA (Fig. 4-3B, clusters #2, #4, and #5). Another 207 proteins (38% of the total) increased gradually after ESA, but did not exceed the 3-fold threshold (Fig. 4-3B, cluster #3). This large increase in protein expression is consistent with previous studies, which show that protein synthesis is required for ecdysteroidogenesis (Dauphin-Villemant et al., 1995; Han and Watson, 2005; Kang and Spaziani, 1995a; Lachaise et al., 1996; Mattson and Spaziani, 1986; Spaziani et al., 1999).

"Targeted" proteomics: the signaling pathway regulating ecdysteroidogenesis

NOS is expressed throughout the central nervous system of insects and crustaceans, in which it is involved in neuronal development and neuromodulation (Aonuma, 2002; Colasanti and Venturini, 2000; Davies, 2000; Johansson and Carlberg, 1994; Johansson and Mellon, 1998; Lee et al., 2000; Scholz and Truman, 2000; Scholz, 2001; Scholz et al., 2002; Schuppe et al., 2001; Talavera et al., 1995; Zou et al., 2002). NOS also appears to be involved with the MIH signal transduction pathway in the YO. Both NOS and NO-sensitive GC are expressed in Y-organs (Kim et al., 2004; Lee et al., 2005). Figure 4-11 presents a hypothetical MIH signaling pathway that is consistent with the available data, including results from the current study.

Fig. 4-11. Hypothetical MIH signaling pathway in the crustacean molting gland (Y-organ). MIH binds to a G protein-coupled receptor, activating adenylyl cyclase (AC); intracellular Ca^{2+} rises when protein kinase A (PKA) activates a membrane Ca^{2+} channel; NO synthase (NOS) is activated when Ca^{2+}/calmodulin (CaM) binds and NOS is dephosphorylated by calcineurin (CaN), a Ca^{2+}/calmodulin-dependent phosphatase; NO activates a NO-sensitive (class I) guanylyl cyclase (GC-I). Activation of a cGMP-dependent protein kinase (cGPK) inhibits expression and/or activities of ecdysteroidogenic proteins, resulting in reduced ecdysteroid synthesis. NOS is inactivated by phosphorylation by PKA, protein kinase C (PKC), and/or other protein kinases.

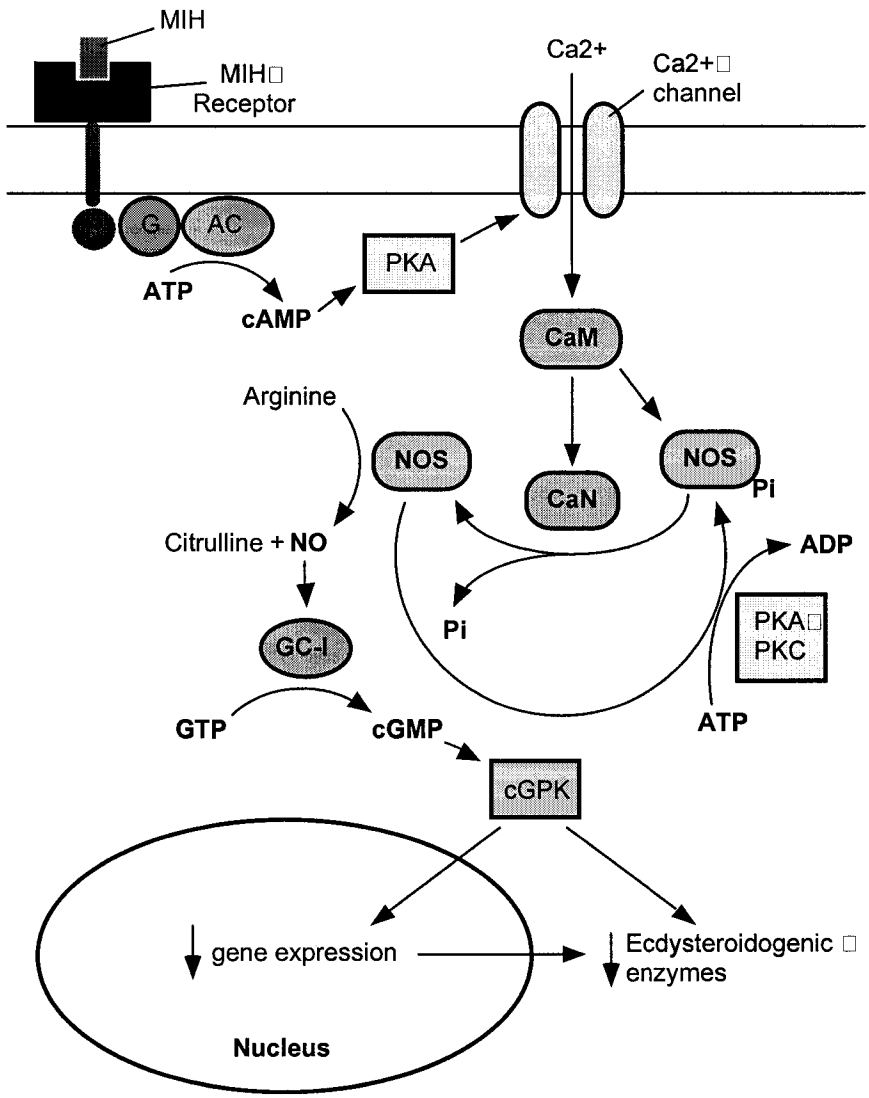

This NO pathway is similar to the mechanism that stimulates fluid secretion in *Drosophila* Malpighian tubules by the decapeptide cardioacceleratory peptide 2b (Kean et al., 2002; MacPherson et al., 2001). According to our model, MIH binding to a G protein-coupled membrane receptor leads to a Ca^{2+}-dependent activation of NOS via CaM and dephosphorylation by CaN (Kone, 2001). Therefore, derepression of the YO by ESA requires inactivation of NOS by phosphorylation (Fig. 4-11). A ~150-kDa phosphoprotein in YO extracts of ES-ablated animals was identified as Gl-NOS. It reacted with an antibody raised against a peptide in the Gl-NOS deduced sequence (Fig. 4-8). Moreover, MALDI-TOF mass spectrometry identified eleven tryptic peptides that matched the theoretical peptide masses based on the Gl-NOS deduced amino acid sequence (Fig. 4-9).

NOS undergoes extensive post-translational modification (Ortiz and Garvin, 2003), which may explain why the observed and theoretical masses of other tryptic peptides did not match. For example, mammalian NOS is phosphorylated/dephosphorylated at numerous sites by a variety of protein kinases/phosphatases (Cordelier et al., 1999) (Bauer et al., 2003; Boo et al., 2002; Fleming et al., 2001; Michell et al., 2002; Mount et al., 2006; Rameau et al., 2004; Song et al., 2005). In the land crab NOS, 27 serine, 4 threonine, and 4 tyrosine phosphorylation sites were predicted with greater than a 0.9 threshold score by the NetPhos 2.0 phosphorylation prediction algorithm (http://www.cbs.dtu.dk/services/NetPhos/). It is unlikely that the matching of the eleven peptides is a coincidence, as the peptides are dispersed throughout the sequence and are not located in conserved regions that may share sequence identities with other oxidoreductases. Moreover, only one of the tyrosines (Y71) and four of the serines (S476,

S565, S952, and S1190) in the putative phosphorylation sites are located in the eleven matching peptides; the 30 other residues are located elsewhere in the sequence.

In addition to NOS, two other phosphoproteins that responded to ESA were found in YO extracts. The identities of the ~12-kDa and ~17-kDa proteins will be elucidated by mass spectrometry, as they may also be involved in neuroendocrine signaling. The Qiagen phosphoprotein purification kit has been used to characterize phosphorylated proteins in yeast and mammalian cells by tandem mass spectrometry (Makrantoni et al., 2005; Metodiev et al., 2004; Puente et al., 2006; Stark and Assaraf, 2006; Ueda et al., 2004). The YO protein eluate from the phosphoprotein column contained additional proteins that were stained with silver but were not detected by the phosphoprotein stain (Fig. 4-4A, compare upper and lower panels). Nonphosphorylated proteins may have bound nonspecifically to the column, as the matrix has less affinity for phosphoproteins than the phosphoprotein stain. Moreover, the phosphoprotein stain is reported to generate more consistent results with better resolution than the ^{32}P-labeling method (Wu et al., 2005). At least some of the nonphosphorylated proteins may have bound to the column by interacting with phosphoproteins, as nondenaturing conditions were used for the phosphoprotein purification.

Proteomic approaches can elucidate signaling mechanisms in the YO, as rapid responses to neuropeptides do not involve changes in gene expression. It can be used to determine the involvement of putative signal transduction components, such as NOS, as well as identify novel components, such as the ~12-kDa and ~17-kDa phosphoproteins. A problem with ESA is that it lacks specificity; it may affect more than the MIH signaling pathway, as the XO is the major source of several neuroendocrine factors that may affect

the YO proteome. However, injection of purified MIH into ES-ablated animals lowers hemolymph ecdysteroid, indicating that the primary effect on the YO is the reduction of MIH (Chang et al., 1987; Nakatsuji and Sonobe, 2004). Experiments are planned that will use purified or recombinant MIH to characterize time- and dose-dependent responses of the YO *in vitro*. Many of the global changes in the proteome probably resulted from transcriptional and post-transcriptional regulation associated with ecdysteroidogenesis. Synthesis of new protein is required for sustained synthesis and secretion of ecdysteroids. Therefore, most of the proteins showing expressional changes in the YO after ESA are likely involved in the uptake and metabolism of cholesterol. Recent advances in mass spectrometry have made it possible to determine protein identities without genomic or EST databases, although such databases would facilitate identification protein products. As a "proof of concept", this study demonstrates that proteomic approaches can be used to understand the complexities of neuropeptide regulation of molting in crustaceans.

CHAPTER FIVE

SUMMARY AND FUTURE DIRECTIONS

Crustaceans, like other arthropods, grow by a periodic shedding their old exoskeleton, a process known as molting or ecdysis. The internal signal controlling the molting cycle is the steroid hormone 20-hydroxyecdysone (Hoffmann and Porchet, 1984). Ecdysteroids are synthesized and secreted from the Y-organs (YOs), a pair of epitheliod glands located in the anterior cephalothoraxes (Lachaise et al., 1993). Regulation of the molting cycle in decapod crustaceans is mainly controlled by the X-organ/sinus gland (XO/SG) complex and the YO. Molt-inhibiting hormone (MIH), is produced in XO/SG complex, and regulates ecdysteroidogenesis in the YO. Eyestalk ablation (ESA) causes a rapid increase of ecdysteroid titers and induces molting (Passano, 1953). However, little information is known about the pathways for inhibition of ecdysteroidogenesis in the YO after MIH triggers the signal cascade from its receptor on the YO membrane.

In an effort to determine which proteins are involved in initiating MIH signaling pathway for Y-organ ecdysteroidogenesis, proteomic (Blackstock and Weir, 1999) and molecular biological approaches were used. The eyestalk is the main endocrine system that produces MIH in crustaceans, and eyestalk ablation (ESA) caused significant increases in hemolymph ecdysteroid of land crabs. However, immunoprecipitation of YO extracts using a blue crab anti-peptide antibody showed that the MIH or MIH-like

peptide(s) was/were not decreased even after 3 days post ESA. The MIH-immunoprecipitated samples were subjected to two-dimensional gel electrophoresis, and then analyzed by both western blot and silver staining. As a result, putative MIHBPs (MIH-binding proteins) were observed only in the YO from intact animals, suggesting that MIHBPs may facilitate and/or stabilize the binding of MIH to its membrane receptor. Therefore, these proteins might be critical triggers for ecdysteroidogenesis. These proteins remain to be identified. However, preliminary tandem mass spectrometry data showed that 3 internal peptide sequences are identical, indicating these proteins are related. The similar binding proteins were identified in secondary limb bud (2° LB), which contains the MIH-like peptide (LAF_{pro}). Since it has been suggested that currently accepted molting control model contains some points to be reconsidered (Chung and Webster, 2005), the determination of MIHBP sequences would be a new guideline to understand crustacean molting regulation mechanisms.

Guanylyl cyclases (GCs) are particularly important signaling molecules for YO activation since the increase in cGMP concentration is considered a key second messenger to inhibit the YOs (Baghdassarian et al., 1996; Saidi et al., 1994). This report describes the first cloning of soluble NO-sensitive GC (two isoforms in Heme-NO-Binding domain) (GC-I) and NO-insensitive GC (GC-III) in crustaceans, as well as differently spliced forms of receptor GC (three isoforms in Ligand-binding domain) (GC-II). The two methods (ES ablation and 20E injection) used to increase hemolymph ecdysteroid levels elicited very different responses by tissues. ES ablation induced a three-fold increase of Gl-GC-II(+18) in claw muscle, suggesting it has a role in molt-induced atrophy (Mykles, 1997). ES ablation increased Gl-GC-Iβ and Gl-GC-III

expression in the YO, suggesting the tissue is compensating for low MIH levels in the hemolymph. 20E at high doses generally had a transient inhibitory effect on the expression of Gl-GC-Iβ and some Gl-GC-II isoforms, most likely resulting from the rapid clearance of 20E from the hemolymph. These data indicate that there are interactions between ES neuropeptides and ecdysteroids that can affect the expression of GCs in tissues. The three GC classes represent diverse GC signaling mechanisms, all of which may play roles in modulating gene expression during molting. The receptor guanylyl cyclases (GC-II) determine those ligands and each isoform we found would have a unique ligand. However, what ligand binds to which isoform still remains to be elucidated.

Total protein extracts of YOs from intact and ES ablated animals were analyzed to discover candidates of molt-regulating factors by two-dimensional gel electrophoresis, image analysis, and proteome clustering. Expression proteomics is potentially a powerful high-throughput target screening system. Regulation of Nitric oxide synthase (NOS) activity by phosphorylation/dephosphorylation is central to our hypothetical MIH signaling pathway in the YO (Kim et al., 2004; Lee et al., 2005). Phosphoproteins purified from the YO were analyzed by two-dimensional gel electrophoresis and phosphoprotein staining. In particular, the regulation of NOS by phosphorylation/dephosphorylation was mainly examined. ES ablation caused significant changes in the levels of phosphoproteins. These proteins were selected as potential candidates for molt-regulating factors. Some of these phosphoproteins were present only in ES ablated YO and showed NOS immuno-reactive signal by land crab NOS antibody. Furthermore, peptide mass fingerprinting (PMF) analysis confirmed that the protein is

land crab NOS. Additional data showed that the NOS was present in cytosol fraction. This result clearly shows that NOS is dephosphorylated to be active after MIH signaling cascade is turned on, and is present in cytosol of the YO. NO activates a NO-sensitive GC (GC-I). Activation of a cGMP-dependent protein kinase (cGPK) inhibits expression and/or activities of ecdysteroidogenic proteins, resulting in reduced ecdysteroid synthesis (Fig. 4-11).

Crutaceans and insects belong to arthropoda and their close phylogenetic relationship implies that crustaceans are particularly sensitive to insecticides. There are large numbers of examples of xenoestrogenic endocrine disruption caused by such insecticides in the marine environment, and the number of the examples has been growing. Therefore, understanding the hormonal regulation of decapod molting and growth is essential to mitigate potential effects of pollutants, including endocrine disruptors (ED). Despite intense effort we still know very little about whole mechanism of crustacean molting and the identity of the MIH receptor still remains unknown. Nonetheless, this research addresses fundamental questions of crustacean molt physiology and endocrinology by demonstrating the MIH signaling pathway.

APPENDICES

Appendix I. Cloning and expression of land crab myostatin (Gl-Mstn). (A) Domain organization of the unprocessed human myostatin protein showing the signal sequence (SS), propeptide, and mature peptide. (B) Deduced amino acid sequence of the mature myostatin peptide for *G. lateralis* (Gl) shares high identity/similarity with human (Hs; #AF01627) and scallop (Ai; #AY553362) myostatin. Sequence identical to *G. lateralis* is represented with dots. Amino acids with similar physiochemical properties to that of the Gl-Mstn residues are shaded in gray. Amino acid differences are shaded in black. Spaces indicate gaps in the sequences to maximize alignments. The RXXR site, at which proteolytic cleavage generates the mature peptide, is conserved. (C) PCR products were amplified using specific primers recognizing myostatin (MSTN) or elongation factor 2 (EF2) from *G. lateralis* claw (CM) and thoracic (TM) muscle. Amplification was carried out using cDNA template isolated from land crab with intact eyestalks (Intact), 1 day post-eyestalk ablation (ESA), and 3 days post-ESA. Hemolymph ecdysteroid levels were: Intact, 14.4 pg/μl; 1 day post-ESA, 49.5 pg/μl; 3 days post-ESA, 208.1 pg/μl. Gl-Mstn mRNA in claw muscle was increased by 3 days post-ESA; Gl-EF2 was constitutively expressed. Inverse image of EtBr-stained gel. Hyun-Woo Kim cloned the Gl-Mstn (part B); Sung Gu Lee examined Gl-Mstn expression (part C).

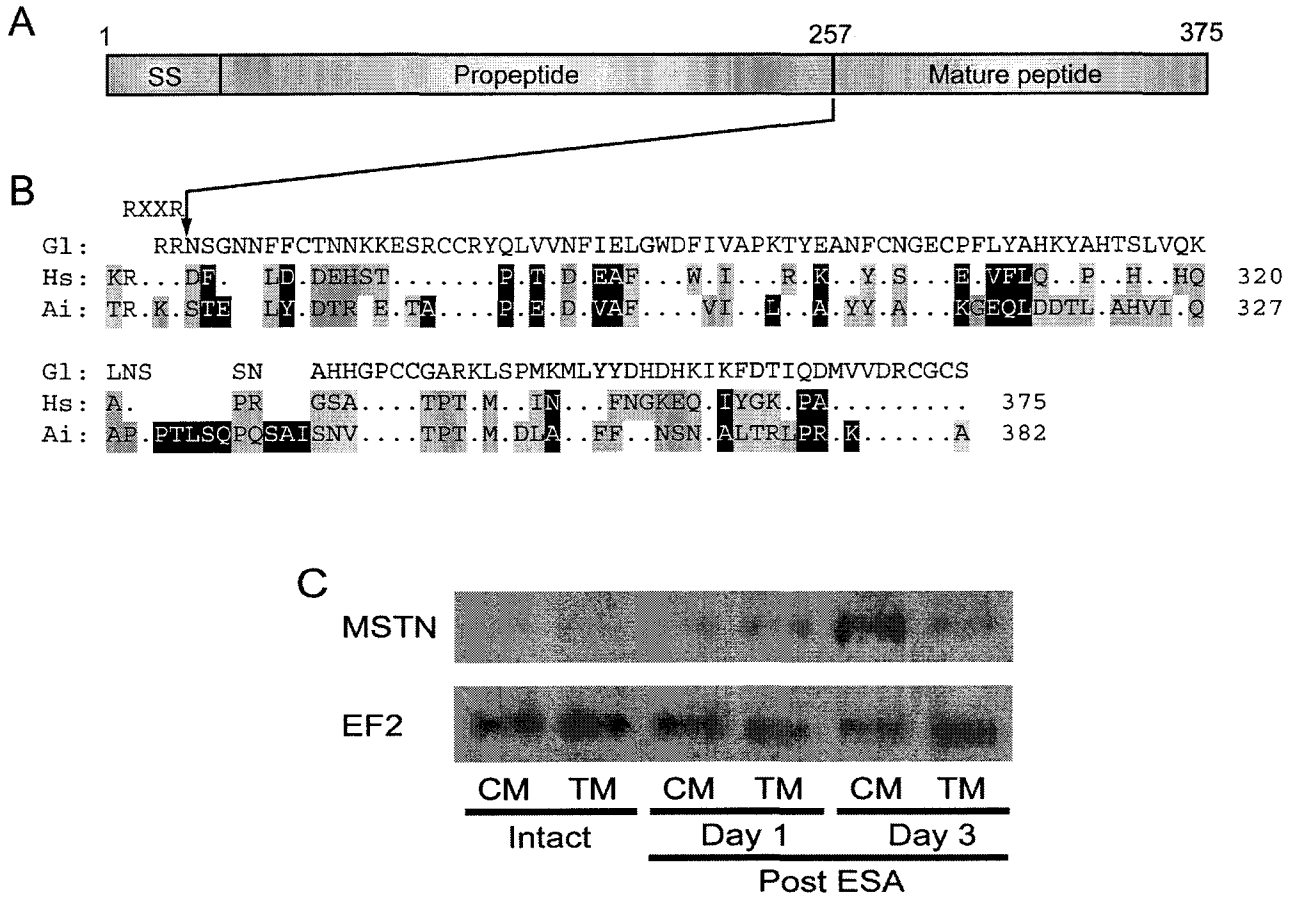

Appendix II. Expression of EcR, RXR isoforms, and E75 in land crab gonadal tissues*. Total RNA 36 from ovary (C), and testis (D) was DNase-treated, reverse-transcribed, and PCR-amplified using sequence-specific primers. EF2 served as an internal standard. Shown is a reverse image of ethidium bromidestained agarose gels of the PCR products. EcR, E75, and RXR were expressed in all tissues, although RXR mRNA was higher in claw muscle than in thoracic muscle. The presence of different RXR isoform cDNAs was determined using forward primers to the three variants in the T box (T), in combination with reverse primers to the 33-amino acid insertion/deletion variants (+33 and -33), the 35-amino acid insertion/deletion variants (+35 and -35), and the two truncations (+33ΔE/F and –33ΔE/F); asterisks identify products of the expected size. Smaller products were generated with the –35 and +35 reverse primers (arrowheads in lanes o, t),

and u), most likely due to the presence of cDNAs lacking the 33-amino acid sequence. Only isoforms containing the T(+12) variant sequence were expressed in thoracic muscle (lanes p-s, t). In contrast, claw muscle expressed isoforms containing the T(+7) and T(+12) variants at similar levels (lanes j-s, t) and isoforms containing the T(+8) variant at low levels (lanes d, g). The gonads expressed more isoforms than skeletal muscles and novel products were obtained with certain primer combinations, which indicate a greater complexity of RXR isoforms in ovary and testis.

---

*The data were published in part of a paper (Kim et al., 2005b).

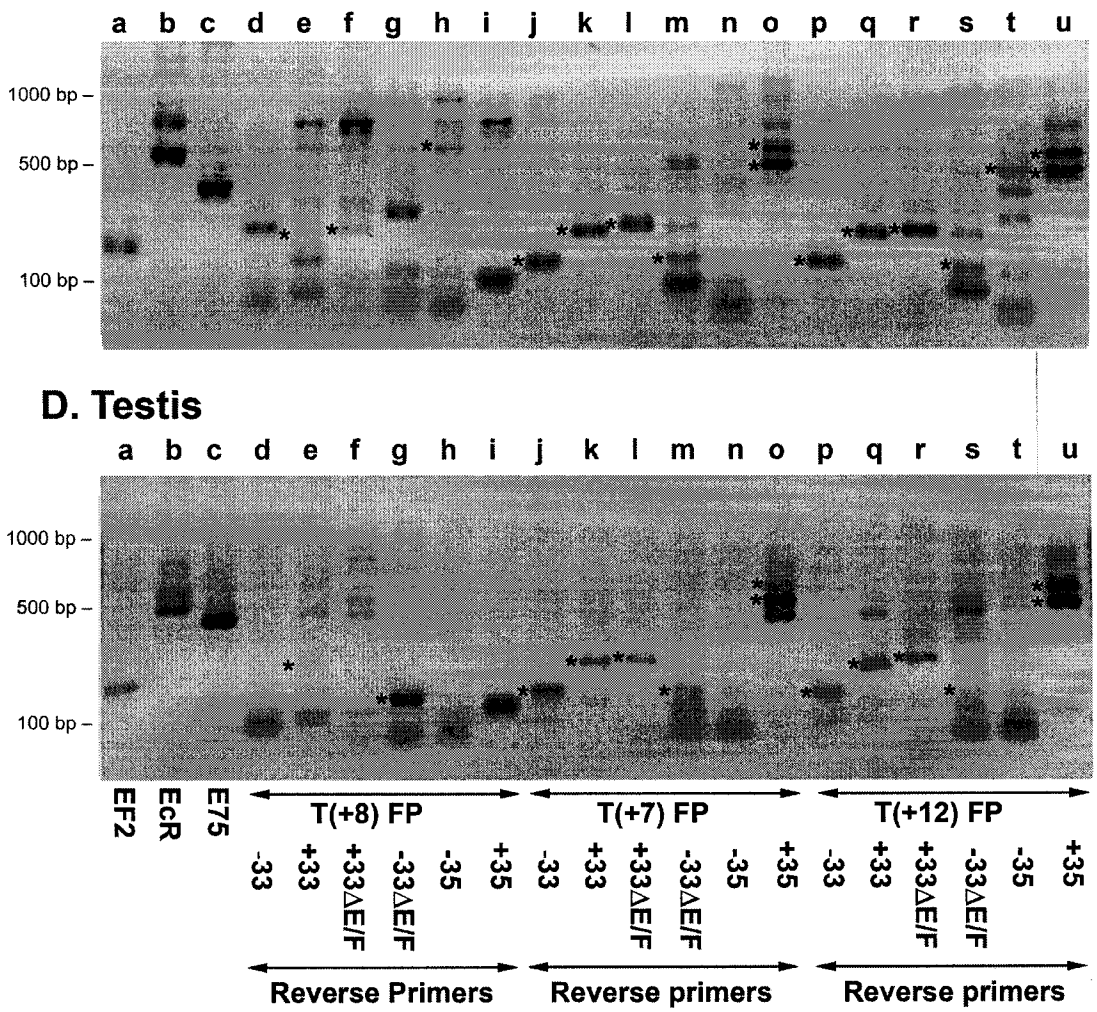

Appendix III. Tissue distributions of land crab NOS. Hybond-P PVDF membrane (Amersham Biosciences) was washed in methanol for 5 min followed by rinsing in transfer buffer (50 mM Tris, 384 mM glycine, 20% methanol). SDS-PAGE gel, which was run with ES ganglia, Y-organ, thoracic ganglia, heart, ovary, testis, gill, integument, and intestine were blotted at 100 V for 1 h. After overnight incubation at 4°C in blocking buffer (20 mM Tris-HCl, pH 7.5, 140 mM NaCl, 0.05% Tween-20, 3% BSA), the membrane was probed with blue crab NOS antiserum (1:2,000, v/v in blocking buffer) and incubated for 2 h at room temperature. After washing in TTBS 3 x 10 min each, the membrane was incubated for 1 h with alkaline phosphatase-conjugated secondary antibody (Sigma, 1:10,000, v/v in blocking buffer), and then washed in TTBS 3 x 10 min each. Finally the blot was developed with BCIP/NBT. Land crab NOS immune-response signals are indicated by dots. Preimmune serum was used as a negative control.

Preimmune serum

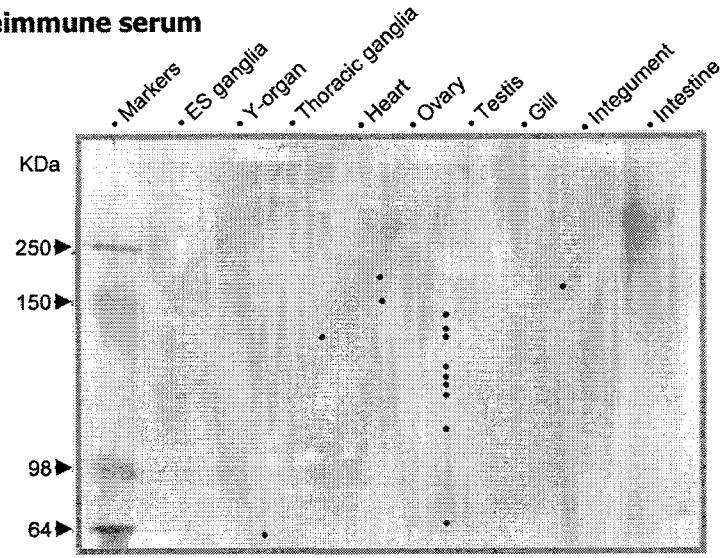

Immune serum

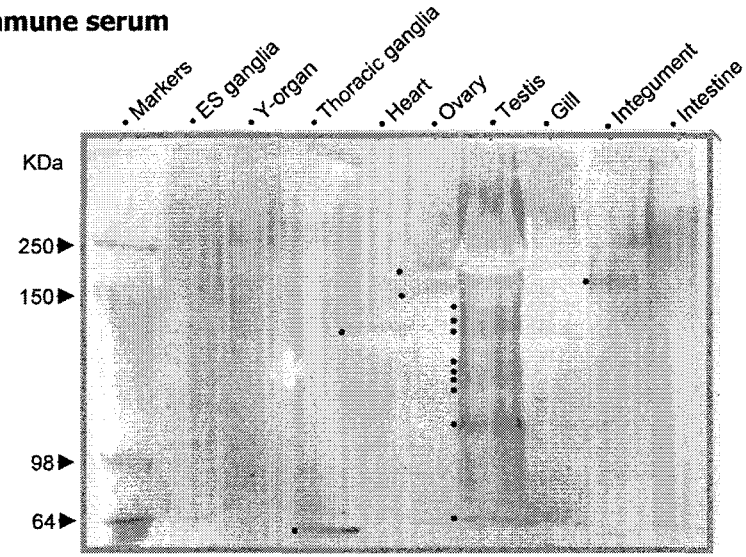

6% gel

1° Ab- 1:2000 / 2° Ab – 1:10,000

(AP-conjugated anti-rabbit mouse Ab)

Appendix IV. Two-dimensional gel electrophoresis analysis of total extracts of limb buds. 1° (A) and 2° (B) limb buds were homogenized in 200 µl lysis buffer (7 M urea, 2 M thiourea, 4% CHAPS, 66 mM dithiothreitol, and 1x protease inhibitor cocktail) using a Dounce homogenizer. The lysate was centrifuged at 40,000 xg for 1 h and the protein concentration in the supernatant was determined with the Bradford reagent (Sigma) using BSA as standard. Before isoelectrofocusing, 0.5% 4-7 IPG buffer (Amersham Biosciences) was added to the protein sample. Protein (20µg, each) was loaded onto 7-cm pH 4-7 linear IPG strips using an in-gel rehydration method. The isoelectrofocusing conditions were as follows: 1 h at 500 V, 1 h at 1,000 V, and at 5,000 V for a total of 17 kVh at 20 °C. After isoelectrofocusing the strips were equilibrated in a buffer containing 30% glycerol, 6 M urea, 2% SDS, 10 mg/ml dithiothreitol, and 0.05 M Tris-HCl (pH 6.8) for 15 min and then for an additional 15 min in equilibration buffer in which 42.5 mg/ml iodoacetamide replaced the dithiothreitol. The strips were positioned at the top of 12.5% polyacrylamide gels with 0.5% agarose containing Laemmli sample buffer. SDS-polyacrylamide gel electrophoresis was performed in Laemmli electrophoresis buffer at 150 V at room temperature. For silver staining, gels were fixed in 40% ethanol and 10% acetic acid for 1 h, rehydrated in 5% ethanol and 5% acetic acid for 2 h, and sensitized in 0.05% (w/v) 2,7-naphthalenedisulfonic acid for 30 min. After three 5-min washes in double-distilled water, the gels were stained in ammoniacal silver nitrate solution for 30 min. After staining the gels were washed 3 times in deionized water for 5 min each. The gels were developed in a solution containing 0.05% (w/v) citric acid and 0.05% formaldehyde for 5 to 10 min. Boxes are shown to indicate spots changed significantly.

(A)

1°-LB(#156) total

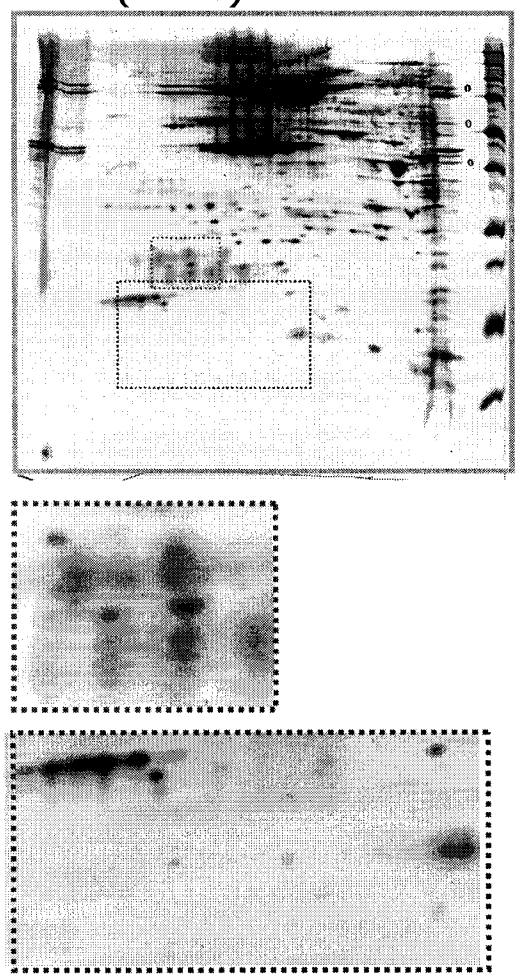

(B)

2°-LB(#166) total

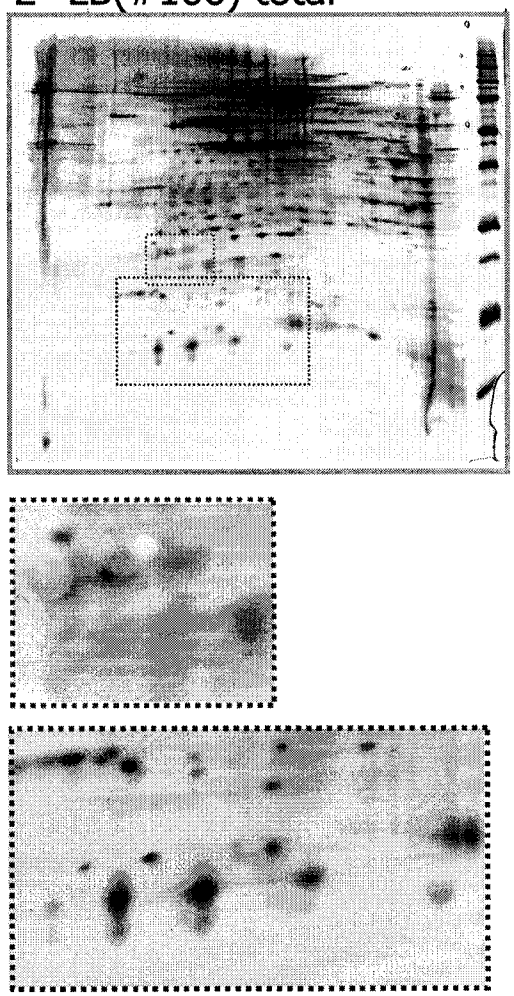

Appendix V. Tandem MS/MS analysis using Agilent Ion-Trap in a nanospray mode.

The MIHBPs were excised from the 2-D gel and in-gel digested by sequencing-grade trypsin (Promega). The tryptic fragments were subjected to tandem MS/MS analysis. The spectra were acquired, and the analyses were done manually. The mass differences between each peak represent the designated amino acids. Mother ions arre shown by blue diamonds on the right side of each spectrum. Sequences are presented in Table 2-1.

(A)

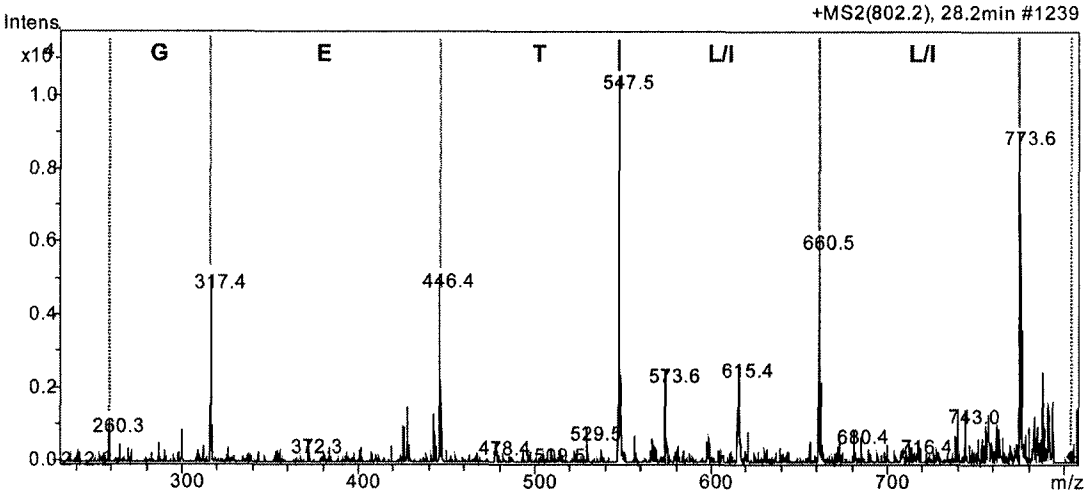

(B)

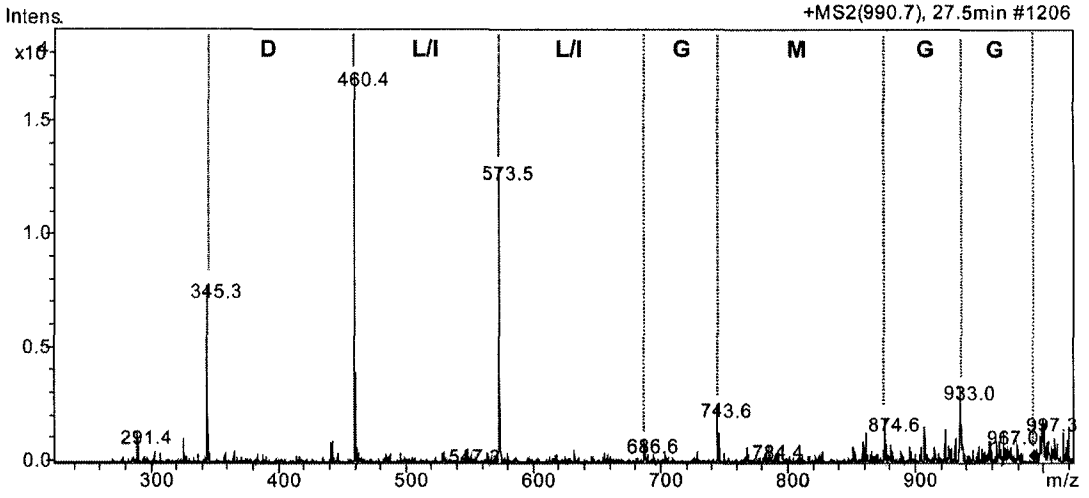

(C)

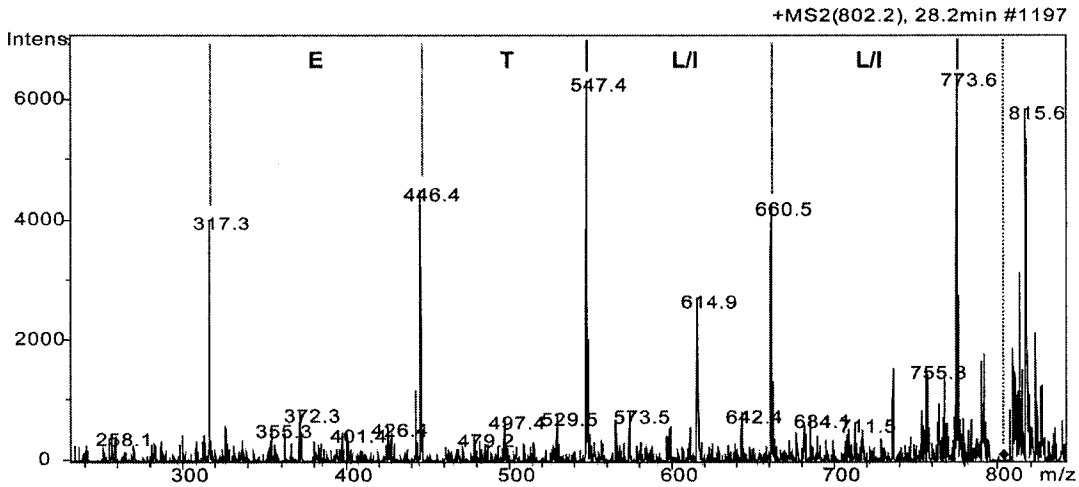

(D)

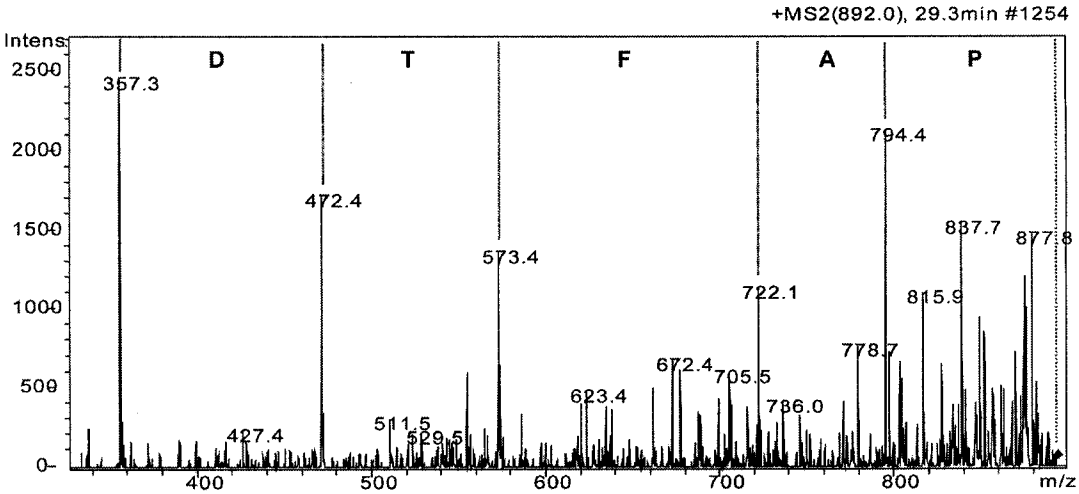

(E)

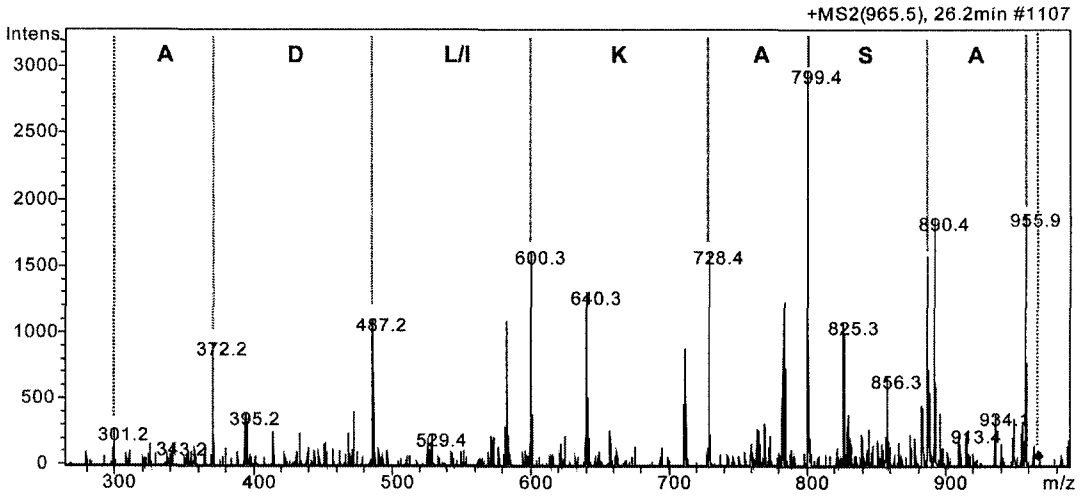

(F)

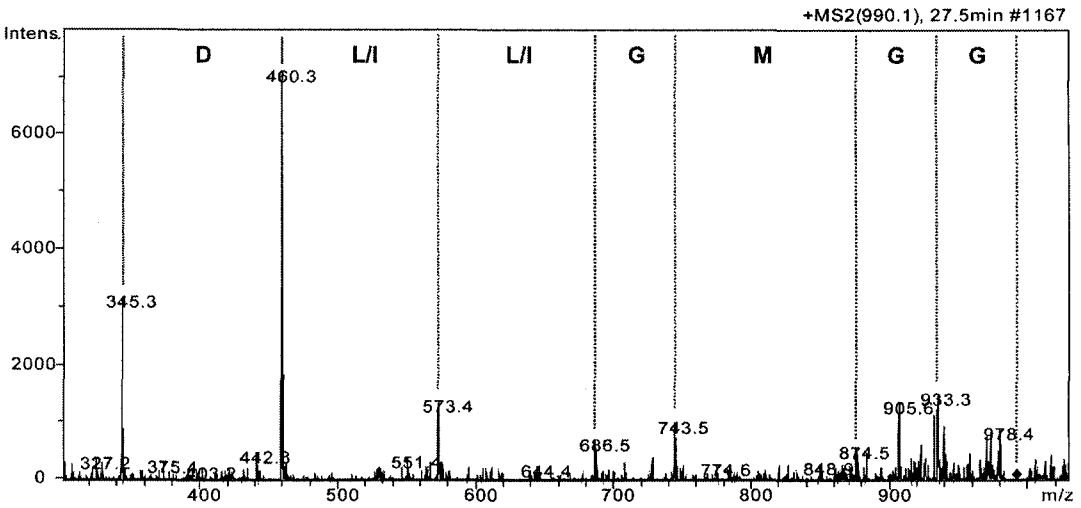

(G)

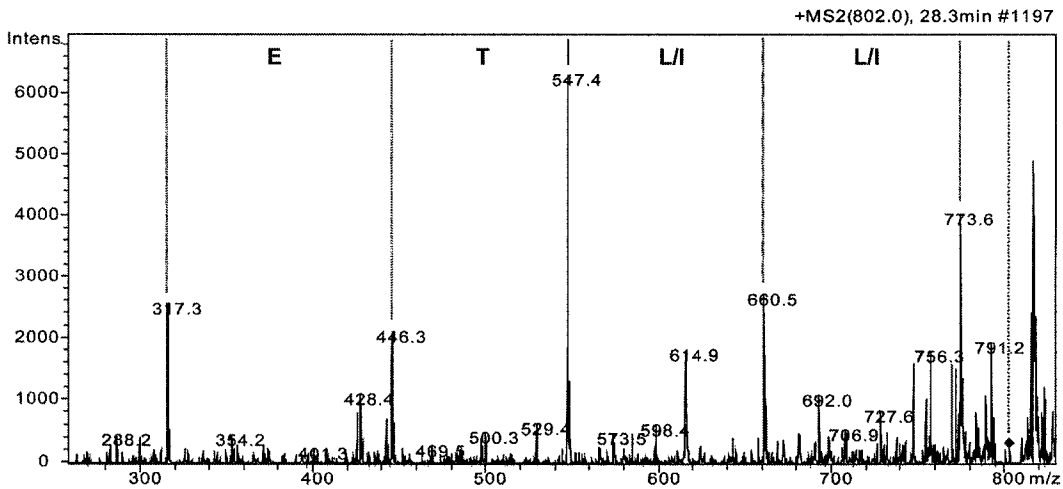

(H)

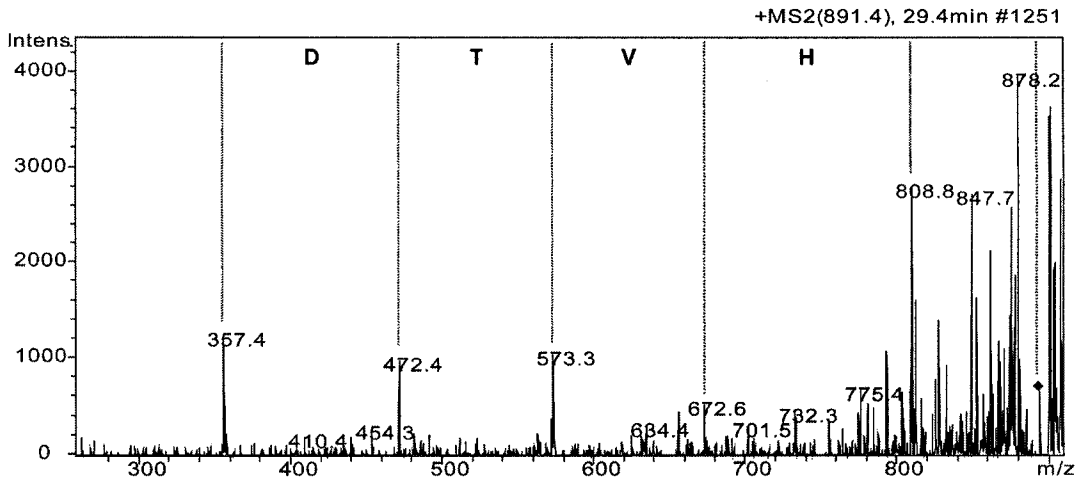

(I)

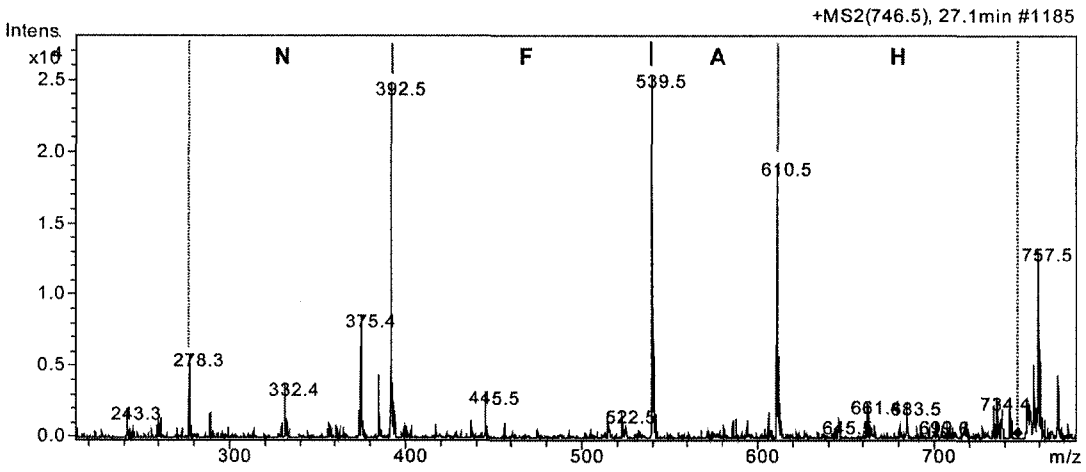

(J)

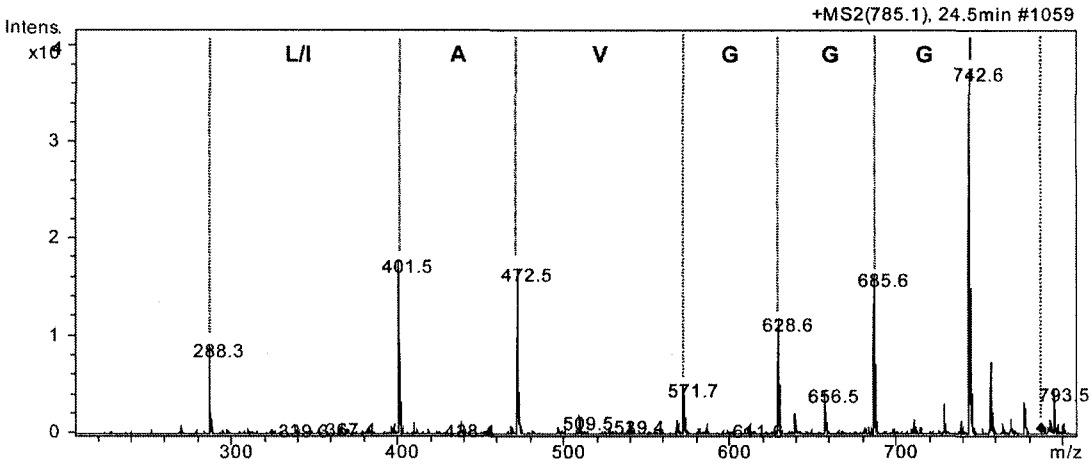

(K)

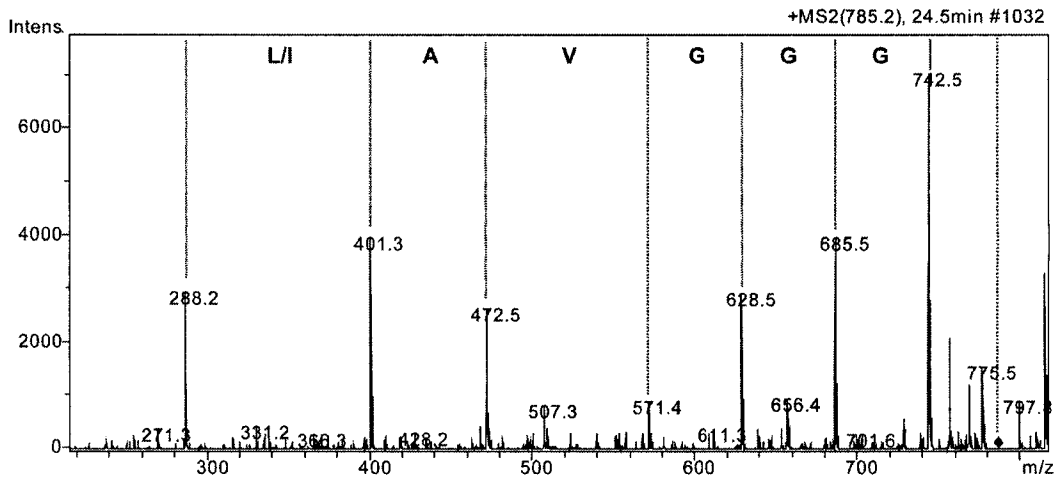

(L)

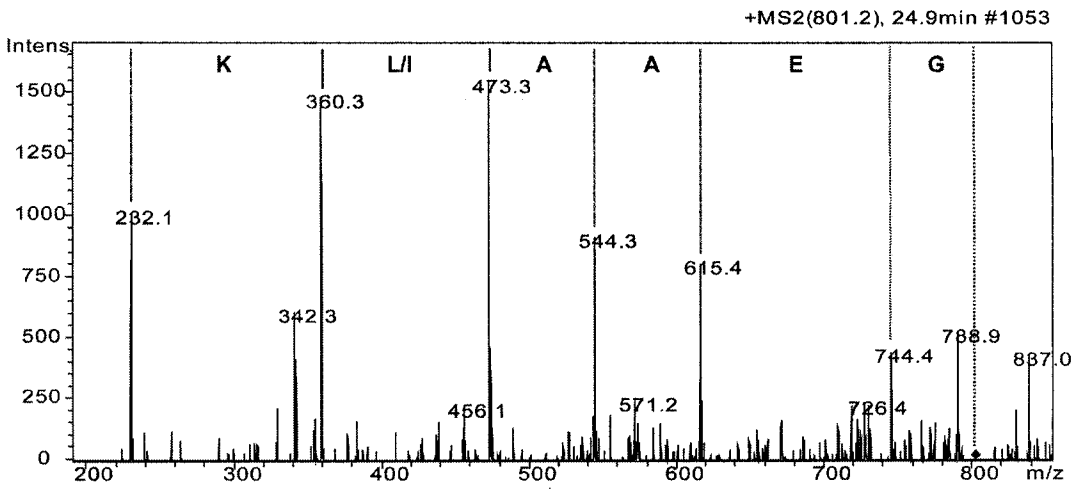

(M)

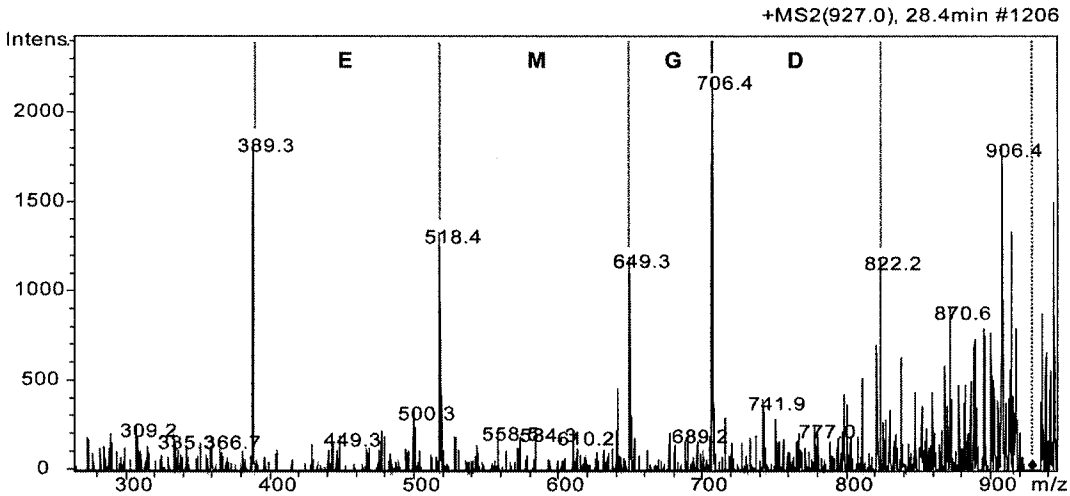

(N)

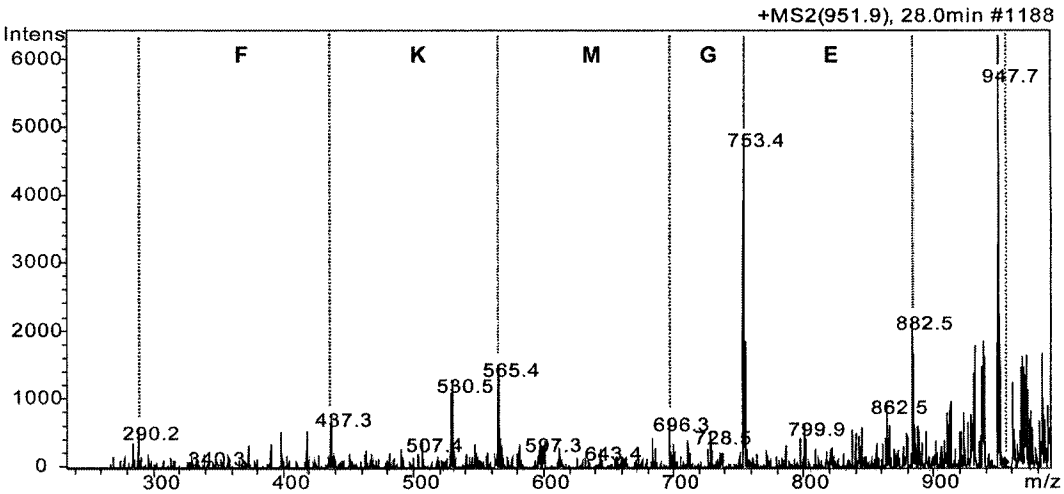

(O)

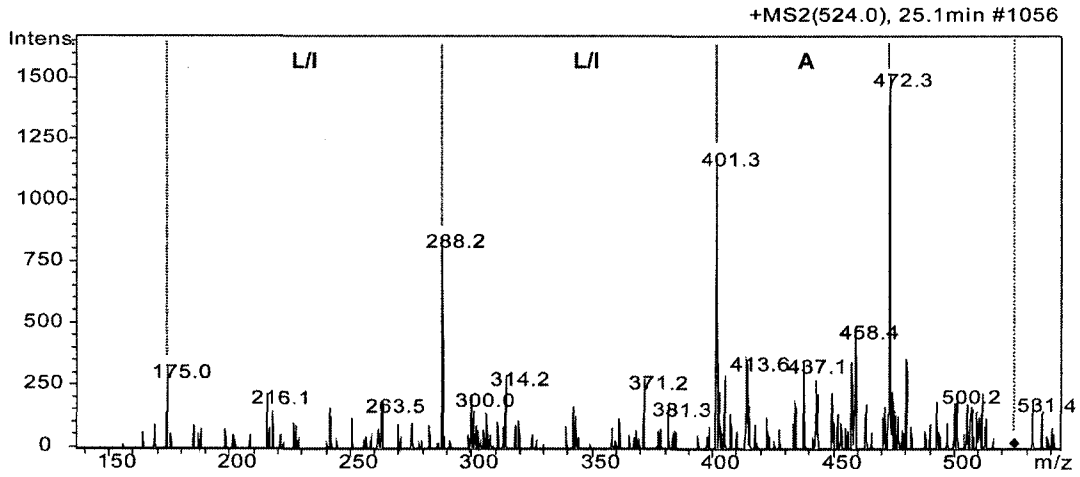

(P)

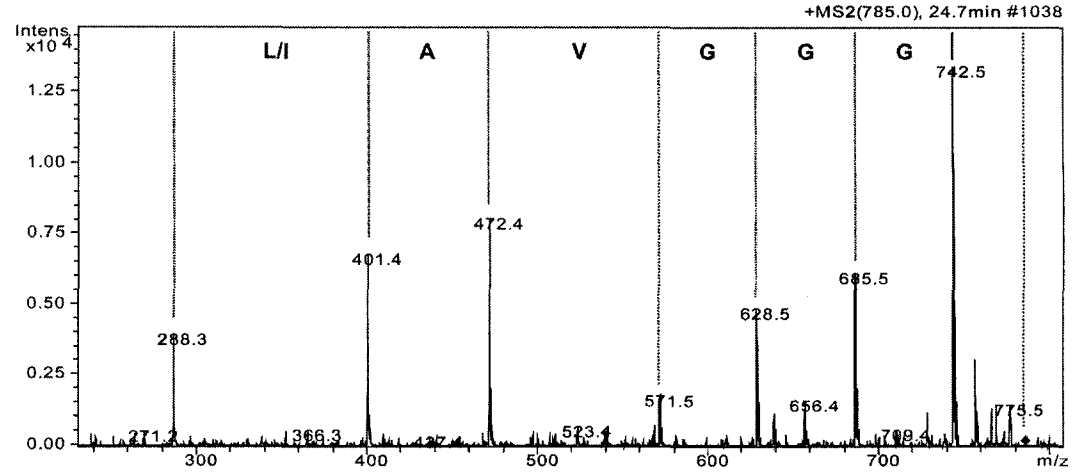

(Q)

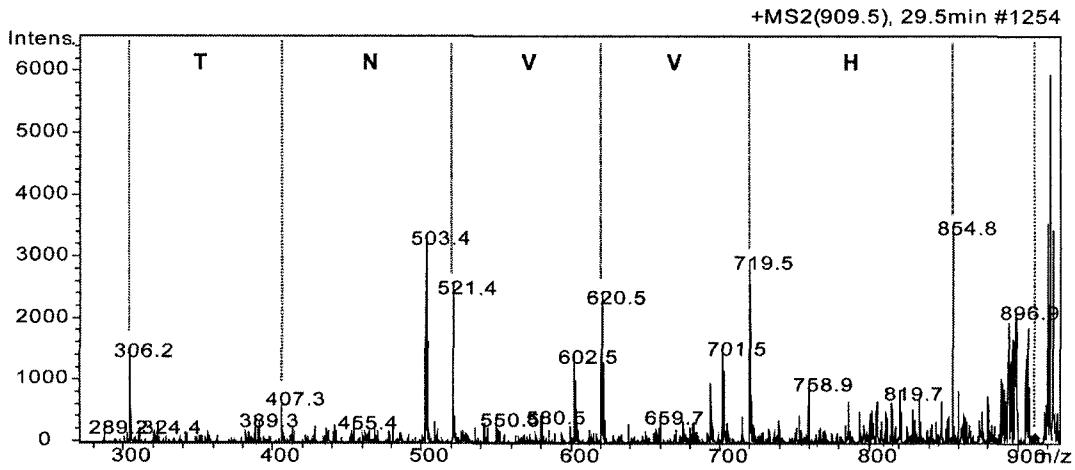

(R)

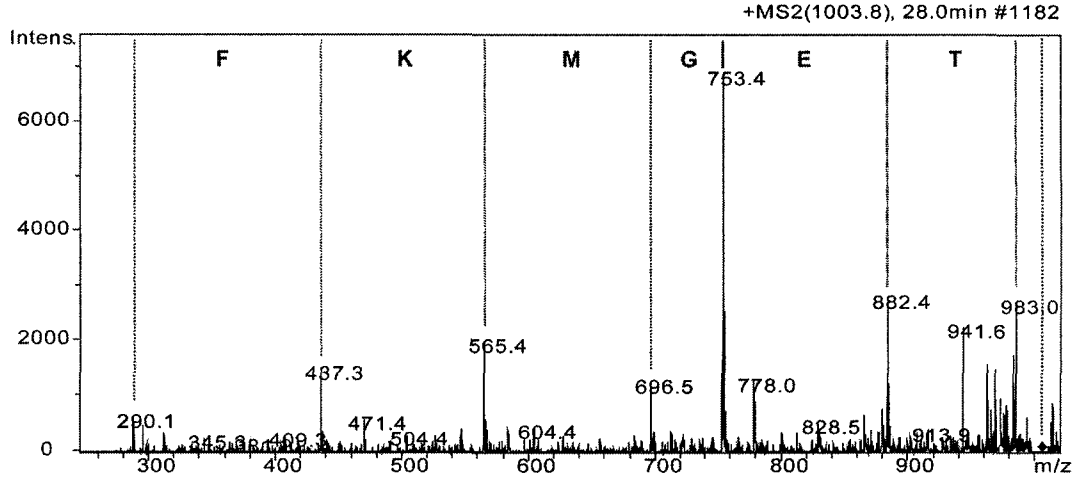

REFERENCES

Aonuma, H. (2002). Distribution of NO-induced cGMP-like immunoreactive neurones in the abdominal nervous system of the crayfish, *Procambarus clarkii*. *Zoological Science* **19**, 969-979.

Asazuma, H., Nagata, S., Katayama, H., Ohira, T. and Nagasawa, H. (2005). Characterization of a Molt-Inhibiting Hormone (MIH) Receptor in the Y-Organ of the Kuruma Prawn, Marsupenaeus japonicus. *Ann N Y Acad Sci* **1040**, 215-8.

Awede, B., Thissen, J. P., Gailly, P. and Lebacq, J. (1999). Regulation of IGF-I, IGFBP-4 and IGFBP-5 gene expression by loading in mouse skeletal muscle. *FEBS Lett.* **461**, 263-267.

Awede, B. L., Thissen, J. P. and Lebacq, J. (2002). Role of IGF-I and IGFBPs in the changes of mass and phenotype induced in rat soleus muscle by clenbuterol. *American Journal of Physiology-Endocrinology and Metabolism* **282**, E31-E37.

Baghdassarian, D., de Besse, N., Saidi, B., Somme, G. and Lachaise, F. (1996). Neuropeptide-induced inhibition of steroidogenesis in crab molting glands: involvement of cGMP-dependent protein kinase. *Gen Comp Endocrinol* **104**, 41-51.

Bauer, P. M., Fulton, D., Boo, Y. C., Sorescu, G. P., Kemp, B. E., Jo, H. and Sessa, W. C. (2003). Compensatory phosphorylation and protein-protein interactions revealed by loss of function and gain of function mutants of multiple serine phosphorylation sites in endothelial nitric-oxide synthase. *J Biol Chem* **278**, 14841-9.

Bayol, S., Jones, D., Goldspink, G. and Stickland, N. C. (2004). The influence of undernutrition during gestation on skeletal muscle cellularity and on the expression of genes that control muscle growth. *British Journal of Nutrition* **91**, 331-339.

Bivalacqua, T. J., Champion, H. C., Usta, M. F., Cellek, S., Chitaley, K., Webb, R. C., Lewis, R. L., Mills, T. M., Hellstrom, W. J. G. and Kadowitz, P. J. (2004). RhoA/Rho-kinase suppresses endothelial nitric oxide synthase in the penis: A mechanism for diabetes-associated erectile dysfunction. *Proceedings of the National Academy of Sciences of the United States of America* **101**, 9121-9126.

Bjellqvist, B., Ek, K., Righetti, P. G., Gianazza, E., Gorg, A., Westermeier, R. and Postel, W. (1982). Isoelectric focusing in immobilized pH gradients: principle, methodology and some applications. *J Biochem Biophys Methods* **6**, 317-39.

Blackstock, W. P. and Weir, M. P. (1999). Proteomics: quantitative and physical mapping of cellular proteins. *Trends Biotechnol* **17**, 121-7.

Böcking, D. and Sedlmeier, D. (1994). Protein phosphorylation in the molting gand of the crayfish, *Orconectes limosus* - Role of cyclic nucleotides, calcium, and molt inhibiting hormone (MIH). *Invertebrate Reproduction & Development* **26**, 237-245.

Boo, Y. C., Hwang, J., Sykes, M., Michell, B. J., Kemp, B. E., Lum, H. and Jo, H. (2002). Shear stress stimulates phosphorylation of eNOS at Ser(635) by a protein kinase A-dependent mechanism. *Am J Physiol Heart Circ Physiol* **283**, H1819-28.

Borst, D. W., Wainwright, G. and Rees, H. H. (2002). In vivo regulation of the mandibular organ in the edible crab, *Cancer pagurus*. *Proceedings of the Royal Society of London Series B-Biological Sciences* **269**, 483-490.

Bredt, D. S., Ferris, C. D. and Snyder, S. H. (1992). Nitric oxide synthase regulatory sites. Phosphorylation by cyclic AMP-dependent protein kinase, protein kinase C, and calcium/calmodulin protein kinase; identification of flavin and calmodulin binding sites. *Journal Of Biological Chemistry* **267**, 10976-10981.

Buchholz, C. and Adelung, D. (1980). The ultrastructural basis of steroid production in the Y-organ and the mandibular organ of the crabs Hemigrapsus nudus (Dana) and Carcinus maenas L. *Cell Tissue Res* **206**, 83-94.

Buechler, W. A., Nakane, M. and Murad, F. (1991). Expression of soluble guanylate cyclase activity requires both enzyme subunits. *Biochem Biophys Res Commun* **174**, 351-7.

Bulau, P., Meisen, I., Reichwein-Roderburg, B., Peter-Katalinic, J. and Keller, R. (2003). Two genetic variants of the crustacean hyperglycemic hormone (CHH) from the Australian crayfish, Cherax destructor: detection of chiral isoforms due to posttranslational modification. *Peptides* **24**, 1871-9.

Bulau, P., Okuno, A., Thome, E., Schmitz, T., Peter-Katalinic, J. and Keller, R. (2005). Characterization of a molt-inhibiting hormone (MIH) of the crayfish, Orconectes limosus, by cDNA cloning and mass spectrometric analysis. *Peptides* **26**, 2129-36.

Carlisle, D. B. and Dohrn, P. F. R. (1953). Studies on Lysmata seticaudata Risso (Crustacea Decapoda). II. Experimental evidence for a growth- and moult-accelerating factor obtainable from eyestalks. *Pubbl. Staz. Zool. Nopoli* **24**, 69-83.

Cesi, V., Vitali, R., Tanno, B., Giuffrida, M. L., Sesti, F., Mancini, C. and Raschella, G. (2004). Insulin-like Growth Factor Binding Protein 5: Contribution to Growth and Differentiation of Neuroblastoma Cells. *Ann N Y Acad Sci* **1028**, 59-68.

Chan, S. M., Chen, X. G. and Gu, P. L. (1998). PCR cloning and expression of the molt-inhibiting hormone gene for the crab (*Charybdis feriatus*). *Gene* **224**, 23-33.

Chan, S. M., Gu, P. L., Chu, K. H. and Tobe, S. S. (2003). Crustacean neuropeptide genes of the CHH/MIH/GIH family: implications from molecular studies. *General and Comparative Endocrinology* **134**, 214-219.

Chang, E. S. (1985). Hormonal control of molting in decapod Crustacea. *American Zoologist* **25**, 179-185.

Chang, E. S. (1989). Endocrine regulation of molting in Crustacea. *Rev. Aquatic Sci. I.*, 131-158.

Chang, E. S. (1993). Comparative endocrinology of molting and reproduction: Insects and crustaceans. *Annu.Rev.Entomol.* **38**, 161-180.

Chang, E. S. and Bruce, M. J. (1980). Ecdysteroid titers of juvenile lobsters following molt induction. *Journal of Experimental Zoology* **214**, 157-160.

Chang, E. S., Bruce, M. J. and Newcomb, R. W. (1987). Purification and amino acid composition of a peptide with molt-inhibiting activity from the lobster, *Homarus americanus*. *General and Comparative Endocrinology* **65**, 56-64.

Chang, E. S., Chang, S. A., Beltz, B. S. and Kravitz, E. A. (1999). Crustacean hyperglycemic hormone in the lobster nervous system: Localization and release from cells in the subesophageal ganglion and thoracic second roots. *J.Comp.Neurol.* **414**, 50-56.

Chang, E. S. and O'Connor, J. D. (1979). Arthropod molting hormones. In *Methods of Hormone Radioimmunoassay*, eds. B. M. Jaffe and H. R. Behrman), pp. 797-814. New York: Academic Press.

Chung, J. S., Dircksen, H. and Webster, S. G. (1999). A remarkable, precisely timed release of hyperglycemic hormone from endocrine cells in the gut is associated with ecdysis in the crab *Carcinus maenas*. *Proceedings of the National Academy of Sciences USA* **96**, 13103-13107.

Chung, J. S. and Webster, S. G. (2003). Moult cycle-related changes in biological activity of moult-inhibiting hormone (MIH) and crustacean hyperglycaemic hormone (CHH) in the crab, Carcinus maenas. From target to transcript. *Eur J Biochem* **270**, 3280-8.

Chung, J. S. and Webster, S. G. (2005). Dynamics of in vivo release of molt-inhibiting hormone and crustacean hyperglycemic hormone in the shore crab, Carcinus maenas. *Endocrinology* **146**, 5545-5551.

Chung, J. S., Wilkinson, M. C. and Webster, S. G. (1996). Determination of the amino acid sequence of the moult-inhibiting hormone from the edible crab, *Cancer pagurus*. *Neuropeptides* **30**, 95-101.

Chung, J. S., Wilkinson, M. C. and Webster, S. G. (1998). Amino acid sequences of both isoforms of crustacean hyperglycemic hormone (CHH) and corresponding precursor-related peptide in *Cancer pagurus*. *Regul. Pept.* **77**, 17-24.

Colasanti, M. and Venturini, G. (2000). Nitric oxide in invertebrates. *Molecular Neurobiology* **17**, 157-174.

Collins, M. O., Yu, L., Coba, M. P., Husi, H., Campuzano, L., Blackstock, W. P., Choudhary, J. S. and Grant, S. G. N. (2005). Proteomic analysis of in vivo phosphorylated synaptic proteins. *Journal Of Biological Chemistry* **280**, 5972-5982.

Collmann, C., Carlsson, M. A., Hansson, B. S. and Nighorn, A. (2004). Odorant-evoked nitric oxide signals in the antennal lobe of Manduca sexta. *Journal of Neuroscience* **24**, 6070-6077.

Cooper, R. L. and Ruffner, M. E. (1998). Depression of synaptic efficacy at intermolt in crayfish neuromuscular junctions by 20-hydroxyecdysone, a molting hormone. *J.Neurophysiol.* **79**, 1931-1941.

Cordelier, P., Esteve, J. P., Rivard, N., Marletta, M., Vaysse, N., Susini, C. and Buscail, L. (1999). The activation of neuronal NO synthase is mediated by G-protein betagamma subunit and the tyrosine phosphatase SHP-2. *Faseb J* **13**, 2037-50.

Cromarty, S. I. and Kass-Simon, G. (1998). Differential effects of a molting hormone, 20-hydroxyecdysone, on the neuromuscular junctions of the claw opener and abdominal flexor muscles of the American lobster. *Comp.Biochem.Physiol.[A]* **120**, 289-300.

Crown, A. L., Cottle, K., Lightman, S. L., Falk, S., Mohamed-Ali, V., Armstrong, L., Millar, A. B. and Holly, J. M. P. (2002). What is the role of the insulin-like growth factor system in the pathophysiology of cancer cachexia, and how is it regulated? *Clinical Endocrinology* **56**, 723-733.

Dauphin-Villemant, C., Bocking, D. and Sedlmeier, D. (1995). Regulation of Steroidogenesis in Crayfish Molting Glands - Involvement of Protein-Synthesis. *Molecular and Cellular Endocrinology* **109**, 97-103.

Davies, S. A. (2000). Nitric oxide signalling in insects. *Insect Biochemistry and Molecular Biology* **30**, 1123-1138.

Dawson, T. M., Sasaki, M., Gonzalez-Zulueta, M. and Dawson, V. L. (1998). Regulation of neuronal nitric oxide synthase and identification of novel nitric oxide signaling pathways. *Prog Brain Res* **118**, 3-11.

De Kleijn, D. P. V. and Van Herp, F. (1995). Molecular biology of neurohormone precursors in the eyestalk of Crustacea. *Comparative Biochemistry and Physiology [B]* **112B**, 573-579.

Dell, S., Sedlmeier, D., Böcking, D. and Dauphin-Villemant, C. (1999). Ecdysteroid biosynthesis in crayfish Y-organs: Feedback regulation by circulating ecdysteroids. *Arch.Insect Biochem.Physiol.* **41**, 148-155.

Dhingra, V., Gupta, M., Andacht, T. and Fu, Z. F. (2005). New frontiers in proteomics research: A perspective. *International Journal Of Pharmaceutics* **299**, 1-18.

Dircksen, H., Böcking, D., Heyn, U., Mandel, C., Chung, J. S., Baggerman, G., Verhaert, P., Daufeldt, S., Plösch, T., Jaros, P. P. et al. (2001). Crustacean hyperglycaemic hormone (CHH)-like peptides and CHH-precursor-related peptides from pericardial organ neurosecretory cells in the shore crab, *Carcinus maenas*, are putatively spliced and modified products of multiple genes. *Biochemical Journal* **356**, 159-170.

Dircksen, H. and Soyez, D. (1998). The lobster thoracic ganglia-pericardial organ neurosecretory system: a large source of novel crustacean hyperglycemic hormone-like peptide. In *Recent Developments in Comparative Endocrinology and Neurobiology Proceedings of the 19th Conference for European Comparative Endocrinologists.*, (ed. E.

W. Roubos, Wendelaar Bonga, S.E., Vaudry, H., De Loof, A.). Nijmegen: European Society for Comparative Endocrinology, Univ. of Nijmegen.

Drach, P. (1939). Meu et cycle d'intermue chez les Crustaces Decapodes. *Ann. Inst. Oceanogr.* **19**, 103-391.

Durica, D. S., Wu, X. H., Anilkumar, G., Hopkins, P. M. and Chung, A. C. K. (2002). Characterization of crab EcR and RXR homologs and expression during limb regeneration and oocyte maturation. *Molecular and Cellular Endocrinology* **189**, 59-76.

Eisen, M. B., Spellman, P. T., Brown, P. O. and Botstein, D. (1998). Cluster analysis and display of genome-wide expression patterns. *Proc Natl Acad Sci U S A* **95**, 14863-8.

Fleming, I., Fisslthaler, B., Dimmeler, S., Kemp, B. E. and Busse, R. (2001). Phosphorylation of Thr(495) regulates Ca(2+)/calmodulin-dependent endothelial nitric oxide synthase activity. *Circ Res* **88**, E68-75.

Foerster, J., Harteneck, C., Malkewitz, J., Schultz, G. and Koesling, D. (1996). A functional heme-binding site of soluble guanylyl cyclase requires intact N-termini of alpha 1 and beta 1 subunits. *Eur J Biochem* **240**, 380-6.

Friebe, A., Wedel, B., Harteneck, C., Foerster, J., Schultz, G. and Koesling, D. (1997). Functions of conserved cysteines of soluble guanylyl cyclase. *Biochemistry* **36**, 1194-8.

Gharahdaghi, F., Weinberg, C. R., Meagher, D. A., Imai, B. S. and Mische, S. M. (1999). Mass spectrometric identification of proteins from silver-stained polyacrylamide gel: a method for the removal of silver ions to enhance sensitivity. *Electrophoresis* **20**, 601-5.

Ghosh, D. K. and Salerno, J. C. (2003). Nitric oxide synthases: Domain structure and alignment in enzyme function and control. *Frontiers in Bioscience* **8**, D193-D209.

Gobom, J., Nordhoff, E., Mirgorodskaya, E., Ekman, R. and Roepstorff, P. (1999). Sample purification and preparation technique based on nano-scale reversed-phase columns for the sensitive analysis of complex peptide mixtures by matrix-assisted laser desorption/ionization mass spectrometry. *J Mass Spectrom* **34**, 105-16.

Gorg, A., Postel, W., Domscheit, A. and Gunther, S. (1988). Two-dimensional electrophoresis with immobilized pH gradients of leaf proteins from barley (Hordeum vulgare): method, reproducibility and genetic aspects. *Electrophoresis* **9**, 681-92.

Goy, M. F. (1990). Activation of membrane guanylate cyclase by an invertebrate peptide hormone. *Journal Of Biological Chemistry* **265**, 20220-20227.

Goy, M. F. (2005). Nitric oxide: An inhibitory retrograde modulator in the crustacean heart. *Comparative Biochemistry And Physiology A-Molecular & Integrative Physiology* **142**, 151-163.

Goy, M. F., Mandelbrot, D. A. and York, C. M. (1987). Identification and Characterization of a Polypeptide from a Lobster Neurosecretory Gland That Induces Cyclic-Gmp Accumulation in Lobster Neuromuscular Preparations. *Journal of Neurochemistry* **48**, 954-966.

Grieneisen, M. L. (1992). The biosynthesis of ecdysteroids by prothoracic glands of *Manduca sexta*. Chapel Hill: University of North Carolina.

Grieneisen, M. L. (1994). Recent advances in our knowledge of ecdysteroid biosynthesis in insects and crustaceans. *Insect Biochem.Mol.Biol.* **24**, 115-132.

Gu, P. L. and Chan, S. M. (1998). The shrimp hyperglycemic hormone-like neuropeptide is encoded by multiple copies of genes arranged in a cluster. *FEBS Lett.* **441**, 397-403.

Han, D. W. and Watson, R. D. (2005). Trimeric G proteins in crustacean (Callinectes sapidus) Y-organs: Occurrence and functional link to protein synthesis. *Journal Of Experimental Zoology Part A-Comparative Experimental Biology* **303A**, 441-447.

Harteneck, C., Wedel, B., Koesling, D., Malkewitz, J., Bohme, E. and Schultz, G. (1991). Molecular cloning and expression of a new alpha-subunit of soluble guanylyl cyclase. Interchangeability of the alpha-subunits of the enzyme. *Febs Letters* **292**, 217-22.

Hoffman, D. L. (1967). The structure of lymphogenous tissue of a caridean shrimp previously described as Y-organ (molting gland). *Can.J.Zool.* **45**, 886-889.

Hoffmann, J. and Porchet, M. (1984). Biosynthesis, metabolism, and mode of action of invertebrate hormones. Berlin ; New York: Springer-Verlag.

Hopkins, P. M. (1983). Patterns of serum ecdysteroids during induced and uninduced proecdysis in the fiddler crab, Uca pugilator. *Gen Comp Endocrinol* **52**, 350-6.

Hopkins, P. M. (1992). Hormonal control of the molt cycle in the fiddler crab *Uca pugilator*. *American Zoologist* **32**, 450-458.

Hughes, J. T., Sullivan,j. j., and Schleser (1972). Enhancement of lobster growth. *Science* **177**, 1110-1111.

Iyer, L. M., Anantharaman, V. and Aravind, L. (2003). Ancient conserved domains shared by animal soluble guanylyl cyclases and bacterial signaling proteins. *BMC Genomics* **4**, 5.

Jagota, A. (2000). Data Analysis and Classification for Bioinformatics: Bioinformatics by the Bay Press.

Jain, A. K., Murty, M. N. and Flynn, P. J. (1999). Data clustering: a review. *ACM Computing Surveys* **31**, 264-323.

Janin, A. K. and Dubes, R. C. (1988). Algorithms for Clustering Data. In *Prentice Hall, Englewood.* NJ.

Jenkin, P. M. and Hinton, H. E. (1966). Apolysis in arthropod moulting cycles. *Nature* **211**, 871.

Johansson, K. U. I. and Carlberg, M. (1994). NADPH-diaphorase histochemistry and nitric oxide synthase activity in deutocerebrum of the crayfish, *Pacifastacus leniusculus* (Crustacea, Decapoda). *Brain Research* **649**, 36-42.

Johansson, K. U. I. and Mellon, D. (1998). Nitric oxide as a putative messenger molecule in the crayfish olfactory midbrain. *Brain Research* **807**, 237-242.

Kajimura, S., Aida, K. and Duan, C. (2005). Insulin-like growth factor-binding protein-1 (IGFBP-1) mediates hypoxia-induced embryonic growth and developmental retardation. *Proc Natl Acad Sci U S A.*

Kang, B. K. and Spaziani, E. (1995a). Uptake of high-density lipoprotein by Y-organs of the crab Cancer antennarius: III. Evidence for adsorptive endocytosis and the absence of lysosomal processing. *J Exp Zool* **273**, 425-33.

Kang, B. K. and Spaziani, E. (1995b). Uptake of high-density lipoprotein by Y-organs of the crab, *Cancer antennarius.* I. Characterization in vitro and effects of stimulators and inhibitors. *Arch.Insect Biochem.Physiol.* **30**, 61-75.

Kang, B. K. and Spaziani, E. (1995c). Uptake of high-density lipoprotein by Y-organs of the crab, *Cancer antennarius*. II. Formal characterization of receptor-mediation with isolated membranes. *Arch.Insect Biochem.Physiol.* **30**, 77-91.

Karlson, P. and Hoffmeister, H. (1963). Zur biogenese des ecdysons. I. Umwandlung von cholesterin in ecdyson. *Hoppe-Seylers Zeitschrift Physiol. Chem.* **331**, 298-300.

Katayama, H., Nagata, K., Ohira, T., Yumoto, F., Tanokura, M. and Nagasawa, H. (2003). The solution structure of molt-inhibiting hormone from the kuruma prawn *Marsupenaeus japonicus*. *Journal Of Biological Chemistry* **278**, 9620-9623.

Kean, L., Cazenave, W., Costes, L., Broderick, K. E., Graham, S., Pollock, V. P., Davies, S. A., Veenstra, J. A. and Dow, J. A. T. (2002). Two nitridergic peptides are encoded by the gene capability in *Drosophila melanogaster*. *American Journal of Physiology* **282**, R1297-R1307.

Keller, R. (1992). Crustacean neuropeptides: Structures, functions and comparative aspects. *Experientia* **48**, 439-448.

Kim, H. W., Batista, L. A., Hoppes, J. L., Lee, K. J. and Mykles, D. L. (2004). A crustacean nitric oxide synthase expressed in nerve ganglia, Y-organ, gill and gonad of the tropical land crab, *Gecarcinus lateralis*. *Journal of Experimental Biology* **207**, 2845-2857.

Kim, H. W., Chang, E. S. and Mykles, D. L. (2005a). Three calpains and ecdysone receptor in the land crab, Gecarcinus lateralis: sequences, expression, and

effects of elevated ecdysteroid induced by eyestalk ablation. *Journal of Experimental Biology* **208**, 3177-3197.

Kim, H. W., Lee, S. G. and Mykles, D. L. (2005b). Ecdysteroid-responsive genes, RXR and E75, in the tropical land crab, Gecarcinus lateralis: Differential tissue expression of multiple RXR isoforms generated at three alternative splicing sites in the hinge and ligand-binding domains. *Molecular and Cellular Endocrinology* **242**, 80-95.

Klein, J. M., Mangerich, S., De Kleijn, D. P. V., Keller, R. and Weidemann, W. M. (1993). Molecular cloning of crustacean putative molt-inhibiting hormone (MIH) precursor. *FEBS Lett.* **334**, 139-142.

Koglin, M. and Behrends, S. (2003). A functional domain of the alpha1 subunit of soluble guanylyl cyclase is necessary for activation of the enzyme by nitric oxide and YC-1 but is not involved in heme binding. *J Biol Chem* **278**, 12590-7.

Kone, B. C. (2001). Molecular biology of natriuretic peptides and nitric oxide synthases. *Cardiovascular Research* **51**, 429-441.

Kozlova, T. and Thummel, C. S. (2000). Steroid regulation of postembryonic development and reproduction in Drosophila. *Trends in Endocrinology and Metabolism* **11**, 276-280.

Kummer, G. and Keller, R. (1993). High-affinity binding of crustacean hyperglycemic hormone (CHH) to hepatopancreatic plasma membranes of the crab *Carcinus maenas* and the crayfish *Orconectes limosus*. *Peptides* **14**, 103-108.

Lachaise, A., Le Roux, A., Hubert, M. and Lafont, R. (1993). The molting gland of crustaceans: localization, activity, and endocrine control (a review). *Journal of Crustacean Biology* **13**, 198-234.

Lachaise, F., Goudeau, M., Carpentier, G., Saidi, B. and Goudeau, H. (1992). Eyestalk ablation in female crabs: Effects on egg characteristics. *Journal of Experimental Zoology* **261**, 86-96.

Lachaise, F., Meister, M. F., Hetru, C. and Lafont, R. (1986). Studies on the biosynthesis of ecdysone by the Y-organs of Carcinus maenas. *Mol Cell Endocrinol* **45**, 253-61.

Lachaise, F., Somme, G., Carpentier, G., Granjeon, E., Webster, S. and Baghdassarian, D. (1996). A transaldolase - An enzyme implicated in crab steroidogenesis. *Endocrine* **5**, 23-32.

Lang, C. H., Fan, J., Cooney, R. and Vary, T. C. (1996). IL-1 receptor antagonist attenuates sepsis-induced alterations in the IGF system and protein synthesis. *Am.J.Physiol.Endocrinol.Metab.* **270**, E430-E437.

Lee, C. Y., Zou, H. S., Yau, S. M., Ju, Y. R. and Liau, C. S. (2000). Nitric oxide synthase activity and immunoreactivity in the crayfish *Procambarus clarkii*. *Neuroreport* **11**, 1273-1276.

Lee, K. J., Elton, T. S., Bej, A. K., Watts, S. A. and Watson, R. D. (1995). Molecular cloning of a cDNA encoding putative molt-inhibiting hormone from the blue crab, *Callinectes sapidus*. *Biochem.Biophys.Res.Commun.* **209**, 1126-1131.

Lee, K. J. and Watson, R. D. (2002). Antipeptide antibodies for detecting crab (*Callinectes sapidus*) molt-inhibiting hormone. *Peptides* **23**, 853-862.

Lee, S. G., Kim, H. W., Bader, B. D., Chang, E. S. and Mykles, D. L. (2005). Effects of elevated ecdysteroid on expression of three guanylyl cyclases in tropical land crab, *Gecarcinus lateralis*. *Integr. Comp. Biol.* **45**, 1158.

Lee, S. G., Kim, H. W., Bader, B. D., Chang, E. S. and Mykles, D. L. (2006). Three guanylyl cyclases in the tropical land crab, Gecarcinus lateralis: cloning and tissue expression in response to elevated ecdysteroid. *Journal of Experimental Biology*, submitted.

Lee, S. G. and Mykles, D. L. (2006). Proteomics and signal transduction in the crustacean molting gland. *Integr. Comp. Biol.*, submitted.

Liu, H. F., Lai, C. Y., Watson, R. D. and Lee, C. Y. (2004). Molecular cloning of a putative membrane form guanylyl cyclase from the crayfish *Procambarus clarkii*. *Journal of Experimental Zoology* **301A**, 512-520.

Lu, W. Q., Wainwright, G., Webster, S. G., Rees, H. H. and Turner, P. C. (2000). Clustering of mandibular organ-inhibiting hormone and moult-inhibiting hormone genes in the crab, *Cancer pagurus*, and implications for regulation of expression. *Gene* **253**, 197-207.

Lucas, K. A., Pitari, G. M., Kazerounian, S., Ruiz-Stewart, I., Park, J., Schulz, S., Chepenik, K. P. and Waldman, S. A. (2000). Guanylyl cyclases and signaling by cyclic GMP. *Pharmacological Reviews* **52**, 375-413.

MacPherson, M. R., Pollock, V. P., Broderick, K. E., Kean, L., O'Connell, F. C., Dow, J. A. T. and Davies, S. A. (2001). Model organisms: New insights into ion channel and transporter function. L-type calcium channels regulate epithelial fluid transport in *Drosophila melanogaster*. *American Journal of Physiology* **280**, C394-C407.

Mahadevan, A., Lappe, J., Rhyne, R. T., Cruz-Bermudez, N. D., Marder, E. and Goy, M. F. (2004). Nitric oxide inhibits the rate and strength of cardiac contractions

in the lobster *Homarus americanus* by acting on the cardiac ganglion. *Journal of Neuroscience* **24**, 2813-2824.

Makrantoni, V., Antrobus, R., Botting, C. H. and Coote, P. J. (2005). Rapid enrichment and analysis of yeast phosphoproteins using affinity chromatography, 2D-PAGE and peptide mass fingerprinting. *Yeast* **22**, 401-14.

Maniere, G., Vanhems, E., Gautron, F. and Delbecque, J. P. (2003). Inhibition of ovarian steroidogenesis by cyclic GMP in a fly. *Journal of Endocrinology* **177**, 35-44.

Marco, H. G., Hansen, I. A., Scheller, K. and Gade, G. (2003). Molecular cloning and localization of a cDNA encoding a crustacean hyperglycemic hormone from the South African spiny lobster, Jasus lalandii. *Peptides* **24**, 845-51.

Marshman, E. and Streuli, C. H. (2002). Insulin-like growth factors and insulin-like growth factor binding proteins in mammary gland function. *Breast Cancer Res* **4**, 231-9.

Mattson, M. P. and Spaziani, E. (1985). Cyclic AMP mediates the negative regulation of Y-organ ecdysteroid production. *Mol Cell Endocrinol* **42**, 185-9.

Mattson, M. P. and Spaziani, E. (1986). Regulation of Y-organ ecdysteroidogenesis by molt-inhibiting hormone in crabs: involvement of cyclic AMP-mediated protein synthesis. *General and Comparative Endocrinology* **63**, 414-423.

Mazerbourg, S., Callebaut, I., Zapf, J., Mohan, S., Overgaard, M. and Monget, P. (2004). Update on IGFBP-4: regulation of IGFBP-4 levels and functions, in vitro and in vivo. *Growth Horm IGF Res* **14**, 71-84.

Metodiev, M. V., Timanova, A. and Stone, D. E. (2004). Differential phosphoproteome profiling by affinity capture and tandem matrix-assisted laser desorption/ionization mass spectrometry. *Proteomics* **4**, 1433-8.

Michell, B. J., Harris, M. B., Chen, Z. P., Ju, H., Venema, V. J., Blackstone, M. A., Huang, W., Venema, R. C. and Kemp, B. E. (2002). Identification of regulatory sites of phosphorylation of the bovine endothelial nitric-oxide synthase at serine 617 and serine 635. *J Biol Chem* **277**, 42344-51.

Morton, D. B. (2004). Invertebrates yield a plethora of atypical guanylyl cyclases. *Molecular Neurobiology* **29**, 97-115.

Morton, D. B. and Simpson, P. J. (2002). Cellular signaling in eclosion hormone action. *Journal of Insect Physiology* **48**, 1-13.

Mount, P. F., Fraser, S. A., Watanabe, Y., Lane, N., Katsis, F., Chen, Z.-P., Kemp, B. E. and Power, D. A. (2006). Phosphorylation of Neuronal and Endothelial Nitric Oxide Synthase in the Kidney with High and Low Salt Diets. *Nephron Physiology* **102**, 36-50.

Mykles, D. L. (1997). Crustacean muscle plasticity: Molecular mechanisms determining mass and contractile properties. *Comparative Biochemistry and Physiology* **117B**, 367-378.

Nakatsuji, T. and Sonobe, H. (2004). Regulation of ecdysteroid secretion from the Y-organ by molt-inhibiting hormone in the American crayfish, Procambarus clarkii. *General and Comparative Endocrinology* **135**, 358-364.

Nighorn, A., Byrnes, K. A. and Morton, D. B. (1999). Identification and characterization of a novel beta subunit of soluble guanylyl cyclase that is active in the

absence of a second subunit and is relatively insensitive to nitric oxide. *Journal Of Biological Chemistry* **274**, 2525-2531.

Nighorn, A., Gibson, N. J., Rivers, D. M., Hildebrand, J. G. and Morton, D. B. (1998). The nitric oxide-cGMP pathway may mediate communication between sensory afferents and projection neurons in the antennal lobe of *Manduca sexta*. *Journal of Neuroscience* **18**, 7244-7255.

Nighorn, A., Simpson, P. J. and Morton, D. B. (2001). The novel guanylyl cyclase MsGC-I is strongly expressed in higher-order neuropils in the brain of *Manduca sexta*. *Journal of Experimental Biology* **204**, 305-314.

Nilsson-Ehle, H., Bengtsson, B. A., Lindstedt, G. and Mellstrom, D. (2005). Insulin-like growth factor-1 is a predictor of blood haemoglobin concentration in 70-yr-old subjects. *Eur J Haematol* **74**, 111-6.

Oddy, V. H. and Owens, P. C. (1996). Insulin-like growth factor I inhibits degradation and improves retention of protein in hindlimb muscle of lambs. *Am.J.Physiol.Endocrinol.Metab.* **271**, E973-E982.

Ortiz, P. A. and Garvin, J. L. (2003). Trafficking and activation of eNOS in epithelial cells. *Acta Physiologica Scandinavica* **179**, 107-114.

Padayatti, P. S., Pattanaik, P., Ma, X. and van den Akker, F. (2004). Structural insights into the regulation and the activation mechanism of mammalian guanylyl cyclases. *Pharmacol Ther* **104**, 83-99.

Pampusch, M. S., Johnson, B. J., White, M. E., Hathaway, M. R., Dunn, J. D., Waylan, A. T. and Dayton, W. R. (2003). Time course of changes in growth factor

mRNA levels in muscle of steroid-implanted and nonimplanted steers. *Journal of Animal Science* **81**, 2733-2740.

Passano, L. M. (1953). Neurosecretory control of molting in crabs by the X-organ sinus gland complex. *Physiologia comparata et Eecolgia* **3**, 155-189.

Passano, L. M. (1960). Low temperature blockage of molting in *Uca pugnax*. *Biological Bulletin* **118**, 129-136.

Pavloff, M. S. and Goy, M. F. (1990). Purification and chemical characterization of peptide-G1, an invertebrate neuropeptide that stimulates cyclic GMP metabolism. *Journal of Neurochemistry* **55**, 788-797.

Potter, L. R. (2005). Domain analysis of human transmembrane guanylyl cyclase receptors: Implications for regulation. *Frontiers In Bioscience* **10**, 1205-1220.

Prabhakar, S., Short, D. B., Scholz, N. L. and Goy, M. F. (1997). Identification of nitric oxide-sensitive and -insensitive forms of cytoplasmic guanylate cyclase. *Journal of Neurochemistry* **69**, 1650-1660.

Puente, L. G., Borris, D. J., Carriere, J. F., Kelly, J. F. and Megeney, L. A. (2006). Identification of candidate regulators of embryonic stem cell differentiation by comparative phosphoprotein affinity profiling. *Mol Cell Proteomics* **5**, 57-67.

Pyriochou, A. and Papapetropoulos, A. (2005). Soluble guanylyl cyclase: more secrets revealed. *Cellular Signalling* **17**, 407-413.

Rabilloud, T., Valette, C. and Lawrence, J. J. (1994). Sample application by in-gel rehydration improves the resolution of two-dimensional electrophoresis with immobilized pH gradients in the first dimension. *Electrophoresis* **15**, 1552-8.

Rameau, G. A., Chiu, L. Y. and Ziff, E. B. (2004). Bidirectional regulation of neuronal nitric-oxide synthase phosphorylation at serine 847 by the N-methyl-D-aspartate receptor. *J Biol Chem* **279**, 14307-14.

Ranga Rao, K. (1965). Isolation and partial characterization of the molt-inhibiting hormone of the crustacean eyestalk *Experientia* **21**, 593-594.

Rees, H. (1989). Pathways of biosynthesis of ecdysone. In *Ecdysone From Chemistry to Mode of Action*, vol. 152-190 (ed. J. Koolman): Georg Thieme Verlag. Stuttgart, Germany.

Rees, H. H. and Isaac, R. E. (1985). Biosynthesis and metabolism of ecdysteroids and methods of isolation and identification of the free and conjugated compounds. *Methods Enzymol* **111**, 377-410.

Riediger, W., Hergenhahn, H. G. and Sedlmeier, D. (1989). Calmodulin-Stimulated Particulate Guanylate-Cyclase in Crayfish Hepatopancreas. *International Journal of Biochemistry* **21**, 333-336.

Rosenzweig, S. A. (2004). What's new in the IGF-binding proteins? *Growth Horm IGF Res* **14**, 329-36.

Saidi, B., de Besse, N., Webster, S. G., Sedlmeier, D. and Lachaise, F. (1994). Involvement of cAMP and cGMP in the mode of action of molt-inhibiting hormone (MIH) a neuropeptide which inhibits steroidogenesis in a crab. *Mol.Cell.Endocrinol.* **102**, 53-61.

Sanchez, J. C., Rouge, V., Pisteur, M., Ravier, F., Tonella, L., Moosmayer, M., Wilkins, M. R. and Hochstrasser, D. F. (1997). Improved and simplified in-gel

sample application using reswelling of dry immobilized pH gradients. *Electrophoresis* **18**, 324-7.

Santos, E. A. and Keller, R. (1993). Crustacean hyperglycemic hormone (CHH) and the regulation of carbohydrate metabolism: Current perspectives. *Comp.Biochem.Physiol.[A]* **106A**, 405-411.

Santos, E. A., Nery, L. E., Keller, R. and Goncalves, A. A. (1997). Evidence for the involvement of the crustacean hyperglycemic hormone in the regulation of lipid metabolism. *Physiol Zool* **70**, 415-20.

Schmidt, P. M., Schramm, M., Schroder, H., Wunder, F. and Stasch, J. P. (2004). Identification of residues crucially involved in the binding of the heme moiety of soluble guanylate cyclase. *J Biol Chem* **279**, 3025-32.

Schmiege, D. L., Ridgway, R. L. and Moffett, S. B. (1992). Ultrastructure of autotomy-induced atrophy of muscles in the crab *Carcinus maenas*. *Can.J.Zool.* **70**, 841-851.

Scholz, N. and Truman, J. W. (2000). Invertebrate models for studying NO-mediated signaling. In *Handbook of Chemical Neuroanatomy*, vol. 17 eds. H. W. M. Steinbusch J. De Vente S. R. Vincent A. Bjorklund and T. Hokfelt), pp. 417-441: Elsevier Science B.V.

Scholz, N. L. (2001). NO/cGMP signaling and the flexible organization of motor behavior in crustaceans. *American Zoologist* **41**, 292-303.

Scholz, N. L., Chang, E. S., Graubard, K. and Truman, J. W. (1998). The NO/cGMP pathway and the development of neural networks in postembryonic lobsters. *Journal of Neurobiology* **34**, 208-226.

Scholz, N. L., de Vente, J., Truman, J. W. and Graubard, K. (2001). Neural network partitioning by NO and cGMP. *Journal of Neuroscience* **21**, 1610-1618.

Scholz, N. L., Goy, M. F., Truman, J. W. and Graubard, K. (1996). Nitric oxide and peptide neurohormones activate cGMP synthesis in the crab stomatogastric nervous system. *Journal of Neuroscience* **16**, 1614-1622.

Scholz, N. L., Labenia, J. S., De Vente, J., Graubard, K. and Goy, M. F. (2002). Expression of nitric oxide synthase and nitric oxide-sensitive guanylate cyclase in the crustacean cardiac ganglion. *Journal of Comparative Neurology* **454**, 158-167.

Schuppe, H., Aonuma, H. and Newland, P. L. (2001). Distribution of NADPH-diaphorase-positive ascending interneurones in the crayfish terminal abdominal ganglion. *Cell and Tissue Research* **305**, 135-146.

Sedlmeier, D. (1988). The crustacean hyperglycemic hormone (CHH) releases amylase from the crayfish midgut gland. *Regul Pept* **20**, 91-8.

Sedlmeier, D. and Fenrich, R. (1993). Regulation of ecdysteroid biosynthesis in crayfish Y-organs: I. Role of cyclic nucleotides. *Journal of Experimental Zoology* **265**, 448-453.

Sedlmeier, D. and Keller, R. (1981). The Mode of Action of the Crustacean Neurosecretory Hyperglycemic Hormone .1. Involvement of Cyclic-Nucleotides. *General and Comparative Endocrinology* **45**, 82-90.

Serrano, L., Blanvillain, G., Soyez, D., Charmantier, G., Grousset, E., Aujoulat, F. and Spanings-Pierrot, C. (2003). Putative involvement of crustacean hyperglycemic hormone isoforms in the neuroendocrine mediation of osmoregulation in the crayfish *Astacus leptodactylus*. *Journal of Experimental Biology* **206**, 979-988.

Simpson, P. J., Nighorn, A. and Morton, D. B. (1999). Identification of a novel guanylyl cyclase that is related to receptor guanylyl cyclases, but lacks extracellular and transmembrane domains. *Journal Of Biological Chemistry* **274**, 4440-4446.

Skinner, D. M. (1962). The structure and metabolism of a crustacean integumentary tissue during a molt cycle. *Biological Bulletin* **123**, 635-647.

Skinner, D. M. (1985). Molting and regeneration. In *The Biology of Crustacea*, eds. D. E. Bliss and L. H. Mantel), pp. 43-146. New York: Academic Press.

Smith, S. L. (1985). Regulation of ecdysteroid titer: synthesis. In *Comprehensive Insect Physiology, Biochemistry and Pharmacology*, vol. 7 eds. G. A. Kerkut and L. I. Gilbert), pp. 295-341: Pergamon Press.

Song, T., Hatano, N., Kume, K., Sugimoto, K., Yamaguchi, F., Tokuda, M. and Watanabe, Y. (2005). Inhibition of neuronal nitric-oxide synthase by phosphorylation at Threonine1296 in NG108-15 neuronal cells. *FEBS Lett* **579**, 5658-62.

Soyez, D. and Kleinholz, L. H. (1977). Molt-inhibiting factor from the crustacean eyestalk. *Gen Comp Endocrinol* **31**, 233-42.

Soyez, D., Van Herp, F., Rossier, J., Le Caer, J. P., Tensen, C. P. and Lafont, R. (1994). Evidence for a conformational polymorphism of invertebrate neurohormones. D-amino acid residue in crustacean hyperglycemic peptides. *J Biol Chem* **269**, 18295-8.

Spaziani, E., Jegla, T. C., Wang, W. L., Booth, J. A., Connolly, S. M., Conrad, C. C., Dewall, M. J., Sarno, C. M., Stone, D. K. and Montgomery, R. (2001). Further studies on signaling pathways for ecdysteroidogenesis in crustacean Y-organs. *American Zoologist* **41**, 418-429.

Spaziani, E. and Kater, S. B. (1973). Uptake and turnover of cholesterol- 14 C in Y-organs of the crab Hemigrapsus as a function of the molt cycle. *Gen Comp Endocrinol* **20**, 534-49.

Spaziani, E., Mattson, M. P., Wang, W. N. L. and McDougall, H. E. (1999). Signaling pathways for ecdysteroid hormone synthesis in crustacean Y-organs. *American Zoologist* **39**, 496-512.

Stark, M. and Assaraf, Y. G. (2006). Loss of Sp1 function via inhibitory phosphorylation in antifolate-resistant human leukemia cells with down-regulation of the reduced folate carrier. *Blood* **107**, 708-15.

Stasiv, Y., Regulski, M., Kuzin, B., Tully, T. and Enikolopov, G. (2001). The *Drosophila* nitric oxide synthase gene (dNOS) encodes a family of proteins that can modulate NOS activity by acting as dominant negative regulators. *Journal Of Biological Chemistry* **276**, 42241-42251.

Steele, C. G. H. and Vafapoulou, X. (1989). Ecdysteroid titer profiles during growth and development of arthropods. In *Ecdysone. From Chemistry to Mode of Action*, (ed. J. Koolman), pp. 221-231. Georg Thieme Verlag: Stuttgart, Germany.

Stephens, G. C. (1955). Induction of molting in the crayfish, Cambarus, by modification of daily photoperiod. *Biol Bull (Woods Hole, Mass.)* **108**, 235-241.

Sunahara, R. K., Beuve, A., Tesmer, J. J., Sprang, S. R., Garbers, D. L. and Gilman, A. G. (1998). Exchange of substrate and inhibitor specificities between adenylyl and guanylyl cyclases. *J Biol Chem* **273**, 16332-8.

Svanberg, E., Frost, R. A., Lang, C. H., Isgaard, J., Jefferson, L. S., Kimball, S. R. and Vary, T. C. (2000). IGF-I/IGFBP-3 binary complex modulates sepsis-induced

inhibition of protein synthesis in skeletal muscle. *Am.J.Physiol.Endocrinol.Metab.* **279**, E1145-E1158.

Talavera, E., Martinezlorenzana, G., Leonolea, M., Sanchezalvarez, M., Sanchezislas, E. and Pellicer, F. (1995). Histochemical distribution of NADPH-diaphorase in the cerebral ganglion of the crayfish *Cambarellus montezumae*. *Neuroscience Letters* **187**, 177-180.

Truman, J. W. and Riddiford, L. M. (1999). The origins of insect metamorphosis. *Nature* **401**, 447-452.

Ueda, K., Kosako, H., Fukui, Y. and Hattori, S. (2004). Proteomic identification of Bcl2-associated athanogene 2 as a novel MAPK-activated protein kinase 2 substrate. *J Biol Chem* **279**, 41815-21.

Umphrey, H. R., Lee, K. J., Watson, R. D. and Spaziani, E. (1998). Molecular cloning of a cDNA encoding molt-inhibiting hormone (MIH) of the crab, *Cancer magister*. *Molecular and Cellular Endocrinology* **136**, 145-149.

Vensel, W. H., Spaziani, E. and Ostegaard, L. S. (1984). Cholesterol turnover and ecdysone content in tissues of normal and de-eyestalked crabs (*Cancer antennarius*). *J. Exp. Zool.* **229**, 383-392.

Von Gliscynski, U. and Sedlmeier, D. (1993). Regulation of ecdysteroid biosynthesis in crayfish Y-organs: II. Role of cyclic nucleotide-dependent protein kinases. *Journal of Experimental Zoology* **265**, 454-458.

Waddy, S. L., Aiken, D. E. and de kleijn, D. P. V. (1995). Control of growth and reproduction. In *Biology of the Lobster Homarus americanus*, (ed. J. R. Factor), pp. 217-266. San Diego: Academic Press, Inc.

Wang, Y. and Marsden, P. A. (1995). Nitric oxide synthases: gene structure and regulation. *Adv Pharmacol* **34**, 71-90.

Watson, R. D., Lee, K. J., Qiu, S. H., Luo, M., Umphrey, H. R., Roer, R. D. and Spaziani, E. (2001). Molecular cloning, expression, and tissue distribution of crustacean molt-inhibiting hormone. *American Zoologist* **41**, 407-417.

Watson, R. D. and Spaziani, E. (1985). Biosynthesis of ecdysteroids from cholesterol by crab Y-organs, and eyestalk suppression of cholesterol uptake and secretory activity, in vitro. *Gen Comp Endocrinol* **59**, 140-8.

Webster, S. G. (1991). Amino acid sequence of putative moult-inhibiting hormone from the crab *Carcinus maenas*. *Proc. R. Soc. Lond. [Biol.]* **244**, 247-252.

Webster, S. G. (1993). High-affinity binding of putative moult-inhibiting hormone (MIH) and crustacean hyperglycaemic hormone (CHH) to membrane-bound receptors on the Y-organ of the shore crab *Carcinus maenus*. *Proc. R. Soc. Lond. [Biol.]* **251**, 53-59.

Wedel, B., Humbert, P., Harteneck, C., Foerster, J., Malkewitz, J., Bohme, E., Schultz, G. and Koesling, D. (1994). Mutation of His-105 in the beta 1 subunit yields a nitric oxide-insensitive form of soluble guanylyl cyclase. *Proc Natl Acad Sci U S A* **91**, 2592-6.

Weis, J. S. (1976). Effects of environmental factors on regeneration and molting in fiddler crabs. *Biol Bull* **150**, 152-62.

White, M. E., Johnson, B. J., Hathaway, M. R. and Dayton, W. R. (2003). Growth factor messenger RNA levels in muscle and liver of steroid-implanted and nortimplanted steers. *Journal of Animal Science* **81**, 965-972.

Willig, A. and Keller, R. (1976). Biosynthesis of alpha- and beta-ecdysone by the crayfish Orconectes limosus in vivo and by its Y-organs in vitro. *Experientia* **32**, 936-7.

Wu, J., Lenchik, N. J., Pabst, M. J., Solomon, S. S., Shull, J. and Gerling, I. C. (2005). Functional characterization of two-dimensional gel-separated proteins using sequential staining. *Electrophoresis* **26**, 225-37.

Wu, X. H., Hopkins, P. M., Palli, S. R. and Durica, D. S. (2004). Crustacean retinoid-X receptor isoforms: distinctive DNA binding and receptor-receptor interaction with a cognate ecdysteroid receptor. *Molecular and Cellular Endocrinology* **218**, 21-38.

Yang, L. S., Gordon-Krajcer, W. and Ksiezak-Reding, H. (1997). Tau released from paired helical filaments with formic acid or guanidine is susceptible to calpain-mediated proteolysis. *J.Neurochem.* **69**, 1548-1558.

Yasuda, A., Yasuda, Y., Fujita, T. and Naya, Y. (1994). Characterization of crustacean hyperglycemic hormone from the crayfish (*Procambarus clarkii*): Multiplicity of molecular forms by stereoinversion and diverse functions. *General and Comparative Endocrinology* **95**, 387-398.

Yu, X. L., Chang, E. S. and Mykles, D. L. (1999). Characterization of a factor in secondary limb regenerates that suspends molting in the land crab. *American Zoologist* **39**, 76A.

Yu, X. L., Chang, E. S. and Mykles, D. L. (2001). Characterization of limb autotomy factor-proecdysis, a polypeptide that inhibits molting in the land crab. *Am. Zool.* **41**, 1635.

Yu, X. L., Chang, E. S. and Mykles, D. L. (2002). Characterization of limb autotomy factor-proecdysis (LAF_{pro}), isolated from limb regenerates, that suspends molting in the land crab *Gecarcinus lateralis*. *Biological Bulletin* **202**, 204-212.

Yu, X. L. and Mykles, D. L. (1997). A factor in limb regenerates that suspends molting in the land crab, *Gecarcinus lateralis*. *American Zoologist* **37**, 154A.

Yu, X. L. and Mykles, D. L. (1998). Secondary limb regenerates contain a factor that suspends molting in the land crab. *American Zoologist* **38**, 42A.

Zhao, Y., Schelvis, J. P., Babcock, G. T. and Marletta, M. A. (1998). Identification of histidine 105 in the beta1 subunit of soluble guanylate cyclase as the heme proximal ligand. *Biochemistry* **37**, 4502-9.

Zheng, J., Lee, C. Y. and Watson, R. D. (2006). Molecular cloning of a putative receptor guanylyl cyclase from Y-organs of the blue crab, Callinectes sapidus. *Gen Comp Endocrinol.*

Zhou, R., Diehl, D., Hoeflich, A., Lahm, H. and Wolf, E. (2003). IGF-binding protein-4: biochemical characteristics and functional consequences. *J Endocrinol* **178**, 177-93.

Zou, H. S., Chang, Y. Z., Chen, S. C., Yau, S. M., Shen, Y. L. and Lee, C. Y. (2002). Localization of NADPH-diaphorase and nitric oxide synthase activity in the eyestalk of the crayfish, *Procambarus clarkii*. *Zoological Studies* **41**, 244-250.